THE ROLE OF TCF7L2 ON BONE METABOLISM

By

AJAI KAILEY

A thesis submitted to the University of Birmingham for the degree of Masters By Research

Institute of Metabolism and Systems
College of Medical and Dental Sciences
University of Birmingham
July 2023

Abstract

People living with Type 2 Diabetes, especially post-menopausal women, have been found to be associated with having a greater risk of developing bone fractures. The single nucleotide polymorphism (SNP) rs7903146 for *Transcription Factor 7-like 2* (*Tcf7l2)*, characterized by a C to T nucleotide substitution within intron 4 of *Tcf7l2*, has been found to have the greatest association with T In an earlier study looking at the role of *Tcf7l2* on adipose tissue function, we found that adipocyte-specific *Tcf7l2* knockout mice had altered plasma osteocalcin content, indicating a potential defect in osteoblast function. The aim of this investigation was to identify whether adipocyte-specific knockout of *TCF7L2* loss of bone cell number and bone cell mass. I also aimed to identify whether the *Tcf7l2* rs7903146 SNP resulted in impaired human osteoblast function. I found that average osteoblast area was significantly greater within homozygous adipocyte-specific *Tcf7l2* knockout mice compared to heterozygous adipocyte-specific *Tcf7l2* knockout mice, when fed a NC diet. Preliminary data from human osteoblast cultures suggests homozygote carriers of the rs7903146 SNP have reduced median expression of the bone formation marker Osteocalcin. However, homozygous carriers of the rs7903146 SNP had greater secretion of uncarboxylated and carboxylated Osteocalcin a heterozygous carrier of the rs7903146 SNP. However, more work is needed to confirm these preliminary results. This investigation can be used as a starting point to determine the influence of the *Tcf7l2* rs7903146 SNP on osteoblast function and adipocyte specific knockout of *Tcf7l2* on osteoblast and osteoclast function, potentially linking *Tcf7l2* with T2D associated osteoporosis.

Acknowledgements.

I would like to take this opportunity to thank Dr Gabriela Da Silva Xavier and Dr Caroline Gorvin for their help and support throughout this project. I would also like to thank to all the staff at the Institute of Metabolism and Systems who taught me how to use specific equipment. I am also very grateful for our collaborators in Denmark, Morten S. Hansen and Morten Frost, who collected, prepared and sent osteoblasts to us for our investigation. I would like to thank Marie-Sophie Nguyen-Tu for their work involving Adipocyte-specific deletion of TCF7L2 within mice, as their mouse model was used in my mouse investigation. Finally, I would like to thank Jasbir, my family and friends for their help and support throughout my academic studies.

Table of Contents

List of abbreviations

adenomatous polyposis coli (APC)
adenosine triphosphate (ATP)
Homozygous adipose tissue specific knockout of *Tcf7l2* (ATCF7L2-KO(hom))
heterozygous adipose tissue specific knockout of *Tcf7l2* adipose tissue (ATCF7L2-KO(het))
Adipose tissue specific knockout of *Tcf7l2* (ATCF7L2-KO)
advanced glycated end products (AGEs)
alpha ketoglutamate (alpha-KG)
Biological apatite (BAp)
Bone gamma-carboxyglutamate (*Bglap)*
Bone gamma-carboxyglutamate 2 (*Bglap2)*
bone mineral density (BMD)
casein kinase 1α (CK-1α)
CCAAT-enhancer binding protein α (C/EBPα)
DHAP-dihydroxyacetone phosphate,
Diacylglycerol (DAG)
dominant negative form of *TCF7L2* within male mice (hTCF7L2LDN)
enhancer binding protein α (C/EBPα)
Exon 11 of TCF7L2 removal in mature adipocytes (ΔE11-TCF7L2)
Forkhead box O (FOXO)
genome wide association studies (GWAS)
Glucagon (gcg)
Glucagon-like peptide-1 (GLP1)
Glucose stimulated insulin secretion (GSIS),
Glucose transporter 2 (GLUT2)
Glucose-6-phosphate (G6P)
Gly3P- Glycerol 3-phosphate,
glycogen synthase kinase-3 (GSK3)
heterozygous carrier of the risk allele (TCF7L2het)
high fat diet (HFD)
homozygous carriers of the rs7903146 SNP of TCF7L2 (TCF7L2hom)
Insulin receptor (InsR)
Insulin receptor substrate (IRS)
insulin receptor substrate 1 (IRS1)
Interleukin 1 beta (IL-1β)
intracellular bipartite transcription factor (β-cat)
knockout of Lrp5 (Lrp5-/-)
low density lipoprotein receptor related 5 (LRP5)
mesenchymal stem cells (MSCs)
msh homeobox homolog 2 (Msx2),
Nicotinamide adenine dinucleotide (NAD+)
Nicotinamide nucleotide transhydrogenase (Nnt)
normal chow (NC)

Nuclear factor kappa-light-chain- enhancer of activated B cells (NF-κB)
oral glucose tolerance test (OGTT),
osteocalcin (OST)
osteoprotegerin (OPG)
Oxaloacetate (OAA)
Peroxisome proliferator-activated receptor gamma 2 (PPARγ2)
phosphatidylinositol (3,4,5)-triphosphate (PIP_3)
phosphatidylinositol 3 kinase (PI3K),
phosphatidylinositol 4,5-bisphosphate (PIP_2)
Protein kinase B kinases (AKT)
Protein kinase C (PKC)
receptor activator for nuclear factor k B (RANK)
runt-related transcription factor 2 (Runx2)
single nucleotide polymorphism (SNP)
Small Interfering RNA (siRNA)
Standard error of the mean (SEM)
Transcription factor (TCF)
Transcription factor 7- like 2 (TCF7L2)
Triacylglycerides (TAG)
Tricarboxylic acid cycle (TCA cycle)
tumour protein p53 (*Tp53)*
Tumour protein p53- inducible nuclear protein 1 *(Tp53inp1)*
Type 2 diabetes mellitus (T2D)
Uncoupling protein 2 (UCP2)
Wild type (WT)
Wingless (WI)
Wingless-related integration site (Wnt)

CHAPTER 1
Introduction

In this project I will explore the effects of the loss of function of the gene encoding Transcription Factor 7-like 2 (*Tcf7l2*) in adipocytes on bone function. Single nucleotide polymorphisms in *Tcf7l2* have been implicated in increased risk of type 2 diabetes (T2D). In this introduction section I will first summarise current information on T2D. This will include summarising T2D pathogenesis, complications of T2D, whole body metabolism control and how tissues involved in controlling whole body metabolism are affected by T2D. Then, I will focus on describing bone structure and function. This section on bone will also cover bone cell differentiation, cross talk between bone cells, how bone remodelling occurs and describe how bone also acts as an endocrine organ. I will explore the link between T2D and an increased risk of bone fracture. Next, I will introduce the polygenic nature of T2D and introduce the gene in question, *Tcf7l2*. TCF7L2 is a transcription factor associated with the Wnt signalling pathway, so I will briefly describe Wnt signalling. I will then give an overview of the literature surrounding the role of *Tcf7l2* within tissues involved in energy homeostasis. Towards the end, I will provide an overview of how Wnt signalling influences bone formation and bone resorption. Following from this, I will discuss the preliminary data that underpins the research question. Finally, the sequence of these sections will lead to the formulation of the hypothesis.

1.1 Overview of Type 2 Diabetes

T2D is one of the most common non-communicable diseases and cases have been predicted to increase at an alarming rate worldwide (Olokoba, Obateru and Olokoba, 2012; Trikkalinou *et al*. 2017). The number of people worldwide living with T2D has been predicted to rise to 552 million people by the year 2030 and 642 million by 2040 (Olokoba, Obateru and Olokoba, 2012; Trikkalinou *et al*. 2017). The treatment of T2D is a serious worldwide financial burden and has negative effects on quality of life (Hex *et al*., 2012; Okoronkwo *et al*. 2015; Assaad-Khalil *et al*. 2017; Cannon *et al*. 2018; Moucheraud *et al*. 2019; Ganasegeran *et al*. 2020). There is also an increasing trend of T2D development within children and adolescents (Chen, Magliano and Zimmet, 2011). T2D is a condition characterized by hyperglycaemia, reduced insulin sensitivity and lack of insulin secretion (Olokoba, Obateru and Olokoba, 2012; Ali, 2013; Roden and Shulman, 2019; Galicia-Garcia *et al*. 2020). As a result, the loss of insulin signaling induces a decrease in glucose transportation into muscle, liver and adipose tissue (Olokoba, Obateru and Olokoba, 2012). T2D is thought to develop as a result of genetic predispositions and environmental factors (Chen, Magliano and Zimmet, 2011). The environmental and behavioral factors thought to increase risk of T2D are lack of activity, obesity, smoking, alcohol intake, stress and a high fat diet (reviewed in van Dam, 2002; Ali, 2013; Da Silva Xavier *et al*., 2013). In recent years, literature has focused more about understanding the causes of T2D beyond the environment and lifestyle factors which has given exciting insights into the pathogenesis of T2D. Progression of T2D can be described as following stages: prediabetic to diabetes stage, decrease in the acute insulin response, initiation of medication and failure of medication to control blood glucose (Fonseca, 2009). Research has also revealed that T2D is associated with aging and chronic inflammation (Palmer, *et al*. 2015; Palmer, *et al*. 2019).

1.1.1 Current Understanding Of how T2D Develops

A western diet and overnutrition is thought to be responsible for the systemic low-grade inflammation which leads to T2D development (Galicia-Garcia *et al*. 2020), Rehman and Akash, 2016). This is because excessive eating results in hyperlipidemia and hyperglycaemia (Rehman and Akash, 2016; Galicia-Garcia *et al*. 2020). When this is paired with a sedentary lifestyle, there is an imbalance between energy expenditure and energy intake which results in the production of reactive oxygen species (ROS) (Galicia-Garcia *et al*. 2020). The excess supply of free fatty acids and glucose results in excessive oxidative phosphorylation which increases electron supply to the electron transport chain within cellular mitochondria (Rebolledo and Actis Dato, 2005; Galicia-Garcia *et al*. 2020). This in turn causes reduction of oxygen to form superoxide (O_2^-) by respiratory chain complex I and complex II (Rebolledo and Actis Dato, 2005; Stefan and Ulrich, 2012; Galicia-Garcia *et al*. 2020). ROS activate pathways that initiate expression of proinflammatory mediators, increase free radical formation and Inhibit antioxidant defense mechanisms (Manna and Jain, 2015; Rehman and Akash, 2016; Galicia-Garcia *et al*. 2020). The increase in systemic proinflammatory mediators is thought to drive peripheral tissue inflammation and beta cell damage (Rehman and Akash, 2016). This eventually results in Insulin resistance and reduced Insulin secretion. ROS can also induce mitochondrial protein, membrane lipid and DNA damage (Galicia-Garcia *et al*. 2020). This results in impaired mitochondrial function and mitochondrial apoptosis (Galicia-Garcia *et al*. 2020). The role of mitochondrial damage and the link to T2D has been well documented and is associated with liver insulin resistance, reduced ATP synthesis by reduced oxidative metabolism, impaired insulin secretion from pancreatic beta cells, impairment of peripheral neurons and the central nervous system (reviewed by Pinti *et al*. 2019)

To understand how insulin resistance develops, it is important to understand insulin signaling (sumarised in figure 1). Insulin binds to the Insulin receptor which activates autophosphorylation of the Insulin receptor and Insulin receptor substrate (IRS) proteins by a tyrosine kinase (Haeusler *et al*. 2018). A protein kinase, phosphatidylinositol 3 kinase (PI3K), then binds with IRS proteins which results in the phosphorylation of phosphatidylinositol 4,5-bisphosphate (PIP_2) to form phosphatidylinositol (3,4,5)-triphosphate (PIP_3) (Boucher, Kleinridders and Kahn 2014). Next, PIP_3 interacts with phosphoinositide-dependent kinase (PDK-1) which phosphorylates Protein kinase B (AKT) kinases to activate further AKT kinase phosphorylation, which is carried out by mTOR complex 2 (mTORC-2) (Boucher, Kleinridders and Kahn 2014; Haeusler *et al*. 2018). AKT kinases activate other kinases that initiate downstream signals of insulin (Boucher, Kleinridders and Kahn 2014). AKT initiates downstream phosphorylation reactions which activates glucose transport, metabolism, survival, cell cycle/ cell growth and glycogen synthesis (Boucher, Kleinridders and Kahn 2014). AKT phosphorylates Forkhead box O (FOXO) transcription factors and prevents their entry into the nucleus (Boucher, Kleinridders and Kahn 2014). As a result, transcription factors belonging to this family can not initiate expression of genes controlling lipid synthesis and gluconeogenesis (Boucher, Kleinridders and Kahn 2014). PDK-1 also phosphorylates and activates Protein kinase C (PKC) which also plays an important role in glucose transport (Boucher, Kleinridders and Kahn 2014).

Insulin signalling also controls another signalling pathway, which is the Grb2-SOS-Ras-MAPK pathway responsible for inducing gene expression and cell proliferation (Boucher, Kleinridders and Kahn 2014). T2D is associated with the activation of Serine and Threonine protein kinases, that ultimately results in the Serine and Threonine phosphorylation of insulin receptor substrate-1 (IRS-1) and AKT (sumarised in figure 2) (Boucher, Kleinridders and Kahn 2014). Serine phosphorylation prevents the Tyrosine phosphorylation of IRS proteins and results in systemic insulin resistance within peripheral tissues (Rehman and Akash, 2016). Therefore, systemic inflammation and widespread mitochondrial dysfunction could help explain, at least in part, how T2D results in peripheral tissue insulin resistance and decreased insulin secretion. As a result, complications arise due to the widespread effects of T2D pathogenesis.

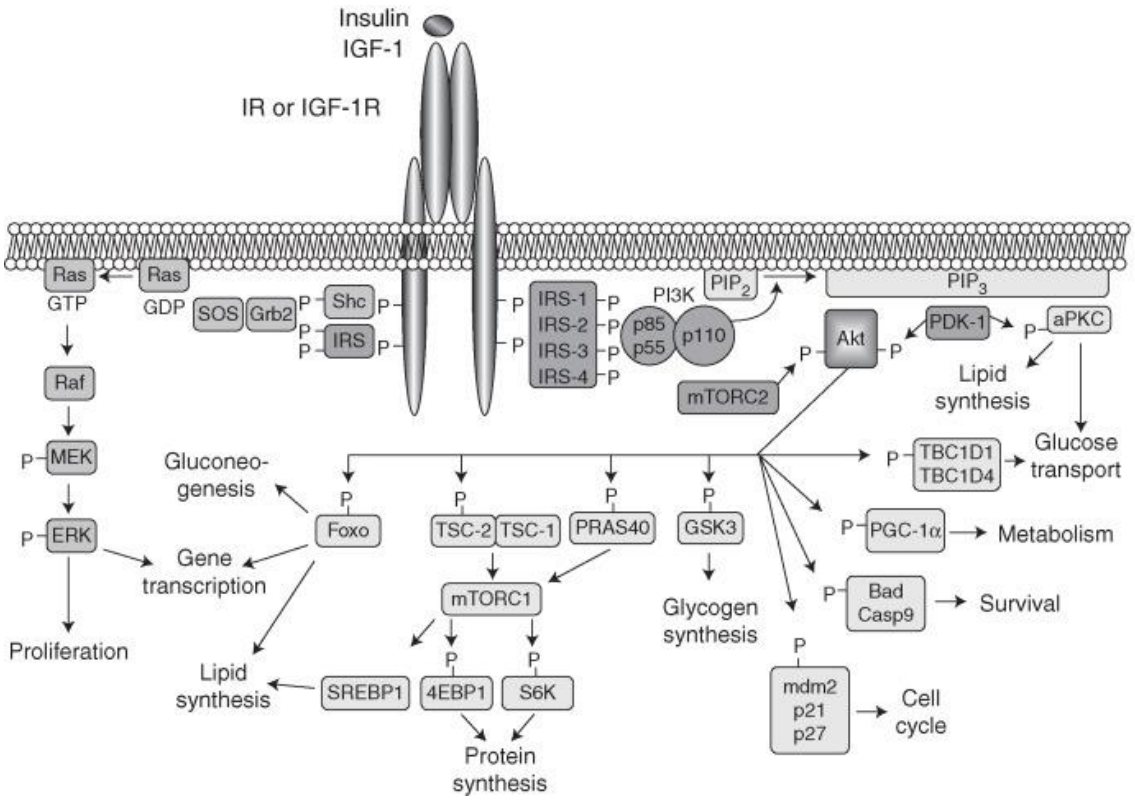

Figure 1- Insulin signaling pathway and the effects of Insulin. Insulin activates phosphorylation of the insulin receptor and the IRS proteins to initiate phosphotylation of AKT. AKT kinase activity then reduced gluconeogenesis and lipid synthesis and upregulates protein synthesis, glycogen synthesis, cell cycle, cell survival and glucose transport. Insulin signaling also activates the Ras-Raf-MEK-ERK pathway which contols cell proliferation and gene expression. Adapted from BOUCHER, J., KLEINRIDDERS, A. & KAHN, C. R. 2014. Insulin Receptor Signaling in Normal and Insulin-Resistant States. *Cold Spring Harbor Perspectives in Biology,* 6**,** a009191-a009191.

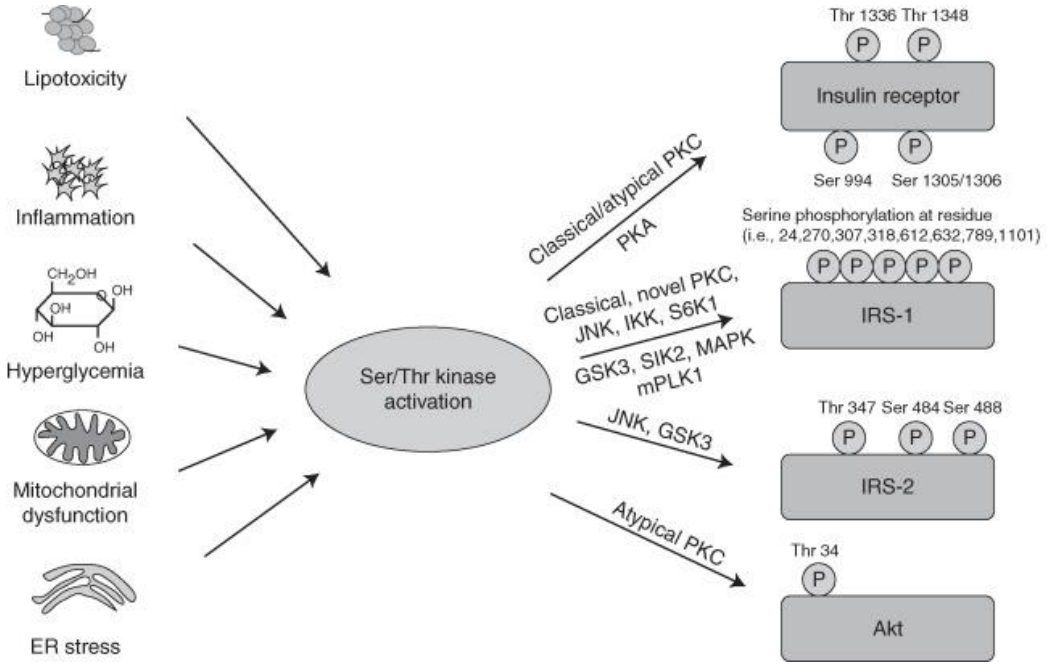

Figure 2- Mechanisms of insulin resistance. Lipotoxicity, systemic inflammation, hyperglycaemia, mitochondrial dysfunction and endoplasmic reticulum stress all lead to inappropriate phosphorylation of Serine and Threonine of IRS proteins (Boucher, Kleinridders and Kahn 2014). The inflammatory responses that occur because of lipotoxicity, hyperglycaemia, mitochondrial dysfunction and endoplasmic reticulum stress increases the production of ROS which induces widespread oxidative stress (Rehman and Akash, 2016). Oxidative stress activates pathways that induces atypical serine phosphorylation. As a result, inappropriate phosphorylation of IRS proteins and the Insulin receptor leads to Insulin resistance (Boucher, Kleinridders and Kahn 2014; Rehman and Akash, 2016). Adapted from: BOUCHER, J., KLEINRIDDERS, A. & KAHN, C. R. 2014. Insulin Receptor Signaling in Normal and Insulin-Resistant States. *Cold Spring Harbor Perspectives in Biology,* 6**,** a009191-a009191.

1.1.2 Complications of T2D

T2D results in many different complications affecting different parts of the body (outlined in table 1).

Atherosclerosis.

The microvascular and macrovascular complications of T2D are associated with atherosclerosis (Poznyak *et al*. 2020). Atherosclerosis is an inflammatory disorder that results in thickening of the intimal layer of blood vessels and formation of atherosclerotic plaques (Poznyak *et al*. 2020). Hyperglycaemia initiates atherosclerosis by causing the glycation of proteins which results in the formation of advanced glycation end products (AGES) (Schleicher and Friess, 2007; Katakami, 2018; Poznyak *et al*. 2020). AGEs bind to the receptor for Advanced glycation end products (RAGE) which induces cytokine release, vasoconstriction, expression of adhesion molecules, clot formation and vascular smooth muscle cell migration (Katakami, 2018; Poznyak *et al*. 2020). Hyperglycaemia also results in excessive glycolysis, this leads to an increase in glucose metabolites, activation of PKC pathway, activation of the polyol pathway, activation of the hexosamine pathway and excessive electron transport which all result in ROS production (Giacco and Brownlee, 2010; Katakami, 2018). Therefore, the balance between ROS production and the defensive antioxidant system is affected. (Katakami, 2018). As a result, excessive ROS presence induces DNA, protein and cell membrane damage as well as expression of cytokines, chemokines, adhesion molecules and other molecules involved in driving atherosclerosis (Katakami, 2018). This eventually results endothelial cell damage, increased endothelial permeability and tissue damage which perpetuates atherosclerosis (Aronson and Rayfield 2002; Katakami, 2018). Damaged blood vessels release cytokines, chemokines and express adhesion molecules which results in the influx of monocytes to the affected area (Katakami, 2018). Monocytes then mature into macrophages (Katakami, 2018). T2D results in hyperlipidemia because of lipoprotein release from the liver and increased lipolysis within adipose tissue (Erion , Park and Lee, 2016). Atheromas develop when low-density lipoproteins (LDLs) enter the endothelial space where they are modified and taken up by macrophages resulting in the formation of foam cells (Katakami, 2018). The presence of modified LDLs results in the production of growth factors that enable vascular smooth muscle cell migration into the intimal layer (Katakami, 2018). Vascular smooth muscle cells also uptake LDLs to form foam cells (Katakami, 2018). Vascular smooth muscle cells produce an ineffective fibrous atherosclerotic lesion cap (Martos-Rodríguez *et al*. 2021). The rupturing of fibrous caps initiates a thrombotic response resulting in T2D atherosclerotic associated complications (La Sala *et al*. 2019; Libby *et al*., 2019; Martos-Rodríguez *et al*. 2021).

Immune system dysfunction

T2D patients have a higher risk of developing infections (Muller *et al*. 2005; Carey *et al*. 2018; (Berbudi *et al.*, 2020). This could possibly explained by experimental evidence indicating impaired cytokine production, defective leukocyte recruitment, defective recognition of pathogens and immune cell dysfunction (reviewed in Berbudi *et al.*, 2020). The polyol pathway, AGE production, PKC pathway and proinflammatory activity also drive the development of neuropathic defects within T2D patients (Yagihashi *et al*. 2011).

Neuropathy

Hyperglycaemia is thought to initiate pathways to increase inflammation that impairs the functions of sensory, motor, autonomic, and peripheral nerves as a result of nerve fiber

damage, loss of nerve axons and nerve blood vessel damage (Syafril, 2018). The development of mitochondrial damage may also be responsible for neuropathy (Dlasková *et al.*, 2010). Neuropathy has been linked to structural changes of nerve mitochondria within human and rats (Dlasková *et al.*, 2010). This involves a decrease in electron transport chain proteins and reduced tricarboxylic acid cycle intermediates within dorsal root ganglia of db/db mice (Dlasková *et al.*, 2010). This implies T2D risk could result in impaired energy production within the peripheral nervous system. This has been confirmed within the central nervous system as brain mitochondria from a T2D mouse model showed a reduced mitochondrial membrane potential and ATP/ADP ratio, which suggests impaired aerobic respiration control (Dlasková *et al.*, 2010).

Alzheimer's Disease

T2D within humans and rats has also been associated with an increased risk of dementia and development of Alzheimer's disease (Peila *et al*. 2002; Moreira *et al*. 2003; (Movassat *et al.*, 2019). Alzheimer's disease (AD) is characterized by the in ability to create new memories, deterioration of cognitive function and behavioral changes (Moreira *et al*. 2003). AD is associated with the accumulation of amyloid-β and neurofibrillary tangles (NFTs) (Murphy and Levine, 2010). Reduced insulin and IGF signaling within the brain has been associated with an increase in expression of amyloid-β precursor protein and glycogen synthase kinase-3β (Moreira *et al*. 2003; Movassat *et al.*, 2019). Glycogen synthase kinase-3β activity is involved in phosphorylation of Tau, a protein that is a main component of NFTs (Moreira *et al*. 2003; (Movassat *et al.*, 2019). Therefore insulin resistance and impaired insulin signalling could be important in removal of amyloid-β plaques and NFTs (De la Monte, 2012; Moreira *et al*. (2003); (Movassat *et al.*, 2019). Amyloid beta peptides were shown to negatively affect brain mitochondrial function within Goto-Kakizaki Rats (Movassat *et al*. 2019) It was found that mitochondrial functional defects were exacerbated by diabetes presence, age and amyloid-β plaques (Moreira *et al*. 2003; Dlasková *et al*., 2010). This implies T2D increases the risk of mitochondrial defects which could result in the development of Alzheimer's. Insulin has found to be important for neuron survival, regeneration and synapse function which could explain why loss of insulin signaling results in impaired cognitive functions (Moreira *et al*. 2003; (Movassat *et al.*, 2019).

Foot Ulcers

Neuropathy is also responsible for the formation of diabetic foot ulcers (Moreira *et al*. 2003; (Movassat *et al.*, 2019). Diabetic patients develop foot ulcers because of inflammation inducing peripheral neuropathy, peripheral blood arterial disease and an increased risk of infection due to impairment of the immune system (Moreira *et al*. 2003; (Movassat *et al.*, 2019). As a result, diabetic patients are more at risk of lower limb infections which can become gangrenous, resulting in lower limb amputations (Moreira *et al*. 2003; (Movassat *et al.*, 2019).

Periodontitis

T2D has been related to the development of poor oral health and an increased risk of periodontitis (Jansson *et al*. 2006; Preshaw *et al*. 2012; Zhou Wu *et al*. 2020; Laouali *et al*. 2021). Periodontitis is chronic inflammatory disease that results in separation of bleeding, tooth mobility, teeth drifting and tooth loss (Preshaw *et al*. 2012).

Table 1- Complications of T2D- List of publications describing the mechanisms for complications associated with T2D.

Type of complications	Complications	References
Microvascular	Neuropathy nephropathy retinopathy	Sami *et al*., 2017; Papatheodorou *et al*. 2018
Macrovascular	Cardiovascular disease Stroke Peripheral artery disease.	Papatheodorou *et al*. 2018
Other	Foot ulcers Dental disease Increased risk of infection Alzheimer's disease.	Papatheodorou *et al*. 2018; Pinti *et al*. 2019

1.2 Overall control of whole body metabolism

In order to understand how T2D diminishes metabolism control, it is important to first understand how metabolism is controlled under normal circumstances. Whole body metabolism is regulated by different tissues and organs that communicate with each other via hormones (summarised in figure 3). After a meal, cells in within the intestinal lumen produce proteins involved in metabolism control. Intestinal cells produce secretin, glucose-dependent insulinotropic peptide (GIP) and glucagon-like peptide 1 (GLP-1) (Gutierrez and Woods, 2011; Röder *et al*. 2016, (Castillo-Armengol, Fajas and Lopez-Mejia, 2019). Secretin, GIP and GLP-1 facilitate insulin secretion from the pancreas (Castillo-Armengol, Fajas and Lopez-Mejia, 2019). Insulin release from the pancreas enables glucose uptake within adipose tissue and skeletal muscle (Castillo-Armengol, Fajas and Lopez-Mejia, 2019). Insulin also initiates pathways that activate glycogen production in skeletal muscle, lipogenesis within the liver, lipogenesis within adipose tissue and inhibits hepatic glucose production (Castillo-Armengol, Fajas and Lopez-Mejia, 2019). GLP1, liver-expressed antimicrobial peptide 2 (LEAP2) and secretin also act on the brain to control food intake and satiety ((Cheng, Chu and Chow, 2011; Ronveaux, Tomé and

Raybould 2015; Castillo-Armengol, Fajas and Lopez-Mejia, 2019) and Insulin can also stimulate signalling within the brain to control food intake (Castillo-Armengol, Fajas and Lopez-Mejia, 2019).

In the fed state, insulin stimulates glucose uptake within adipose tissue via glucose transporter type 4 transport proteins (GLUT 4). Insulin signalling also initiates glycolysis and lipogenesis within adipose tissue (Luo and Liu, 2016). Glycolysis leads to Acetyl-CoA production which is used as a precursor for fatty acid synthesis (Luo and Liu, 2016). Free fatty acids can also be extracted after digestion, from the blood stream, from Triacylglycerides (TAG) present within chylomicrons and very low density lipoproteins (Luo and Liu, 2016). Fatty acids then undergo esterification which enables fatty acids to be stored as TAG containing lipid droplets (Luo and Liu, 2016).

Insulin signaling within skeletal muscle, just as in adipose tissue, results in the uptake of glucose via GLUT4. Glucose is then used as an energy source to facilitate muscle contraction as well as stimulate glycogen synthesis (Argilés *et al*. 2016). In the fed response, transport of glucose into the liver also occurs without the need of Insulin, due to the GLUT 2 transporter (Wu, Fritz and Powers, *et al*. 1998). The liver responds to insulin by favoring glycolysis (Rui, 2014). Just as in skeletal muscle, glucose uptake in the liver is used to initiate glycogenesis (Wu, Fritz and Powers, *et al*. 1998). Within the liver, excess glucose is converted into long chain fatty acids which are combined with glycerol to form TAGs and stored within lipid droplets (Olzmann and Carvalho, 2019). Bile acid release into the small intestine stimulates expression of Fibroblast growth factor 19 (FGF19) (Castillo-Armengol, Fajas and Lopez-Mejia, 2019)). FGF19 targets the liver to decreases bile acid and hepatic glucose production (Castillo-Armengol, Fajas and Lopez-Mejia, 2019). In addition, FGF19 also stimulates glycogen synthesis within the liver (Castillo-Armengol, Fajas and Lopez-Mejia, 2019).

During fasting, The gut releases a hormones called Ghrelin which targets the hypothalamus and increases appetite (Castillo-Armengol, Fajas and Lopez-Mejia, 2019). Ghrelin also promotes lipid synthesis and inhibits fatty acid oxidation within adipose tissue (Castillo-Armengol, Fajas and Lopez-Mejia, 2019). Finally, Ghrelin stimulates glucagon release from pancreas (Castillo-Armengol, Fajas and Lopez-Mejia, 2019). Glucagon acts to oppose the effects of insulin (summarised in figure 4) (Castillo-Armengol, Fajas and Lopez-Mejia, 2019). In the fasting state, glucagon initiates enables lipolysis within adipose tissue (Luo and Liu, 2016). This involves lipase mediated release of glycerol and free fatty acids from stored TAGS (Luo and Liu, 2016). Free fatty acids and glycerol are released into the blood stream and enter the liver (Luo and Liu, 2016). Glucagon also stimulates glycogenolysis within skeletal muscle and subsequently glucose release into the bloodstream (Argilés *et al*. 2016). In severe cases of hypoglycemia skeletal muscle protein degradation can occur which releases amino acids into the bloodstream (Argilés *et al*. 2016).

The liver responds to glucagon which inhibits the actions of insulin and initiates gluconeogenesis, glycogenolysis and lipolysis (Rui, 2014). The liver receives fatty acids and glycerol from the blood (Rui, 2014). Glycerol is phosphorylated within the liver to form Gly3P

which is then as a gluconeogenic precursor (Rui, 2014). The free acids released from adipose tissue are oxidized within the liver to form Acetyl-CoA (Rui, 2014). Acetyl-CoA is then used to produce the ketone bodies: Acetoacetate and β-hydroxybutyrate (Kolb *et al.* 2021). These ketone bodies are converted into back into Acetyl-CoA by extrahepatic tissues to drive oxidative phosphorylation (Kolb *et al*. 2021). The liver also receives amino acids from skeletal muscle which are metabolized into α-ketoacids (Rui, 2014). α-ketoacids serve as precursors to produce TCA cycle metabolites essential for oxidative phosphorylation (Rui, 2014). TAGS, from lipid droplets, are metabolised within the liver to release free fatty acids which can undergo beta oxidation by cellular mitochondria (Rui, 2014). Adipose tissue can release adipokines such as adiponectin and asprosin. Adiponectin release stimulates the activated protein kinase activity (AMPK) signaling pathway within the hypothalamus, which increases appetite (Castillo-Armengol, Fajas and Lopez-Mejia, 2019). Adiponectin positively influences liver insulin sensitivity via AMPK pathway activation (Castillo-Armengol, Fajas and Lopez-Mejia, 2019). Furthermore, adiponectin functions to increase fatty acid oxidation but inhibit lipid synthesis in the liver (Castillo-Armengol, Fajas and Lopez-Mejia, 2019). On the other hand, asprosin targets the liver to increase hepatic glucose production (Castillo-Armengol, Fajas and Lopez-Mejia, 2019). We will now describe how T2D affects the tissues and organs involved in metabolism control.

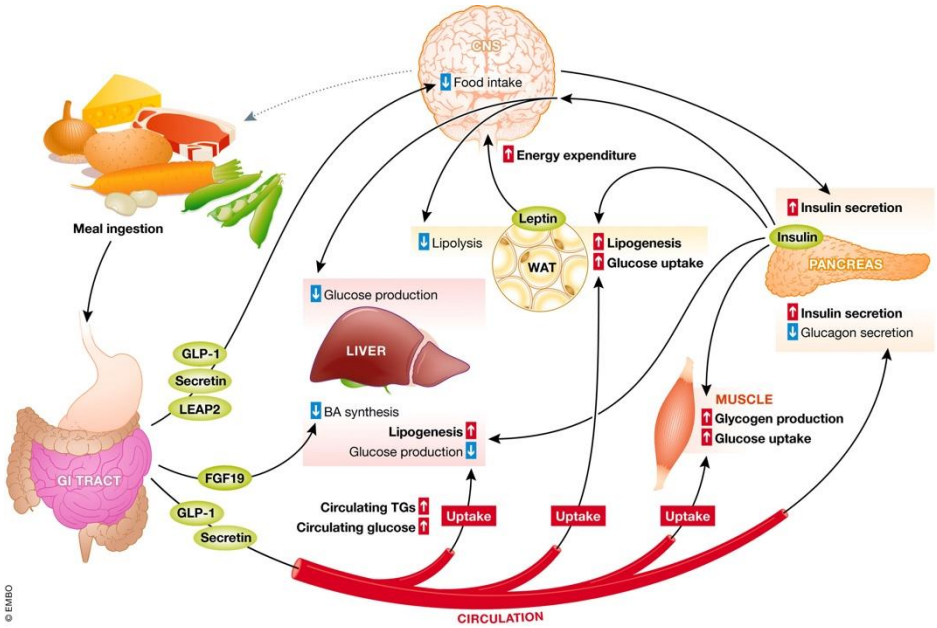

Figure 3- Regulation of metabolism In the fed response. The gut releases hormones that reduce appetite(GLP-1,Secretin,LEAP2). GLP-1 and secretin stimulate insulin secretion and reduce glucagon secretion. Insulin then facilitates glucose uptake within adipose tissue and skeletal enables via glucose transporter type 4 protein (GLUT4). Insulin initiates lipogenesis within the liver and adipose tissue. Insulin also stimulates glycogenesis within skeletal muscle and the liver. On the other hand, Insulin Inhibits lipolysis, glycogenolysis and hepatic gluconeogenesis. BA- Bile acid, FA- fatty acid, GLP-1- Glucagon-like peptide 1, TG- Triglyceride. WAT-white adipose tissue. Figure from**:** Castillo-Armengol, J., Fajas, L. and Lopez-Mejia, I.C.

(2019) Inter-organ communication: a gatekeeper for metabolic health. *EMBO reports*, 20 (9). doi:10.15252/embr.201947903.

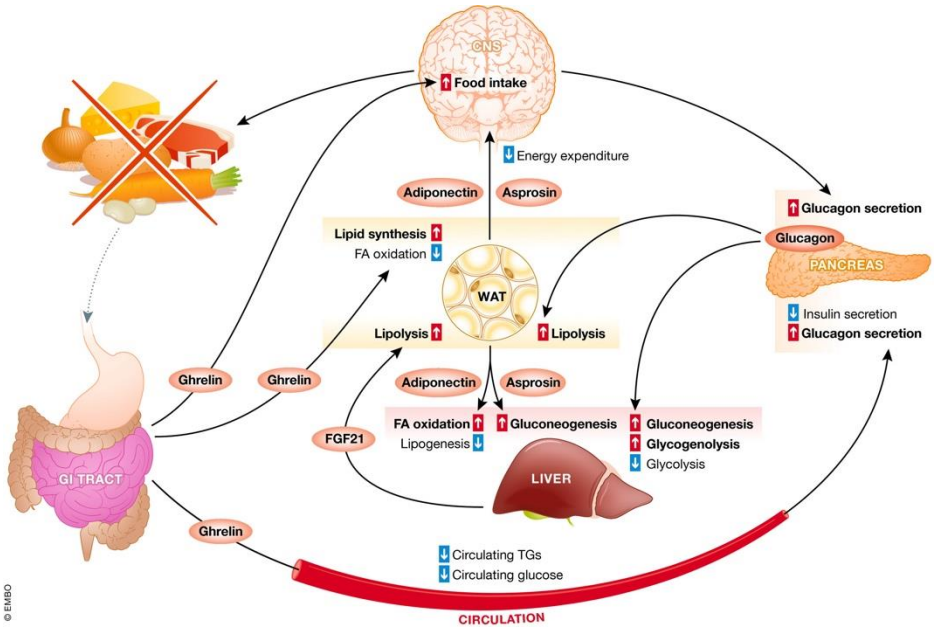

Figure 4- The regulation of metabolism during fasting. During the fasting state the gastrointestinal tract releases Ghrelin. Ghrelin is involved in stimulating food intake, lipid synthesis and inhibits fatty acid oxidation. Ghrelin prevents insulin secretion by preventing localisation of the GLP-1R, the receptor for the GLP1. This therefore diminishes the incretin effect and insulin release. Conversely, Ghrelin stimulates the release of glucagon from pancreatic α-cells. Glucagon acts on the liver to upregulate gluconeogenesis and glycogenolysis. On the other hand, Glucagon inhibits lipogenesis and glycolysis within the liver. Glucagon also stimulates lipolysis within white adipose tissue (WAT). During the fasting state, WAT releases adipokines which also regulate metabolism. WAT releases adiponectin which increases liver insulin sensitivity and increases liver fatty acid oxidation. Asprosin directly stimulates glucose release and is involved in gluconeogenesis. Both Adiponectin and Asprosin have both been linked with promoting feeding and food intake via targeting the central nervous system. Finally, hypothalamic neurons can stimulate parasympathetic glucagon release from pancreatic α-cells. Figure from**:** Castillo-Armengol, J., Fajas, L. and Lopez-Mejia, I.C. (2019) Inter-organ communication: a gatekeeper for metabolic health. *EMBO reports*, 20 (9). doi:10.15252/embr.201947903.

1.2.1 T2D and the Pancreas

To understand the effect of T2D on the pancreas, it is important to understand how the pancreas functions under normal circumstances. The pancreas belongs to the digestive system and is one of the major endocrine organs controlling whole body metabolism (Röder *et al.*, 2016). The Pancreas is known to be made up of 5 cell types: α-cells, β-cells, γ-cells, δ-cells and

pancreatic polypeptide producing cells (Röder *et al*. 2016). The most abundant cells within the pancreas are α-cells and β-cells, and these cells produce Glucagon and Insulin, respectively (Röder *et al*. 2016). Insulin is postprandially released from β-cells due to an increase in glucose within β-cells (Röder *et al*. 2016).

Insulin secretion is stimulated by glucose intake and is mostly dependent upon glycolysis (summarised in figure 5) (Fu , Gilbert and Liu, 2013). Glucose enters β-cells via the glucose transporter 2 (GLUT2) protein and is immediately phosphorylated by glucokinase to form glucose-6-phosphate (G6P) (Fu , Gilbert and Liu, 2013). G6P is then metabolized as a result of glycolysis, which produces pyruvate (Fu , Gilbert and Liu, 2013). Pyruvate is then decarboxylated to form acetyl coenzyme A within the mitochondria, which is further metabolised by the Tricarboxylic acid cycle (TCA) (Fu , Gilbert and Liu, 2013). Pyruvate can also be converted to oxaloacetate, a TCA cycle metabolite, by Pyruvate carboxylase (Jitrapakdee, Vidal-Puig and Wallace, 2006). The increase in cellular ATP concentration leads to closure of ATP sensitive potassium channels; closure of these channels initiates depolarization across the plasma membrane of β-cells which opens voltage gated calcium channels (Fu , Gilbert and Liu, 2013). The influx of calcium is then involved in the fusion of insulin containing vesicles fusion with the cell membrane, and insulin release via exocytosis (Klec *et al*. 2019). Insulin release can also be stimulated by glycerol-3-phosphate being metabolized into Diacylglycerol (Fu , Gilbert and Liu, 2013). DAG can then activate PKC stimulated insulin release (Fu , Gilbert and Liu, 2013). Insulin release can also be stimulated by fatty acids and amino acids (Fu , Gilbert and Liu, 2013). Dysregulation of any of these steps leads to inappropriate regulation of insulin secretion, many drugs for treatment of T2D target these steps to enhance beta cell function (Marín-Peñalver *et al.*, 2016).

T2D has been associated with a decrease in beta cell mass and increase in beta cell apoptosis (Lin and Sun 2010). In obese individuals beta cell mass increases In order to adapt the metabolic demand as a result of high caloric intake (Rhodes, 2005). If T2D develops, beta cell mass then begins to decrease as the cell fails to meet the high metabolic demand (Rhodes, 2005). This then leads to beta cell apoptosis (Rhodes, 2005). It has been hypothesized that the role of cytokines, hyperglycaemia, hyperlipidemia, metabolic stress and inflammation may all converge into a single pathway that induces beta cell apoptosis (Donath *et al*. 2005; Rhodes, 2005). Each of these effects all influence different signaling pathways that induce phosphorylation of insulin receptor substrate 2 which then undergoes ubiquitination, degradation and eventually induces apoptosis of beta cells (Rhodes, 2005). Cytokines are released which leads to immune cell trafficking into the pancreas driving inflammation (Cerf, 2013). ROS and reactive nitrogen species are produced because of this inflammation which induces damage to pancreatic beta cells (Lin and Sun, 2010).

The pancreas is an endocrine organ that is highly active due to high metabolic demand (Donath, 2005). T2D associated hyperinsulinemia leads to excessive endocrine activity and this causes endoplasmic reticulum stress (Harding and Ron 2002, Araki *et al*. 2003). If beta cells are unable to control this excess of insulin production, by decreasing protein synthesis and/or increasing chaperone protein expression, the cells undergo apoptosis (Harding and Ron 2002, Araki *et al*.

2003). Hyperglycaemia and hyperlipidemia may also result in mitochondrial dysfunction within beta cells (Pinti *et al*. 2019). Islets from T2D patients were shown to have lower glucose stimulated insulin secretion (GSIS), ATP production and reduced mitochondrial membrane hyperpolarization compared to islets from control participants (Anello *et al*. 2005). An increase in protein expression of Uncoupling protein 2 (UCP2) was observed in islets from T2D patients compared to control participants (Anello *et al*. 2005). This is important as UCP2 is important in regulating ATP synthesis and preventing proton influx through ATP synthase (Pierelli, *et al)*. Therefore, increased UCP2 expression could explain, at least partially, the decrease in ATP production (Anello *et al*. 2005). Since ATP production regulates insulin release, it is possible that UCP2 upregulation could lead to impaired GSIS (Anello *et al*. 2005).

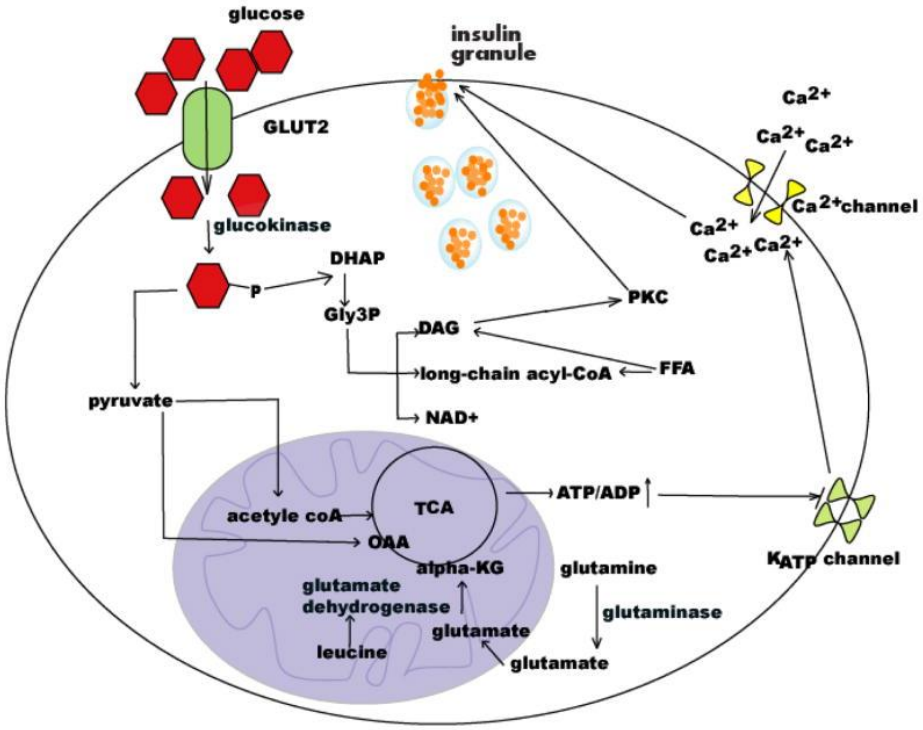

Figure 5- How insulin release is stimulated. Glucose uptake within pancreatic β-cells via Glucose transporter 2 (GLUT2) which is then used as a substrate for aerobic respiration. The increase in the ratio of ATP: ADP inhibits the opening of ATP-sensitive Potassium channels (^{K}ATP channel) which initiates membrane depolarization. Membrane depolarization induces the opening of voltage gated calcium channels (Ca^{2+} channel). It is the influx of calcium which is thought to activate insulin containing granules to fusion with the cell membrane allowing Insulin release. Insulin release can also be stimulated by phosphorylated glucose being metabolized into Diacylglycerol (DAG) which activates Protein kinase C (PKC) associated insulin release. Free fatty acid (FFA) oxidation and amino acid metabolism can also stimulate insulin release (alpha-KG- alpha ketoglutamate, DHAP-dihydroxyacetone phosphate, Gly3P- Glycerol 3-phosphate, NAD+- Nicotinamide adenine dinucleotide, OAA-oxaloacetate) Figure adapted from: FU , Z., GILBERT , E. R. & LIU, D. 2013. Regulation of Insulin Synthesis and Secretion and Pancreatic Beta-Cell Dysfunction in Diabetes. *Current Diabetes Reviews,* 9**,** 25-53.

1.2.2 T2D and Adipose tissue.

There are two types of adipose tissue within humans which are: white adipose tissue and brown adipose tissue (Chloe *et al*. 2016, Luo and Liu, 2016). However, it is white adipose tissue that is involved lipid storage and lipid catabolism (Luo and Liu, 2016). Adipose tissue can release adipokines which have been linked to insulin sensitivity and insulin secretion (Brown, 2012). Adipokines can also induce adipose tissue and systemic inflammation (Rehman and Akash 2016). Examples of Adipokines include leptin, Interleukin 6, Interleukin 1 beta (IL-1β) and Tumour necrosis factor alpha (summarized in table 2).

Adipocytes increase in size as caloric intake increases to enable storage of the excess Triglycerides obtained from a high fat diet (HFD) (Guilherme *et al*. 2008). After continued exposure to a HFD adipocytes begin to secrete adipokines (Rehman and Akash, 2016). Hypertrophic adipocytes begin to secrete the chemokine, monocyte chemoattractant protein-1 (MCP-1) (Guilherme *et al*. 2008). This results in inflammatory cell infiltration, particularly M1 macrophages, into adipose tissue (Guilherme *et al*. 2008). M1 macrophages also play a role in the release of MCP-1 and enable continued macrophage infiltration into adipose tissue (Guilherme *et al*. 2008). The cytokine IL-1β induces adipocyte expression of chemokines such as: MCP-1, Monocyte chemoattractant protein-2, Monocyte chemoattractant protein-3, Monocyte chemoattractant protein-4, C-C Motif Chemokine Ligand 2, Macrophage inflammatory protein-1 alpha and Macrophage inflammatory protein-1 beta to continue driving inflammation within adipose tissue (Rehman and Akash, 2016). The attraction of macrophages then produces cytokines which are then released systemically and induce systemic insulin resistance by activating pathways that impair insulin signaling within adipocytes and peripheral tissues (Rehman and Akash, 2016)

1.2.3 T2D and skeletal muscle

Skeletal muscle of T2D patients have been associated with damaged insulin receptor substrate 1 (IRS1) and impaired phosphorylation of this substrate (Lin and Sun, 2010). The PI3K/AKT pathway is also impaired, which is essential for glucose transportation via activation of the GLUT4 translocation protein (Defronzo and Tripathy 2009; Lin and Sun, 2010; Świderska *et al*. 2020). As a result of this pathway being affected, glycogen synthesis and protein synthesis are also affected within skeletal muscle (Huang *et al*. 2018). This occurs in part due to the systemic presence of free fatty acids, because of adipocyte dysfunction (Lin and Sun, 2010; Defronzo and Tripathy 2009; Guilherme *et al*. 2008). The increase in systemic free fatty acids leads to excess fatty acid uptake by muscles (Loria *et al*. 2013). Inside muscle tissue, lipid metabolites including Diacylglycerol, ceramides and fatty acyl COAs have been linked to inappropriate IRS1 phosphorylation and inhibition of the AKT signaling pathway (Lowell and Shulman, 2005). This results inhibition of insulin signalling (Lowell and Shulman, 2005). Evidence also points towards mitochondrial damage, since T2D patients have reduced phosphocreatine recovery, lowered maximal ATP synthesis and decreased ADP stimulated respiration (Pinti *et al*. 2019).

Table 2- **Role of some Adipokines in T2D.**

Adipokine	Role in T2D
Leptin	Leptin has been associated with decreasing insulin secretion and processing Insulin secretion is inhibited by activating the opening of K_{ATP} channels (Manna and Jain, 2015). As a result, no membrane depolarization occurs which is essential in insulin release.
Adiponectin	Adiponectin is a positive regulator of normal insulin release (Dunmore and Brown, 2013). Amount of adiponectin secretion decreases because of increased adiposity (Dunmore and Brown, 2013).
Tumour necrosis factor- α	Induces of beta cell apoptosis and stimulates serine residue phosphorylation of IRS-1 which results in insulin signaling. (Dunmore and Brown, 2013)
Interleukin-6	Important in developing insulin resistance by activating JNK serine phosphorylation of IRS1, activation of Nuclear factor kappa-light-chain-enhancer of activated B cells (NF-κB) and of cytokine signaling-3 (SOCS-3) (Manna and Jain, 2015)
Interleukin-1	Proinflammatory cytokine, drives insulin resistance, linked to leptin action (Wellen and Hotamisligil, 2005)
Interleukin-18	Proatherogenic molecule (Wellen and Hotamisligil, 2005).
MCP-1	Proatherogenic molecule, promotes Macrophage infiltration (Wellen and Hotamisligil, 2005).

1.2.4 T2D and Liver

The liver is a very metabolically active organ within the body with the ability to control whole body metabolism (Rui, 2014). However, insulin resistance within T2D diabetic patients results in liver damage (Loria *et al*. 2013; Mohamed *et al.*, 2016) . This is because metabolism in the Liver shifts towards production of fatty acids (Crawford, 2005; Feldman, Friedman and Brandt 2020). This leads to steatosis and systemic free fatty acid release (Crawford, 2005; Feldman, Friedman and Brandt 2020). Lipids accumulate in the liver from excess production and deposition (Mohamed *et al.*, 2016). The adipose tissue within the liver begins to secrete adipokines and cytokines that further drive inflammation (Loria *et al*. 2013; (Mohamed *et al.*, 2016). As a result of insulin resistance, the liver continues to undergo gluconeogenesis (Mohamed *et al.*, 2016). Obese insulin resistant patients with nonalcoholic steatosis have been found to have mitochondrial defects, which results in impaired respiration, and this could explain the cause of decreased ATP synthesis within patients (Schmid *et al*. 2011, Pinti *et al*. 2019).

1.2.5 T2D and bone

There is evidence to suggest T2D negatively influences bone quality within patients (Costantini and Conte, 2019) We would like to explore this and identify whether the gene, *Tcf7l2*, could be involved explain the effect of T2D on bone. firstly, I will give an overview of bone structure and function. Then, we will discuss literature regarding the effect of T2D on bone.

1.3 Overview of Bone structure and function

There are a total of 213 bones that make up the human skeletal system (Clarke, 2008). The skeleton provides structural support, enables movement, maintains mineral homeostasis and protects organs (Clarke, 2008). Bone is made up of inorganic salts, organic protein matrix, water and lipids (Clarke, 2008; Florencio-Silva *et al*. 2015). The inorganic salts of bone is mainly made up of phosphate and calcium ions, which form hydroxyapatite ($Ca_{10}(PO_4)_6(OH)_2$) (Clarke, 2008). Bone matrix is made up of collagenous and non-collagenous proteins, which act as a mesh that hydroxyapatite becomes embedded into (Florencio-Silva *et al*. 2015). It is the ultrastructural association of hydroxyapatite and bone matrix proteins that determines bone stiffness (Florencio-Silva *et al*. 2015).

Adult bone is formed of cortical bone and trabecular bone; with the former being the most abundant (refer to figure 6) (Clarke, 2008). Cortical bone is the solid outer layer of bone that surrounds marrow (Walker 2020). Trabecular bone is spongy and porous because of the network of interlinking plates and rods (Clarke, 2008; Oftadeh *et al*., 2015**)**. Trabecular bone is located at either ends of long bones and within vertebral bodies (Clarke, 2008; Oftadeh *et al*., 2015). Trabecular bone allows mechanical load from joints to be transferred to cortical bone (Oftadeh *et al*., 2015; Susan, 2018).

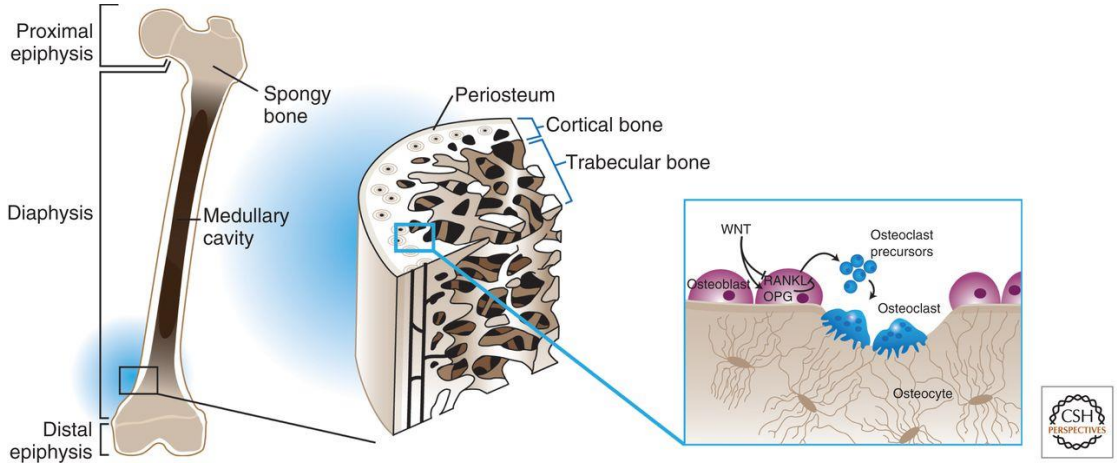

Figure 6- The anatomy of bone. Trabecular bone is found at either end of long bones, whereas cortical bone makes up the outer layer of bones and envelopes bone marrow. Cortical bone is solid to provide strength. Trabecular bone is porous; the interlinking rods give cortical bone its sponge like appearance. Osteoblasts (purple) can be found on the surface of bones, where they form new bone as well as regulate osteoclast activity. Osteoclasts (blue) are involved in bone catabolism and finally osteocytes (brown) orchestrate osteoblast and osteoclast activity. Figure from: Regard, J.B., Zhong, Z., Williams, B.O., et al. (2012) Wnt Signaling in Bone Development

and Disease: Making Stronger Bone with Wnts. *Cold Spring Harbor Perspectives in Biology*, 4 (12): a007997–a007997. doi:10.1101/cshperspect.a007997.

Bone contains different cells which are known as osteoblasts, osteoclasts, osteocytes and bone lining cells (Florencio-Silva *et al*. 2015). Osteoblasts are known to regulate bone formation by synthesizing bone matrix proteins and play an important role in mineral deposition (Clarke, 2008; Florencio-Silva *et al*. 2015). Osteoclasts on the other hand, are responsible for bone resorption (Clarke, 2008). Osteoclasts release hydrogen ions, cathepsin K enzyme and matrix metalloproteinases (Clarke, 2008). This stimulates bone mineral to dissolve and breaks down bone matrix proteins which results in bone resorption (Clarke, 2008). Osteocytes can be found within the bone matrix, and are thought to orchestrate bone resorption and formation (Florencio-Silva *et al*. 2015). Bone lining cells are found on bone surfaces where no bone reformation is occurring, and are thought prevent inappropriate osteoclast association with the bone matrix (Florencio-Silva *et al*. 2015). These bone cells form the basic multicellular unit needed to maintain bone health (Oftadeh *et al*. 2015).

1.3.1 Overview of bone cell differentiation

Osteoblast differentiation

Osteoblasts derive from mesenchymal stem cells from the bone marrow (Ponzetti and Rucci, 2021) (summarised in figure 7). Mesenchymal stem cells commit to a osteo-chondroprogenitor intermediate as a result of many pathways involving bone morphogenic protein signalling, wingless-related integration site (Wnt) signalling , Notch signalling and hedgehog signalling (Thomas and Jaganathan, 2022). These Osteo-chondrocyte progenitor cells then further differentiate into preosteblasts and immature osteoblasts (Ponzetti and Rucci, 2021). This process is controlled by the activity of important master transcription factors called core binding factor α1 (cbaf1), runt-related transcription factor 2 (Runx2), osterix (OSX), drosophila distal-less 5 and Beta catenin (Komori, 2006; Ralston, 2013; Rutkovskiy, Stensløkken and Vaage, 2016; Ponzetti and Rucci, 2021). These immature osteoblasts then become mature osteoblasts as expression of osteogenic genes begins (Ralston, 2013; Rutkovskiy, Stensløkken and Vaage, 2016; Ponzetti and Rucci, 2021). This includes expression of osteocalcin, type I collagen and alkaline phosphatase (Ralston, 2013; Rutkovskiy, Stensløkken and Vaage, 2016; Ponzetti and Rucci, 2021).

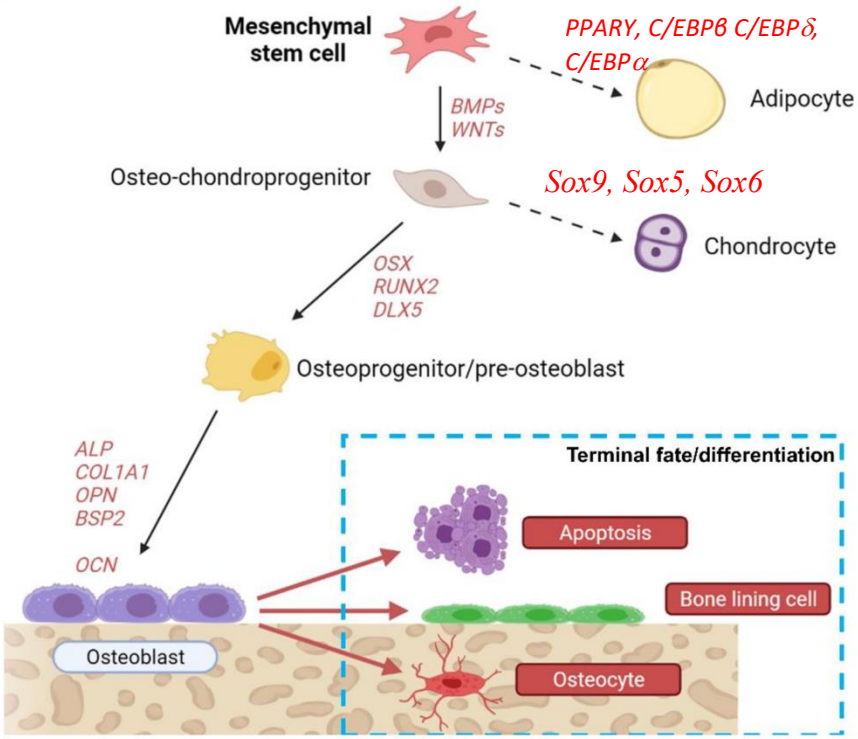

Figure 7- Osteoblast differentiation and cell fate. Multipotent mesenchymal stem cell (MSC) can differentiate into adipocytes, chondrocytes and osteoblasts within bone. Signalling pathways, such as Wnt and BMP, stimulate MSC stem cell differentiation into a osteo-chondrocyte progenitor intermediate cell. Osteo-chondrocyte progenitor differentiate into osteoblasts due to the action master transcription factors (OSX,Runx2,DL5 and cbaf1 etc.) which stimulate the expression of osteoblast specific genes (Alkaline phosphatase, osteocalcin and osteopontin etc.). After bone formation, mature osteoblasts then either undergo apoptosis, differentiate into bone lining cells or differentiate into osteocytes.
Modified figure from: Ponzetti, M. and Rucci, N. (2021) Osteoblast Differentiation and Signaling: Established Concepts and Emerging Topics. *International Journal of Molecular Sciences*, 22 (13): 6651. doi:10.3390/ijms22136651.

Osteoclast differentiation

Osteoclasts derive from cells of haematopoietic cells. Osteoclast differentiation begins with the binding of receptor activator of nuclear factor kappa-B ligand (RANKL) to its receptor (RANK), and the growth factor colony-stimulating factor-1 (CSF-1) (Boyle, Simonet and Lacey, 2003(Ralston, 2013). RANKL and CSF-1 enable hematopoietic cells to differentiate into osteoclasts by stimulating expression of other osteoclastogenic genes and genes associated with osteoclast activity (Boyle, Simonet and Lacey, 2003; Ralston, 2013). Mature osteoclasts form from 10-20 immature osteoclasts (Boyle, Simonet and Lacey, 2003). A protein named Dendritic cell-specific transmembrane protein (DC-STAMP) enables the fusion of immature osteoclasts cells to form multinuclear mature osteoclasts cells (Ralston, 2013)

1.3.2 Crosstalk between bone cells.

Osteoblasts and osteoclasts are able to control differentiation of each other via cell to cell interactions and secretion of soluble factors (summarised in figure 8) (Kim *et al.*, 2020). One of these mechanisms involves the RANKL/RANK/osteoprotegerin regulatory axis (Roux and Orcel, 2000; (Kim *et al.*, 2020). Osteoblasts release RANKL which then binds to its receptor RANK on osteoclasts (Roux and Orcel, 2000; Kim *et al.*, 2020) Activation of the RANK receptor initiates osteoclastogenesis and stimulates bone resorption (Boyle, Simonet and Lacey, 2003)Roux and Orcel, 2000; Boyle, Simonet and Lacey, 2003). Osteoblasts and osteocytes also release osteoprotegerin which acts as a decoy receptor for RANKL (Roux and Orcel, 2000; Kim *et al.*, 2020). Thereby, blocking RANKL association with RANK and inhibiting osteoclast differentiation (Roux and Orcel, 2000). Osteoblasts and osteoclasts can regulate remodelling by cell to cell interactions (Kim *et al.*, 2020). For example, Ephrin B2 (EFNB2), a surface molecule found on osteoclasts, binds to it's receptor located on the cell surface of osteoblasts (Kim *et al.*, 2020). Osteoclasts can then inhbit osteoblast differentiation via this interaction(Kim *et al.*, 2020). The reverse is also possible, whereby osteoblasts influence osteoclast differentiation (Kim *et al.*, 2020).

Table 3- osteoblast and osteoclast derived factors that control bone cell development. Both osteoclasts and osteoblasts secrete a range of factors. These factors can either promote or inhibit the differentiation of osteoblasts and osteoclasts. Table from Kim, J.-M., Lin, C., Stavre, Z., et al. (2020) Osteoblast-Osteoclast Communication and Bone Homeostasis. *Cells*, 9 (9): 2073. doi:10.3390/cells9092073.

Osteoblast-Derived Factor	Influence on osteoblasts
M-CSF	Promotes proliferation and survival of osteoclast precursor
RANKL	Promotes osteoclast differentiation and activation
OPG	Inhibits osteoclastogenesis
WNT5A	Promotes osteoclastogenesis
WNT16	Inhibits osteoclastogenesis
Osteoclast-Derived Factor	Influence on osteoclasts
S1P	Promotes osteoblast migration and survival
SEMA4D	Suppresses osteoblastogenesis
CTHRC1	Recruits stromal cells and induces osteoblastogenesis
C3	Promotes osteoblastogenesis
WNT10B	Promotes osteoblastogenesis
Vesicular RANK	Promotes osteoblastogenesis

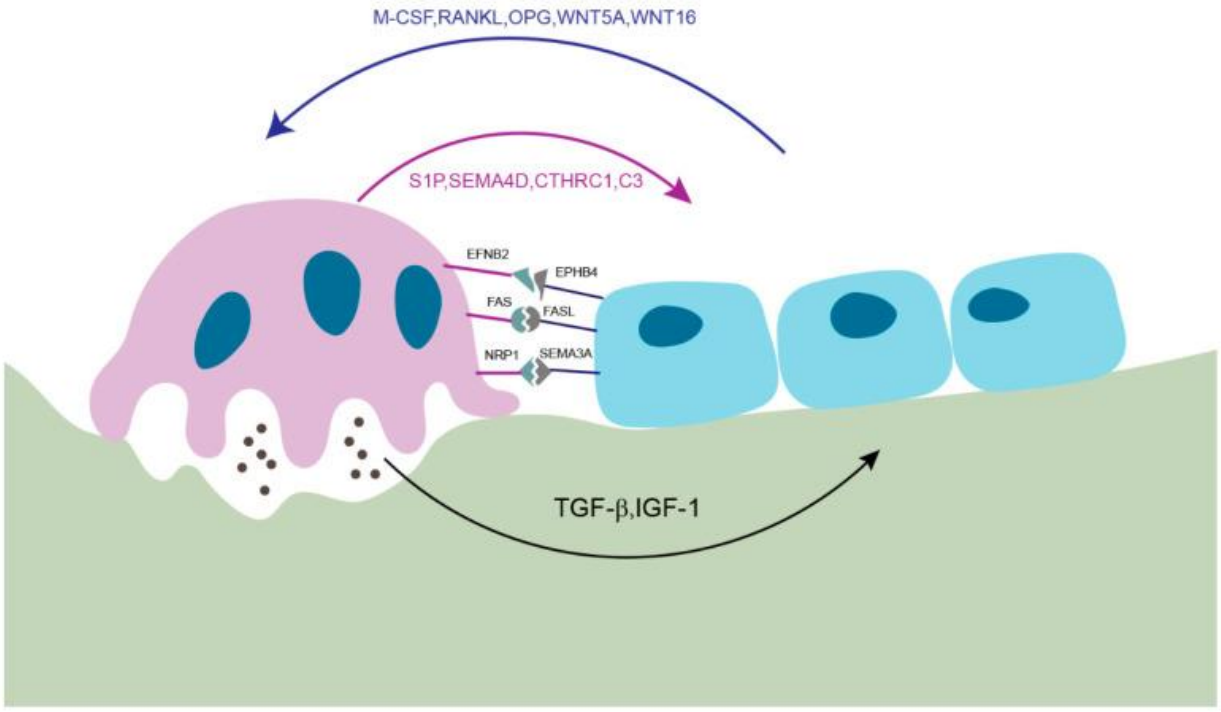

Figure 8- The interaction regulation of bone cell activity via cell to cell communication. Bone cells can regulate the activity of each other via cell to cell interactions (osteoclasts-pink, osteoblasts-blue and bone matrix- green). Ephrin B2 (EFNB2) (located on osteoclasts) binds to its receptor EPH receptor B4. This interaction enables either cell to negatively influence differentiation and activity of the other cell. Fas cell surface death receptor (FAS) is located on osteoclasts, and its association with its ligand (FASL) can stimulate apoptosis of osteoclasts. Semaphorin 3A (SEM3A), present on osteoblasts, binds to its receptor neuropilin-1 (NRP1) on osteoclasts and prevents RANKL signaling and prevents osteoclast differentiation. Osteoblasts secrete M-CSF, RANKL and WNT5A which stimulates osteoclastogenesis. On the other hand, Osteoblasts also release OPG and WNT16 to inhibit osteoclastogenesis. Osteoclasts secrete S1P, CTHRC1, C3, WNT10B and Vesicular RANK which promote osteoblastogenesis. Finally, osteoclasts secrete SEMA4D, this molecule represses osteoblastogenesis. When Osteoclasts degrade the bone matrix proteins are released such as, Transforming growth factor B1 and Insulin like growth factor type 1. These molecules have been linked to activating osteoblastogenesis.
Figure from: Kim, J.-M., Lin, C., Stavre, Z., et al. (2020) Osteoblast-Osteoclast Communication and Bone Homeostasis. *Cells*, 9 (9): 2073. doi:10.3390/cells9092073.

Osteoblasts and osteoclasts can also release soluble molecules that can promote or inhibit development of either bone cells. (summarized in table 3)(Kim *et al.*, 2020). Proteins released from after bone resorption can also influence osteoblast differentiation (Kim *et al.*, 2020). Transforming Growth Factor β1 is released from the bone matrix, and aids mesenchymal stem cell differentiation into osteoblasts (Kim *et al.*, 2020). Finally insulin-like growth factor type 1 also

acts to stimulate osteoblastogenesis, via activation of mammalian target of rapamycin pathway(Kim *et al.*, 2020). I will now discuss the roles of bone cells in bone remodelling.

1.3.3 Bone remodelling and healing.

Bones are exposed to mechanical stress because of daily activities and exercise which results in minor cracks (O'Brien *et al*., 2005; Boskey and Coleman, 2010). These cracks are repaired as a result bone cells facilitating bone remodeling (summarised in figure 9) (Boskey and Coleman, 2010). Bone remodeling is also important for responding to weight gain, athletic training, fracture healing and for maintaining ion homeostasis (Dallas *et al*. 2013; Florencio-Silva *et al*. 2015; (Le *et al.*, 2017).

Bone remodeling begins by osteoclasts precursors migrating to the damaged bone (Ralston, 2013). The osteoclast precursors differentiate into osteoclasts, and bind to the surface of the bone (Ralston, 2013). Osteoclasts then form a seal on the bone surface bone (Ralston, 2013). The Osteoclasts then degrade bone via hydrochloric acid and proteolytic enzyme secretion (Ralston, 2013; Florencio-Silva *et al.*, 2015). Hydroxyapatite is dissolved by hydrocholoric acid in the resorption site, and the proteolytic enzymes can now access the bone matrix to begin protein degradation (Ralston, 2013) Florencio-Silva *et al.*, 2015). Then, osteoclasts detach from the bone surface and undergo apoptosis (Ralston, 2013).

A transition from bone resorption to bone formation occurs, and osteoblast precursors migrate to the bone resorption site (Florencio-Silva *et al*. 2015, (Ralston, 2013; Florencio-Silva *et al.*, 2015). Osteoblast precursors differentiate into mature osteoblasts and begin to form uncalcified bone matrix (Ralston, 2013). The uncalcified bone matrix is mineralized by calcification after approximately 10 days to complete the bone remodelling cycle (Ralston, 2013). Bone mineralisation occurs when vesicles containing calcium ions are secreted into the bone matrix and bind to proteoglycans (Florencio-Silva *et al.*, 2015). The negatively charged proteoglycans attract the stored calcium ions (Florencio-Silva *et al.*, 2015). Proteoglycans are then degraded by enzymes secreted by osteoblast and the free calcium ions enter the vesicle via calcium channels called annexins (Florencio-Silva *et al.*, 2015). Osteoblasts also secrete alkaline phosphatases that enable phosphate release from molecules within bone (Florencio-Silva *et al.*, 2015). Phosphate ions enter the matrix vesicles containing calcium, where hydroxyapatite crystals form (Florencio-Silva *et al.*, 2015). Accumulation of hydroxyapatite crystals within matrix vesicles leads to lysis of the vesicles, and the crystals become embedded across the bone matrix (Florencio-Silva *et al.*, 2015).

After bone formation is complete osteoblasts either undergo apoptosis or differentiate into osteocytes and bone lining cells (refer to figure 7) (Florencio-Silva *et al.*, 2015; Lee *et al.*, 2017) There is currently evidence which suggests that the skeleton has an endocrine role and plays a part in whole body homeostasis.

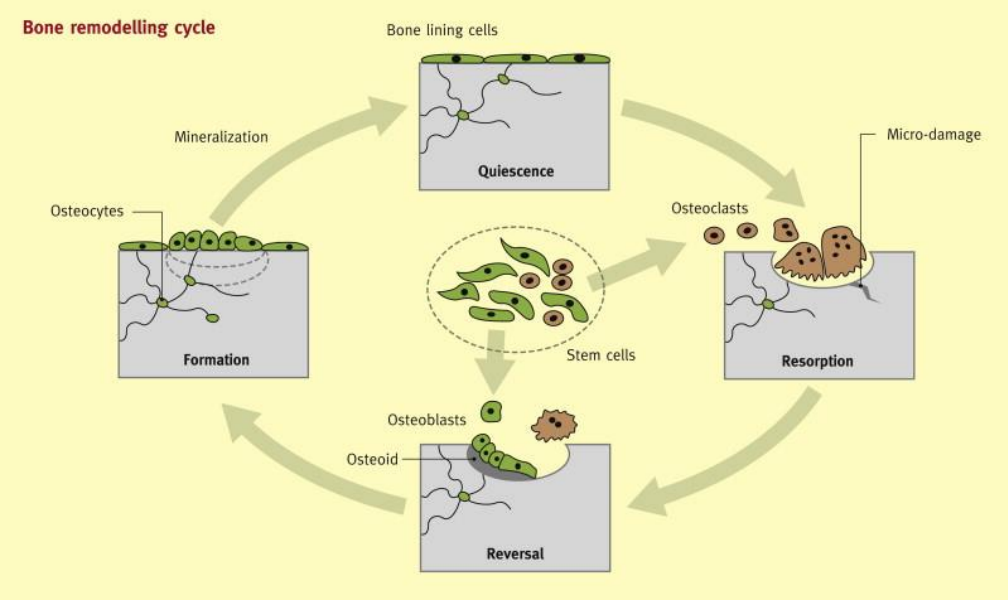

Figure 9- The bone remodeling cycle. Osteoclast precursors migrate to micro damaged sites of bone and initiate the resorption phase once they have differentiated into mature osteoclasts. Osteoclasts migrate away from the bone surface after bone resorption is complete. Osteoblast precursors then migrate to the bone surface during the reversal phase. Osteoblasts precursors differentiate into mature osteoblasts and begin to lay down new bone. Osteoblasts then either undergo apoptosis, become osteocytes, or become bone lining cells. Adapted from Ralston, S. H. (2013) 'Bone structure and metabolism', *Medicine,* 41(10), pp. 581-585.

1.3.4 Role of bone as an endocrine organ in the control of metabolism .

Aside from providing structural support, enabling movement, maintaining mineral homeostasis and protecting organs, bone is an endocrine organ (Clarke, 2008; Zhou *et al.*, 2021). Bone secretes many endocrine factors into the blood stream that have been linked to affect peripheral tissues (summarised in figure figure 10). For example, Bone morphogenic proteins (BMPs) have been linked to upregulating osteogenesis and chondrogenesis (Zhou *et al.*, 2021) . Since then, 20 different BMPs have been identified (Zhou *et al.*, 2021). BMPs have been linked to controlling adipocyte development, adipocyte biological function and insulin secretion from beta cells (Zhou *et al.*, 2021). It is important to note that some of these factors are also produced by other tissues and organs in the body (Zhou *et al.*, 2021). Therefore, it is difficult to determine whether bone derived endocrine factors do indeed perform the same role (Zhou *et al.*, 2021). More research is needed to determine the endocrine influence of bone derived factors. In this study we will focus on the bone derived protein, osteocalcin (OST).

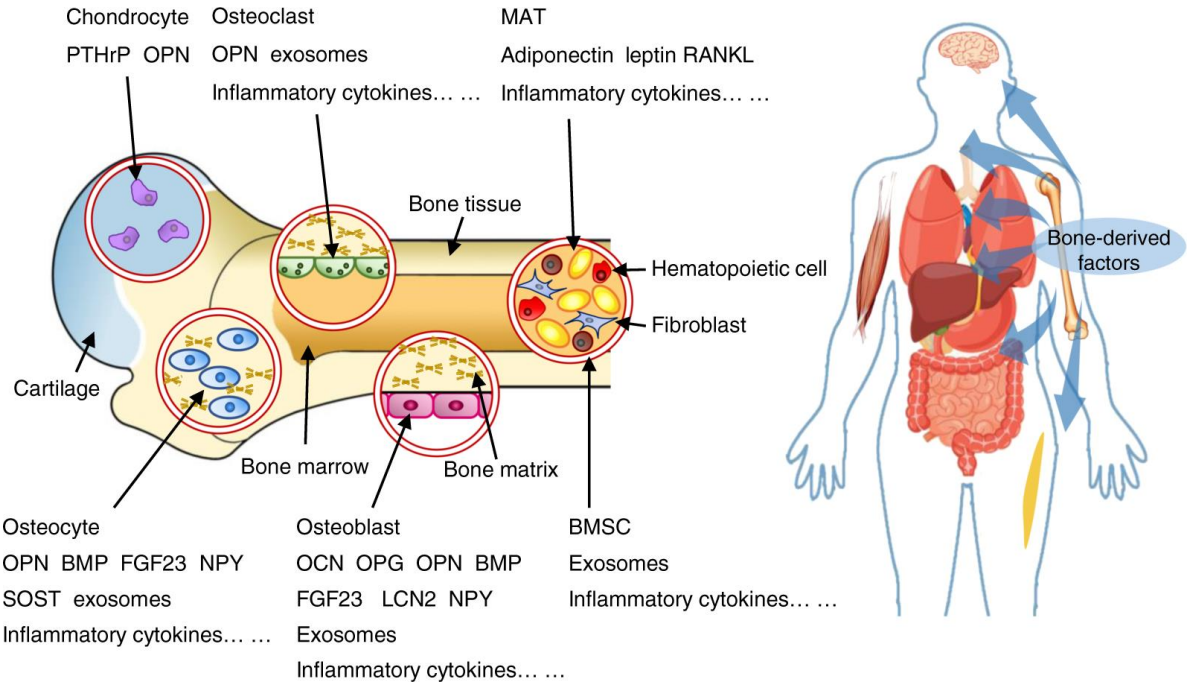

Figure 10- Bone is an endocrine organ that releases many endocrine factors. Chondrocytes, marrow adipose tissue (MAT), osteocytes, osteoblasts and bone marrow stem cells (BMSC) secrete many endocrine factors that have been linked affect the activity of peripheral tissues. Figure from Zhou, R., Guo, Q., Xiao, Y., Guo, Q., Huang, Y., Li, C. and Luo, X. (2021) 'Endocrine role of bone in the regulation of energy metabolism', *Bone Research,* 9(1).

1.3.5 Osteocalcin and control of whole body metabolism

After collagen, OST is most abundant protein found within bone and it is mostly produced by osteoblasts (Komori 2020) OST is encoded by *bone gamma-carboxyglutamate protein (BGLAP)* within humans (located within chromosome 1 at 1q25-31) and rats. In humans, when OST is initially produced it is 98 amino acids long. OST then undergoes posttranslational modifications. OST then undergoes cleavage to remove an endoplasmic reticulum signal sequence forming pro-osteocalcin (Zoch, Clemens and Riddle, 2016). Pro-osteocalcin then undergoes γ-carboxylation at 3 glutamic acid residues (second carboxyl group is added to glutamic acid residues 13, 17, and 20 within mice mouse and at residues 17, 21, and 24 in humans (Delmas *et al*., 2000; Zoch, Clemens and Riddle, 2016). Mature OST (carboxylated OST) is formed after the cleaving of the of the propeptide sequence (Komori 2020). Finally, OST is transferred into vesicles for secretion and released into the bone matrix (Zoch, Clemens and Riddle, 2016).

The carboxylated glutamic acid residues enable OST to bind to calcium ions within hydroxyapatite (Delmas *et al.*, 2000). This association lead to the initial hypothesis that OST is essential for the creation of hydroxyapatite crystals (Zoch *et al*. 2016). Other experiments indicted that OST could inhibit bone mineralization (Zoch *et al*. 2016). Deletion of *Bglap and*

Bglap2 within 129Sv;C57BL/6J mice (OCN-/- mice) revealed an increase in cortical bone, trabecular bone, bone strength, bone formation and bone resorption compared to WT mice (Ducy *et al*. 1996). Bone formation was increased without an increase in osteoblast area, which suggests that lack of OST does not lead to an increase in osteoblast number (Ducy *et al*. 1996). Ovariectomy within OCN-/- mice resulted normal osteoclast function compared to WT mice (Ducy *et al*. 1996; Toshihisa, 2020). Therefore, OST was hypothesized to negatively control bone formation without impairing osteoclast activity (Ducy *et al*. 1996; Toshihisa, 2020). However, Carboxylated OST has been related to be essential for bone strength and preventing excessive bone elasticity (refer to figure 10). This is because OST knockout within mice has shown that OST is needed for correct orientation parallel of biological apatite to collagen in the longitudinal direction of long bones (Komori, 2020; Moriishi *et al*. 2020).

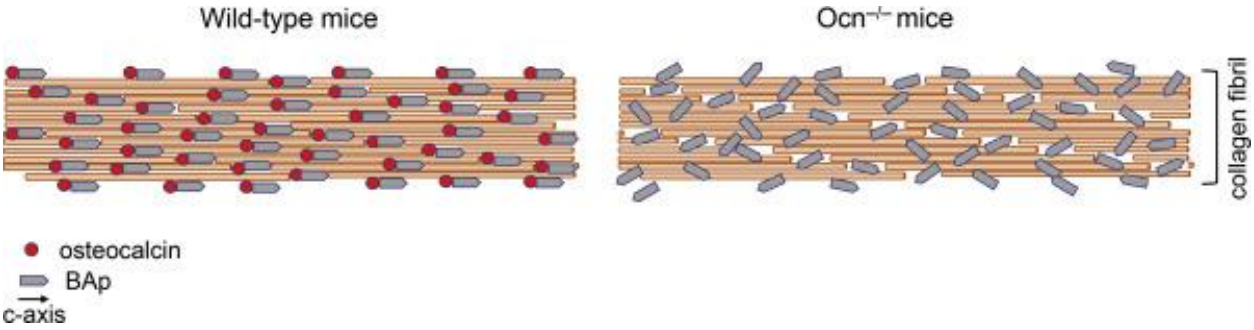

Figure 11- Carboxylated OST associates with biological appatite to maintain bone strength and inhibit bone flexibility. Collagen fibrils are aligned parallel to the longitudinal direction of long bones. In wild type mice it was found that biological apatite (BAp) associates with OST and align parallel to collagen. However, in osteocalcin deficient mice (Ocn-/-) the alignment of biological apatite was affected. This random orientation of BAp was found to strongly influence bone bending after nanoindentation testing. This suggests that the OST influences BAp orientation parallel to collagen, which is important for maintain bone strength. Figure from: Komori , T. (2020) 'What is the function of osteocalcin?', *Journal of Oral Biosciences,* 62(3), pp. 223-227.

Bone has been found to release OST (Zoch *et al*. 2016). OST can be decarboxylated when exposed to an acidic environment (see figure 13). Osteoclasts create an acidic environment during bone resorption, this decrease in pH results in the OST decarboxylation to form uncarboxylated OST (Tangseefa *et al*. 2018). uncarboxylated OST acts as a hormone which targets adipose tissue, The brain, pancreas, skeletal muscle and testes (summarised in Figure 10) (Zoch *et al*. 2016).

OST was found to be upregulated within osteoblasts as a result of Insulin (Lee *et al.*, 2007; Zoch *et al*. 2016). Mice with Osteoblasts lacking the InsR were found to be associated with increased body fat, hyperglycaemia, reduced serum insulin, reduced insulin sensitivity and impaired glucose control (Zoch *et al*. 2016; (Lee *et al.*, 2007). Treating InsR null mice with OST led to an improvement in glucose metabolism, which suggests OST plays an important role in whole body glucose control and tissue Insulin sensitivity (Lee *et al.*, 2007). Evidence also suggests OST is

involved in insulin synthesis, beta cell proliferation and adiponectin release (Tangseefa *et al*. 2018). Daily injections of OST within mice, fed a normal chow and a high fat diet, resulted in improved insulin sensitivity, glucose tolerance and prevention of obesity compared with non-treated mice (Ferron *et al*. 2012). This implies that crosstalk between bone, adipose tissue and the pancreas to control glucose metabolism by increasing insulin secretion through an OST-adiponectin- insulin loop (summarised in figure 12) (Tangseefa *et al*. 2018). OST may also influence insulin release by controlling the secretion of Incretin molecules (Mizokami *et al*. 2013). This Is because Uncarboxylated OST administration to mouse isolated STC-1 cells resulted in a significantly increased dose dependent release of GLP-1 compared with carboxylated OST treated STC-1 cells (Mizokami *et al*. 2013). These results were confirmed in vivo as uncarboxylated OST (7ug/kg) administration to male C57BL/6J mice after a 5 hour fast resulted In a significant increase in serum GLP1 and insulin when compared with control mice (Mizokami *et al*. 2013). Intraperitoneal injection of GLP-1 within male mice resulted in increased insulin levels which was inhibited when admistered with the GLP-1 receptor agonist exendin (Mizokami *et al*. 2013).

Figure 13 summarises the role of Insulin signalling on osteoblasts and the indirect effect on osteoclasts. Insulin binds to the insulin receptor (InsR) on osteoblasts to activate *OST* expression, osteoblast development, differentiation, proliferation (Tangseefa *et al*. 2018). Insulin signalling indirectly enables the expression of *T cell immune regulator* within osteoclasts, which encodes a proton transport protein that facilitates H+ transport into the resorption lacunae created by osteoclasts (Tangseefa *et al*. 2018). The decrease in pH within resorption lacunae enables the decarboxylation of OST which activates OST (Tangseefa, *et al*. 2018).

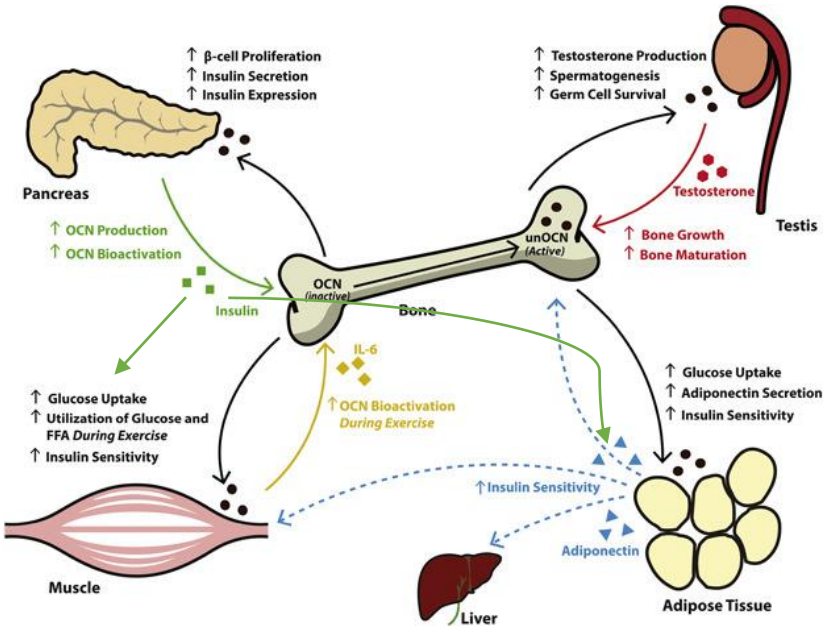

Figure 12- Role of Osteocalcin on whole body metabolism control- Osteocalcin (OCN) secretion is involved in an Osteocalcin-adiponectin-insulin feed forward loop. Uncarboxylated OST (UcOCN) is released from bone into the bloodstream. Uncarboxylated osteocalcin then stimulates adiponectin secretion from adipose tissue, and stimulates insulin secretion from

pancreatic beta cells. Adiponectin, then increases insulin sensitivity within skeletal muscle, the liver and bone. Insulin released, as a result of uncarboxylated osteocalcin secretion, then facilitates glucose uptake within skeletal muscle and adipose tissue. Insulin also upregulates osteocalcin production and bioactivation, this continues the feed forward loop to control whole body metabolism. Skeletal muscle can also release interleukin-6 to stimulate osteocalcin bioactivation. Uncarboxylated Osteocalcin has also been linked to controlling male fertility. Modified Figure adapted from**:** Tangseefa, P., Martin, S. K., Fitter, S., Baldock, P. A., Proud, C. G. and Zannettino, A. C. W. (2018) 'Osteocalcin-dependent regulation of glucose metabolism and fertility: Skeletal implications for the development of insulin resistance', *Journal of Cellular Physiology,* 233(5), pp. 3769-3783.

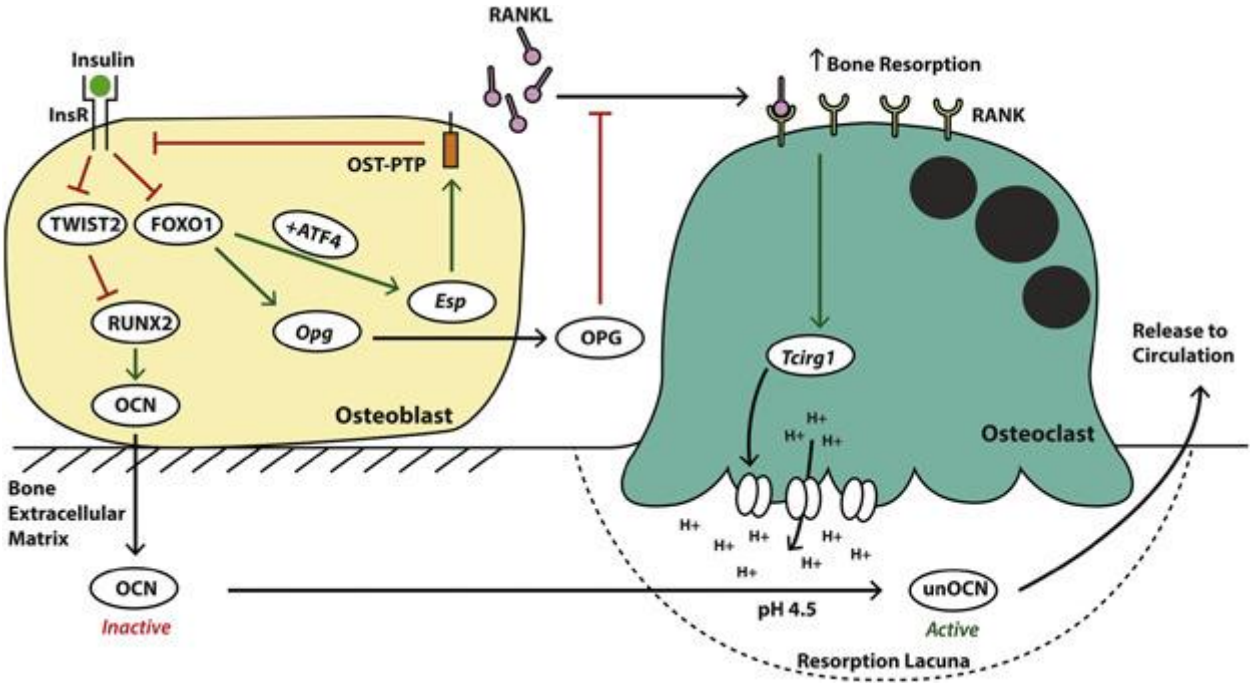

Figure 13- The role of insulin activity in controlling OST production- without insulin signalling, FOXO1 and ATF4 induce the expression of *Esp.* This then leads to the production of OST-PTP, a protein involved in reducing insulin receptor (InsR) signalling. FOXO1 also initiates expression and production of OPG, which is then secreted by osteoblasts and inhibits osteoclast function via binding to RANKL. FOXO1 and TWIST2 inhibit Runx2 activity which prevents Runx2 associated *bglap* expression, and hence inhibits OST production. However, insulin singalling inhibits FOXO1 and TWIST2 activity, this leads to reduced *Opg* expression, *Esp* expression and stimulates *bglap* expression. Therefore insulin signalling is essential for stimulating OST production. Figure adapted from: Tangseefa, P., Martin, S. K., Fitter, S., Baldock, P. A., Proud, C. G. and Zannettino, A. C. W. (2018) 'Osteocalcin-dependent regulation of glucose metabolism and fertility: Skeletal implications for the development of insulin resistance', *Journal of Cellular Physiology,* 233(5), pp. 3769-3783.

T2D has been linked to increased bone porosity (Pritchard *et al*. 2012; Pritchard *et al*. 2013; Patsch *et al*. 2013; Picke *et al*. 2019), decreased bone strength (Howard *et al*. 1996; P. Garnero

et al 2006; Poundarik *et al*. 2015; Picke *et al*. 2019), reduced osteoblasts numbers (Mizokami *et al*. 2013; Picke *et al*. 2019), increased osteoblast apoptosis (Picke *et al*. 2019, increased mesenchymal stem cells (MSC) committing to adipocyte lineage rather than osteoblast lineage (Picke *et al*. 2019), increased adiposity within bone marrow (Mizokami *et al*. 2013) and bone microangiopathy (Picke *et al*. 2019). Investigations have also revealed that T2D is associated with an increased fracture risk.

1.3.6 T2D and increased fracture risk

An increased risk of fracture has been associated with aging ((Staa *et al.*, 2001; Moayeri *et al*. 2017). A metanalysis identified older T2D patients (aged ≥70 years) had a greater relative risk of fracture compared to younger T2D patients (age 50-69) (Moayeri *et al*. 2017). A study revealed patients with T2D who experienced a hypoglycaemic episode were more at risk of fracture and fragility associated fracture compared to patients who are diabetic and did not have a hypoglycaemic event (Ntouva *et al*. 2019).

T2D patients have an increased risk of fractures because of therapeutic low blood sugar levels, which puts patients at an increased risk of falling (Costantini and Conte, 2019). Fractures could also influence balance, changes in posture and impaired muscle strength which could affect movement leading to increased risk of further injury (Costantini and Conte, 2019). It is also important to note that T2D associated complications such as impaired vision, peripheral artery disease leading to bone hypoxia, neuropathy of nerves affecting movement may all lead to an increase in fractures (Costantini and Conte, 2019).

Duration of T2D has also been associated with an increase in fracture risk (Nicodemus and Folsom 2001; Russo *et al*. 2016). Incidence rates for fractures at all sites are greater after the age of 50 within women compared to men (Moayeri *et al*. 2017). The lifetime fracture risk at any site is also greater for women after the age of 50 compared to men (Moayeri *et al*. 2017). This could be explained by the observation that T2D has also been related to an increase risk of fracture within post-menopausal women (Nicodemus and Folsom, 2001). Despite this however, there are no studies that compare the effect of T2D and fracture risk between genders (Russo *et al*. 2016; Moayeri *et al*. 2017). Studies have also shown that fracture healing is could also be impaired in T2D patients which may influence bone strength after a fracture (Murray and Coleman 2019; Picke *et al*. 2019).

1.4 Genetics of T2D.

Genetic studies about T2D inheritance initially began through genetic linkage analysis, which allowed identification of the inheritance of monogenic diabetes caused by high penetrance genes (outlined in table 3) (Risch and Merikangas, 1996; Owen and Hattersley, 2001). Gene candidate studies allowed for the identification of genes such as *KCNJ11*, *PPARG*, *WFS-1*, *IRS1*, *IRS2*, *HNF1 A, HNF1B* (Ali, 2013; Sun *et al*. 2014). It is important to note that the role of these genes in worldwide diabetes presence has reported to be low (Ringel *et al*. 1999; Clement *et al*. 2000; Furuta *et al*. 2002; Le Fur *et al*. 2002; Zhu *et al*. 2003; Sandhu *et al*. 2007; Franks *et al*.

2008; Ali, 2013). Therefore, these genes do not give much information into the inheritance and development of type 2 diabetes (Sacks and Mcdonald, 1996). There must be other genes that are more associated with the prevalence of T2D worldwide.

The introduction of large-scale association tests and genome wide association studies (GWAS) allowed massive collections of data to be analysed and identify genes associated with T2D (Gloyn *et al*. 2003; Saxena *et al*. 2007; Kooner *et al*. 2011). GWAS confirmed the association of genes found by candidate gene studies within the european population and allowed identification of novel genes (Sun *et al*. 2014). GWAS studies revealed how complex development of diabetes is and a revealed a need for understanding how these genes may lead to the development of T2D (Mahajan *et al*. 2018). Interest in *Tcf7l2* began when this gene was found to be associated with the greatest risk of developing T2D within a cohort of Iceland (Grant, *et al*. 2006). This was then confirmed within cohorts from The US, Denmark and France (Grant, *et al*. 2006; Sladek *et al*. 2007; Humphries *et al*. 2006; Mahajan *et al*. 2018). 5 *Tcf7l*2 Single nucleotide polymorphisms (SNPs) were identified as being associated with T2D which are: rs12255372, rs7903146, rs7901695, rs11196205 and rs7895340 (Grant, *et al*. 2006). The rs12255372 and rs7903146 SNPs showed the highest association with T2D (Grant, *et al*. 2006; Guan *et al*., 2016).

The rs7903146 SNP is characterized by a C to T nucleotide substitution mutation within intron 4 of *Tcf7l2,* and the strong association of this SNP with T2D has been confirmed by other studies (Nicod *et al*. 2014). However, this has not been reported in some populations. The SNPs found to be associated with T2D in the Iceland cohort were used to identify the presence of these SNPs within a Pima Indian cohort (Guo *et al*. 2007). It was found that the minor alleles of the common *Tcf7l2* SNPs were not as prevalent within Pima Indians (Guo *et al*. 2007). Neither of the *Tcf7l2* SNPs were associated with T2D and the odds ratio for the rs7903146 T-allele was much lower than previous studies have reported (Guo *et al*. 2007). However, there was a link between high BMI and the T allele of the rs7903146 genotype in terms of diabetes presence (Guo *et al*. 2007). This indicates that despite low prevalence of the SNP there is a still a risk of T2D development if a patient has a high BMI. High BMI was also associated with carriers of the G allele for the rs12255372 SNP, C-allele of rs7895307, C-allele of rs7903146. The rs7903146 SNP and rs1225537 SNP were found to be rare or marginally associated with T2D within the Han Chinese population (Chang *et al*. 2007; Ren *et al*. 2008). However other groups have reported an association between the rs7903146 SNP and T2D (Lin *et al*. 2010; Dou *et al*. 2013). Similar findings have been reported from investigations involving Arab populations. There was a marginal association between disease stage and frequency of the T allele for rs12255372 but the same was not reported for the rs7903146 allele (Saadi *et al*. 2008). No difference was found between the carrier status of risk alleles and markers of T2D such as fasting blood glucose, fasting insulin, 2 hour oral glucose tolerance test (OGTT), insulin resistance and beta cell function (Alsmadi *et al*. 2008, Saadi *et al*. 2008). Despite these findings, it is widely accepted that *Tcf7l2* is the most significant gene associated with risk of diabetes development (Da Silva Xavier *et al*. 2012). This is because, *Tcf7l2* has been found to be associated with T2D in many different cohorts involving participants of different ethnicities across the world (Grant, *et al*.

2006; Herder *et al*., 2008; Sanghera, *et al*. 2008; Cho, *et al*. 2009; Cauchi, 2012; Long, *et al*. 2012)

1.5 Role of *TCF7L2* in tissues involved in energy homeostasis

1.5.1 Wnt signaling

TCF7L2 is a known transcription factor of the Wnt signalling pathway, important in controlling expression of Wnt target genes. (Jin 2008; Ip *et al*. 2012; Chen *et al*. 2018). The name Wnt originates from the combination of the oncogene Int-1 discovered in mice, and the Drosophila ortholog wingless (Maeda *et al.*, 2019). As of today, 19 different Wnt ligands have been discovered in humans (Maeda *et al.*, 2019). Wnt signalling is particularly important in embryogenesis, cell fate determination, motility, polarity, primary axis formation, osteoblastogenesis and organogenesis (summarised in figure 14) (Komiya and Habas, 2008). This may explain why Wnt signalling has been related to cancers, skeletal deformities and birth defects in humans (Komiya and Habas, 2008). Since *Tcf7l2* SNPs have been associated with T2D, it is important to understand the normal function of this gene in tissues. I will review the evidence that may explain the mechanisms by which this gene influences T2D development. Firstly, I will describe Wnt signalling and then outline the role of TCF7L2 in metabolism control. I will also describe the role of Wnt signalling within bone.

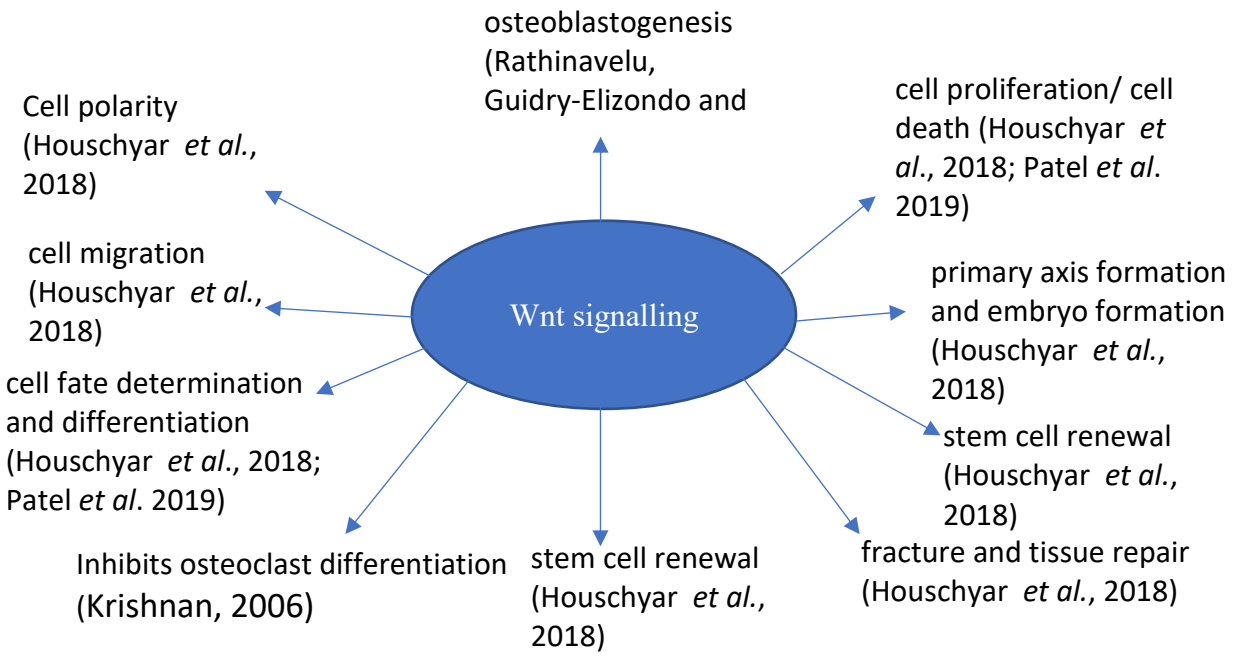

figure 14– The role of Wnt signaling. This figure highlights the importance of WNT signaling. Wnt signaling plays an important role in stem cell renewal, cell proliferation, migration and cell fate determination which may explain why this pathway is implicated in embryo development. The WNT signaling pathway is also important in the development of Osteoblasts which could explain the role of Wnt signaling within fracture repair.

Table 3- Most common maturity onset diabetes of the Young (MODY) genes. These genes are associated with monogenic diabetes. These genes are all Transcription factor mutations, except for MODY2 which is a mutation within glucokinase. Homozygous and heterozygous inheritance of these disorders may influence the phenotype produced. These mutations present as diabetes within patients either from birth, during childhood and early adulthood.

MODY subtype/ Gene	Gene function	When diabetes develops	Effects of mutations/ Complications
MODY1/ *HNF4α*	Transcription factor/expressed where column	Adolescence (Urakami, 2019) Before 25 years (Firdous *et al*., 2018).	Neonates present with hyperinsulinemia and hypoglycaemia (Firdous *et al*., 2018). Diabetes develops as a result of insulin deficiency (Urakami 2019).
MODY2/ Glucokinase	Enzyme	From Birth (Urakami, 2019)	Increased threshold for glucose as a result of excess insulin secretion which leads to hyperglycaemia (Urakami, 2019). Effects of condition reduce over time therefore complications are rare (Urakami, 2019). Heterozygous mutations are associated with minute increases in blood glucose in children. Whereas homozygous mutations results in neonatal diabetes (Firdous *et al*. 2018)
MODY3/ *HNF1α*	Transcription factor	Early adulthood (Urakami, 2019)	Progressive loss of insulin production over time possibly as a result of cell apoptosis (Firdous *et al*., (2018); Urakami (2019)). Complications involve microvascular and macrovascular issues (Urakami, 2019). Patients may also develop renal tubular defects (Urakami, 2019).
MODY4/ *PDX1*	Transcription factor.	Variable-most commonly develops between 17-67 years of age (Nkonge *et al*. 2020).	Pancreatic agenesis, hypoplasia and beta cell defects (Urakami, 2019).
MODY5/ *HNF1β*	Transcription factor	Adolescence/ Early adulthood (Urakami, 2019).	Dyslipidemia, pancreatic hypoplasia, insulin resistance in liver. Many patients develop renal failure later in life (Urakami, 2019). This mutation is associated with other complications such as vaginal aplasia, female genital tract deformation, gout, low birth weight and hyperuricemia (Firdous *et al*., 2018).

MODY6/ NEURO D1	Transcription factor	Homozygous mutations- neonatal diabetes (Urakami, 2019). Heterozygous mutations- diabetes presents during childhood or adulthood (Urakami, 2019).	This transcription factor is essential for development of beta cells and And neurons (Urakami, 2019). As a result of immature beta cell presence patients develop irregular glucose control (Urakami, 2019). Those with homozygous mutation have much worse effects as a result of neonatal diabetes and are associated with learning difficulties (Urakami, 2019).

1.5.2 Canonical Wnt signalling

The canonical Wnt signalling pathway (refer to figure 14) involves Wnt ligands binding to their receptors (frizzled) (Jin 2008; Ip *et al*. 2012). Wnts 1, 2, 3a, 3b, 4, 8, and 10b are known to activate this pathway (Houschyar *et al.*, 2018). Wnt ligands are released from cells via binding to a transmembrane protein, Wntless (WI). The low-density lipoprotein receptor-related proteins 5 (LRP5) and 6 (LRP6) complex (LRP-5/6) prevents the degradation of intracellular bipartite transcription factor (β-cat) via inhibition of proteasome activity (Jin, 2008; Ip *et al*. 2012). This is because β-cat usually associates with a degradation complex made up of adenomatous polyposis coli (APC), axin/conductin, glycogen synthase kinase-3 (GSK3) and casein kinase 1α (CK-1α) that phosphorylates serine residues within β-cat resulting in its degradation (Ip *et al*. 2012). However, Wnt signaling prevents this interaction and enables β-cat to interact with transcription factors associated with the transcription factor (TCF) family genes and begin transcription of Wnt target genes (Jin, 2008; Ip *et al*. 2012)**.**

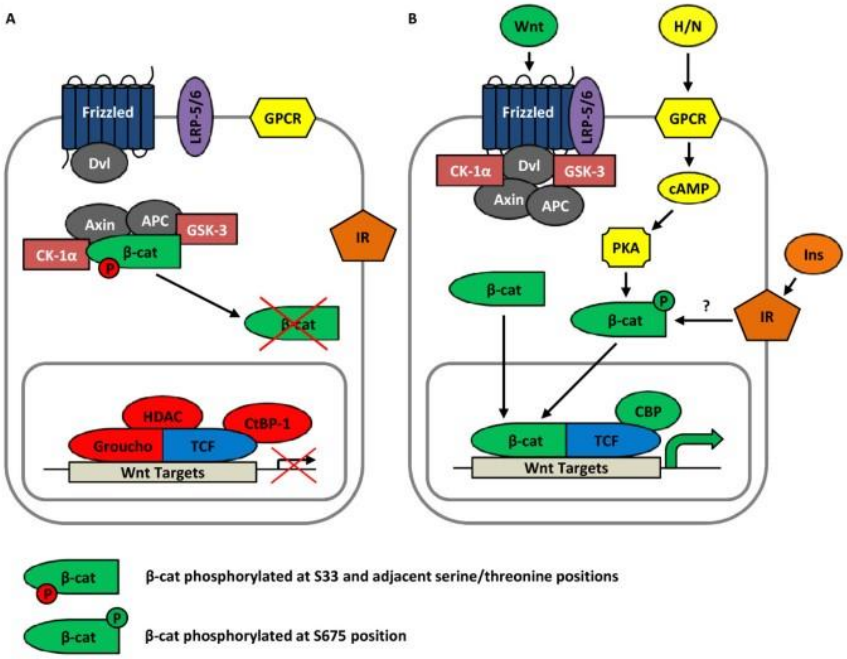

Figure 15- Overview of the Wnt signalling pathway. (A) Without Wnt signalling, serine residues within β-catenin are phosphorylated by the degradation complex made up APC, axin/conductin, GSK-3 and CK-1α (Ip *et al*. 2012). This prevents entry of β-cat into the nucleus resulting in impaired expression of Wnt target genes (Ip *et al*. 2012). (B) As a result of Wnt signalling, the degradation complex associates with the Wnt receptor and Dishevelled (Dvl) (Ip *et al*. 2012). Protein kinase A (PKA) has been found to phosphorylate β-catenin at serine residue 675 which is linked to the expression of Wnt genes (Ichiro Hino *et al.*, 2005). It is possible that β-cat phosphorylation by PKA is initiated by signalling pathways controlled by hormones such as insulin, insulin-like growth factor-1 and GLP-1 (Jin, 2008). Figure from: IP, W., CHIANG, Y.-T. A. & JIN, T. 2012. The involvement of the Wnt signaling pathway and TCF7L2 in diabetes mellitus: The current understanding, dispute, and perspective. *Cell & Bioscience,* 2**,** 28.

1.5.3 Non canonical signalling

Non canonical signalling involves two different signalling pathways: the planar cell polarity pathway (pcp) and the Wnt/Ca2+ pathway (see figure 16) (Komiya and Habas, 2008). The pcp pathway is involved in cell cytoskeleton rearrangement and cell polarisation (Houschyar *et al.*, 2018). This pathway involves activation of Frizzled without the association low density lipoprotein receptor-related proteins 5 and 6 complex (Houschyar *et al.*, 2018). The activation of Dishevelled then activates two GTPases, Rho and Rac. Rho GTPase then activates Rho-asscoiated kinase and mysoin, this enables cytoskeleton rearrangement (Komiya and Habas, 2008). The Rac Gtpase activates the JNK pathway, which activates cytoskeletal changes necessary for cell polarisation (Komiya and Habas, 2008).

Select Wnt ligands can initiate Ca2+ release from the endoplasmic reticulum. Ca2+ activates calcium/calmodulin-dependent kinase (camK11), calcineurin and protein kinase Kinase C (Komiya and Habas, 2008). Wnt/ca2+ signalling controls embryogenesis by influencing dorsal axis formation, embryo ventral cell fate and tissue separation (Komiya and Habas, 2008).

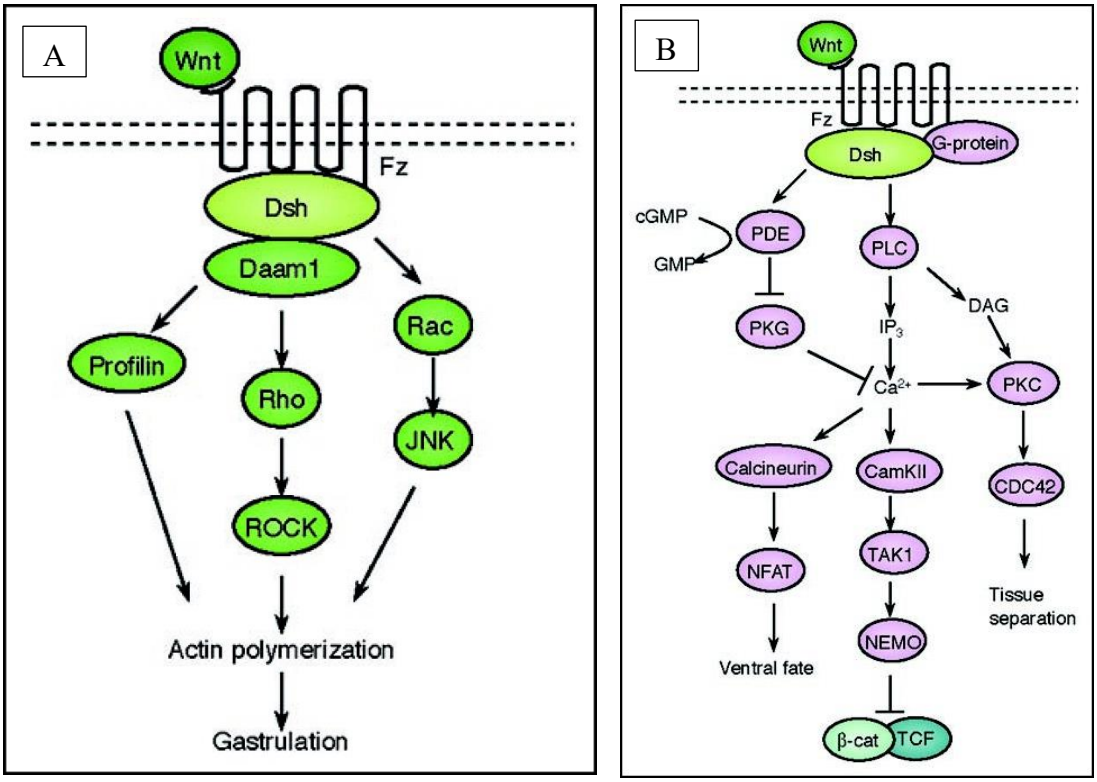

Figure 16- Non canonical Wnt signalling pathways. (A) the planar cell polarity (PCP) pathway is activated when Wnt ligands bind to the frizzled receptor without the co receptors, lipoprotein receptor-related proteins 5 and 6. PCP signalling activates two GTPases, Rho and Rac, and an actin binding protein named Profilin. These two GTPases then activate Rho associated kinase

(ROCK) and the JNK pathway, respectively. The action of ROCK, JNK signalling and profilin results in cytoskeletal changes influencing cell polarization and motility. (B) Wnt signalling can also intitiate Ca2+ release from intracellular calcium stores. Wnt/ca2+ signalling then activates Calcineurin, camK11 and PKC. These control ventral cell fate, dorsal axis formation via inhibiting beta catenin/TCF signalling and tissue sepearation, respectively. Figure from: Komiya, Y. and Habas, R. (2008) 'Wnt signal transduction pathways', *Organogenesis,* 4(2), pp. 68-75.

1.5.4 Overview of TCF7L2 function in different tissues and organs

Experiments have indicated TCF7L2 has important functions in organs and tissues involved in energy homeostasis (summarised in figure 16). Pancreas specific knockout of *Tcf7l2* has been linked to impaired glucose tolerance after oral glucose tolerance tests (Da Silva Xavier *et al*. 2012), controlling the incretin effect (Shu *et al*. 2008), Impaired incretin release (Da Silva Xavier *et al*. 2012), GSIS (Shu *et al*. 2008), controlling beta cell proliferation (Shu *et al*. 2008) and beta cell survival (Shu *et al*. 2008, Shahbazi *et al*., 2013) and regulating beta cell mass and proliferation (Shu *et al*. 2008). Interestingly, human carriers of the *Tcf7l2* rs7903146 SNP (heterozygous-C/T, homozygous-T/T) were found to be associated with a reduced insulin secretion during an early insulin response to an OGTT compared with controls (carriers of CC allele) (Lyssenko *et al*. 2007). A significant decrease in insulin secretion was found after measurement by disposition index and arginine stimulated insulin secretion between CT/TT carriers vs CC carriers (Lyssenko *et al*. 2007). A reduced Incretin effect was confirmed within this investigation as reduced insulin secretion was observed after OGTT within CT/TT carriers compared to CC carriers (Lyssenko *et al*.2007). Manipulation of *Tcf7l2* expression within the liver and liver cells in mouse and rat models have shown TCF7L2 acts to inhibit gluconeogenesis (Norton, *et al*. 2011; Ip *et al*. 2012; Oh *et al*. 2012; Ip *et al*. 2015).

Adipocyte specific knockout of *Tcf7l2* was found to result in an increase in adipocyte specific differentiation markers (Geoghegan *et al*. 2019). Adipocyte specific knockout of TCF7L2 in mice also resulted in impaired glucose tolerance when exposed to a HFD (Geoghegan *et al*. 2019). Insulin resistance was observed, during an Insulin tolerance test, when mice were exposed to a HFD vs normal chow diet (Geoghegan *et al*. 2019). Loss of *Tcf7l2* within adipose tissue also resulted in an increase in fat mass and adipocyte size (Geoghegan *et al*. 2019). This was paired with a downregulation of lipolytic genes and upregulation of genes controlling lipogenesis (Geoghegan *et al*. 2019). In another experiment, mice with heterozygous and homozygous adipocyte specific knockout of *Tcf7l2* were generated and the effect on adipose tissue investigated (Nguyen-Tu *et al*. 2021). Intraperitoneal glucose tolerance and OGTT revealed age associated impaired glucose control in heterozygous and homozygous adipocyte specific *Tcf7l2* knockout male mice, which was independent of insulin resistance (Nguyen-Tu *et al*. 2021). Islets from homozygous adipocyte specific *Tcf7l2* knockout mice displayed impaired GSIS compared to control islets (Nguyen-Tu *et al*. 2021). This suggests TCF7L2 is important in the crosstalk between adipose tissue and pancreatic islets during metabolism control. This could be explained by the decrease in circulating incretin levels, within homozygous and heterozygous adipocyte specific *Tcf7l2* knockout mice, after random feeding when compared with control mice (Nguyen-Tu *et al*. 2021).

Silencing of *Tcf7l2* within 3T3-L1 preadipocytes using viral administered short hairpin RNA showed inhibition of adipogenesis as well as reduced expression and translation of adipogenic transcription factors (Chen *et al*. 2018). Removal of Exon 11 from *Tcf7l2* within mature adipocytes (ΔE11-TCF7L2) led to impaired glucose tolerance along with hyperinsulinemia during an intraperitoneal glucose tolerance test within male and female mice (Chen *et al*. 2018). During an euglycemic hyper insulinemic clamp test, there was an increase in insulin stimulated endogenous glucose production (Chen *et al*. 2018). This indicates that *Tcf7l2* removal from adipose tissue may lead to hepatic insulin resistance (Chen *et al*. 2018). Further investigation involving placing ΔE11-TCF7L2 mice on a HFD revealed increased body weight, fasted hyperglycaemia, increased lipid deposition within the liver and increased inguinal white adipose tissue mass (Chen *et al*. 2018). Based on these studies, *Tcf7l2* activity within adipose tissue important in controlling body weight, glucose tolerance, adipocyte differentiation, crosstalk with the liver, the incretin effect, lipogenic activity, lipolysis and adipocyte size.

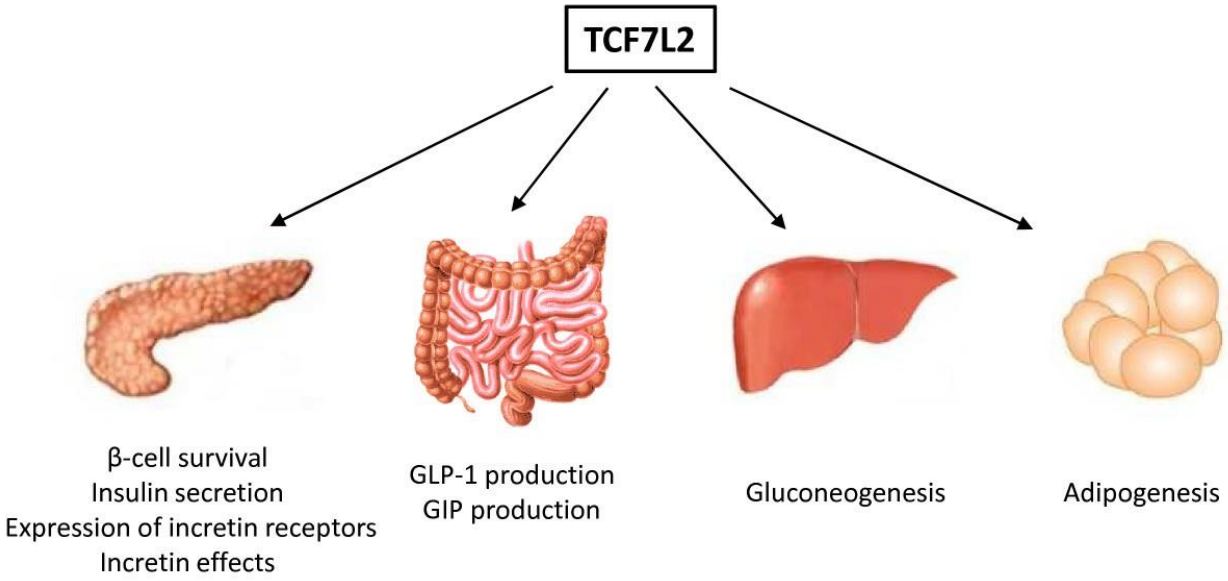

Figure 17- Summary of the action of TCF7L2 in different tissues. Evidence from knockout experiments suggests TCF7L2 has important roles in organs and tissues that are involved in metabolism control. In the pancreas tcf7l2 has been linked to controlling beta cell survival, maintaining beta cell mass, expressing incretin receptros and controlling the incretin effect. TCF7L2 appears to be involved with incretin (GLP-1 and GIP) production within the gastrointestinal tract. Manipulation of *Tcf7l2* expression within the liver and liver cells in mouse and rat models have shown TCF7L2 acts to inhibit gluconeogenesis. Finally, adipocyte specific knockout of *Tcf7l2* was found to result in an increase in adipocyte specific differentiation markers. This suggests TCF7L2 is involved in controlling adipogenesis. Figure from: Ip, W., Chiang, Y.-T.A. and Jin, T. (2012) The involvement of the Wnt signaling pathway and TCF7L2 in diabetes mellitus: The current understanding, dispute, and perspective. *Cell & Bioscience*, 2 (1): 28. doi:10.1186/2045-3701-2-28.

1.5.5 Wnt signalling and bone formation

Wnt signalling has been shown to control osteoblastogenesis and normal bone metabolism (Maeda *et al.*, 2019) (refer to figure 17). The first evidence of Wnt signalling being important came from human investigations. Mutations within genes encoding a Wnt coreceptor, lipoprotein receptor-related proteins 5 (LRP5), was found to be associated with osteoporosis (Gong *et al.*, 2001; Houschyar *et al.*, 2018). This was confirmed in mice, when LRP5 knockout mice displayed low bone mass (Kato *et al.*, 2002). In addition, gain of function mutations within revealed the opposite, whereby bone density increased in humans and mice (Babij *et al.*, 2003).

Mice were engineered to express Wnt10b within bone marrow under the control of the fatty acid binding protein 4 promoter (FABP5-Wnt10b mice) (Bennett *et al.*, 2005). Skeletal bone analysis revealed increased bone mass, increased bone strength and reduced loss of bone in relation to aging (Bennett *et al.*, 2005). Ovariectomy resulted in decreased bone volume/total volume, bone mineral density and trabecular number in wild type mice (Bennett *et al.*, 2005). Whereas ovariectomy bone of wild type mice FABP5-Wnt10b mice did not significantly affect bone volume/total volume, bone mineral density, or trabecular number (Bennett *et al.*, 2005). The group also identified that canonical Wnt signalling was able to stimulate osteoblastogenesis whilst inhibiting adipogenesis of bipotential bone marrow cells (Bennett *et al.*, 2005). Finally, knockout of Wnt10b within mice resulted in decreased bone volume/total volume and bone mineral density when compared with wild type mice (Bennett *et al.*, 2005). This investigation was important because Wnt10b was found to increase expression of osteoblast associate genes such as RUNX2, Dlx5 and OSX and inhinbt the expression of the adipogenic transcription factors, C/EPalpha and PPARγ (Bennett *et al.*, 2005). Other studies have also identified that Wnt10b positively regulates osteogenesis and bone mass (reviewed in Visweswaran *et al.*, 2015). Therefore, Wnt signalling Is important for upregulating differentiation of MSCs into osteoblasts and inhibiting of the MSC differentiation into adipocytes (Maeda *et al.*, 2019). As discussed earlier, the transmembrane protein WI is involved in Wnt ligand release (Regard *et al.*, 2012). Osteoblast specific knockout of Wl within mice resulted in severe decreases in trabecular mass, cortical mass and significantly lower bone formation rate (Regard *et al.*, 2012). Therefore, Wnt ligands seem to be important in osteoblast activity and bone mass maintenance

During bone development removal of β-catenin within osteoblast progenitor cells results in the development of chondrocytes (Regard *et al.*, 2012). Ectopic activation of canonical Wnt signalling has also been linked to inhibit MSCs differentiating into chondrocytes (Regard *et al.*, 2012).Wnt signalling upregulates MSCs differentaion, once MSCs have commited to the osteoblast lineage (Regard *et al.*, 2012). Wnt signalling can also limit the differentiation of early osteoblasts into mature osteoblasts (Regard *et al.*, 2012). Therefore, Wnt signalling is important in controlling MSC differentiation into osteoblasts (see figure 18).

The non canonical Wnt ligand, Wnt5a, has also been shown to activate osteoblast differentiation via controlling the canonical pathway (Maeda *et al.*, 2019). Osteoblast-specific Wnt5a knockout mice decreased bone formation (Maeda *et al.*, 2019). In addition, Wnt receptor expression and coreceptor complex (LRP5/LRP6) was lower within osteoblasts from

Wnt5a knockout mice (Maeda *et al.*, 2019). This was paired with reduced canonical Wnt signalling activation (Maeda *et al.*, 2019). In contrast, over expression of LRP5 within Osteoblast-specific Wnt5a cells resulted in normal canonical signalling and increased osteoblast differentiation (Maeda *et al.*, 2019). Wnt7b has also been shown to increase osteoblast differentiation. This is because transgenic introduction of Wnt7b into mice resulted in increased bone formation and increased bone mass (Maeda *et al.*, 2019).

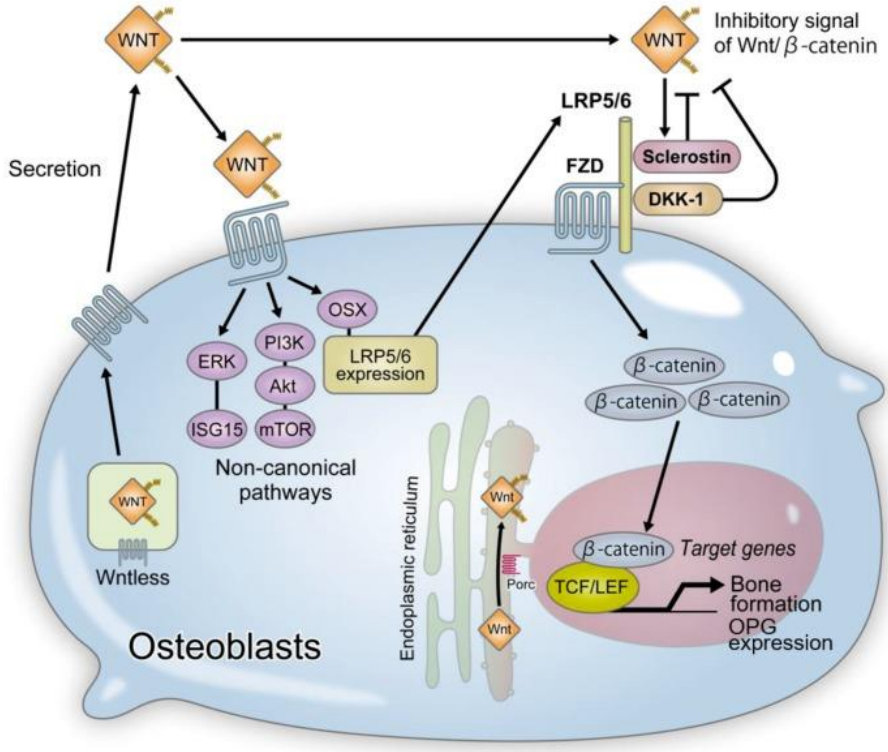

Figure 18-Wnt signalling and osteoblastogenesis. Wnt ligands are producerd and then undergo porcupine (Porc) mediated lipidation by palmitoleic acid. Wnt ligands are then secreted by cells and bind to the frizzled (FZD) receptor and stimulate canonical and non canonical Wnt signaling. When specific Wnt ligands bind to FZD or FZD/ Ror1/2 complexes, non canonical Wnt signalling is initiated. Whereas, when specific Wnt ligands bind to FZD/LRP5/6 complexes canonical Wnt sginalling is stimulated. Wnt5a has been found to initiate non canonical Wnt signalling expression of osterix (OSX). This leads to the expression of LRP5/6 complexes, which in turn promotes osteoblast differentiation. Wnt ligands that initiate canonical signaling induce osteoblastogenesis by increasing expression of osteoblast specific genes, including OPG. Wnt signalling can also be inhibited by the proteins sclerostin and Dickkopf 1 (DKK-1). Akt: Protein kinase B, ERK: Extracellular signal-related kinases, ISG15: Interferon stimulated gene 15 (Figure from: Maeda, K., Kobayashi, Y., Koide, M., et al. (2019) The Regulation of Bone Metabolism and Disorders by Wnt Signaling. *International Journal of Molecular Sciences*, 20 (22): 5525. doi:10.3390/ijms20225525.

1.5.6 Wnt signalling and bone resorption

Wnt signalling is also linked to the control of bone resorption (Refer to figure 19). This is because Canonical Wnt signalling has been linked to surpressing osteoclast differentiation (Maeda *et al.*, 2019. In one study, osteoclast precursor specific knockout of β-catenin resulted in increased osteoclast differentiation (Maeda *et al.*, 2019). Whereas, mice expressing a constitutive form of β-catenin displayed impaired osteoclast development (Kobayashi *et al.*, 2016). In addition, expression of OPG was found to be high within these mice (Kobayashi *et al.*, 2016).

As mentioned earlier, osteoclastogenesis is controlled by a RANKL/RANK/OPG regulatory axis (Roux and Orcel, 2000; Kim *et al.*, 2020) and evidence suggests Wnt signalling controls osteoclastogenesis via this regulatory axis. Loss of β-catenin has been linked to decreased OPG expression (Regard *et al.*, 2012). In addition, Osteoblast specific knockout of β-catenin resulted in increased RANKL expression (Regard *et al.*, 2012). However, Wnt5a has been reported to increase RANK expression within osteoclast precursors, thereby increasing RANKL induced osteoclast differentiation (Kobayashi *et al.*, 2016).The Wnt16 ligand was found to inhibit RANKL associated osteoclast formation within human and mouse osteoclast precursors. This could possibly be explained by a Wnt16 associated increase in the expression of OPG in an osteoblast cell line (Kobayashi *et al.*, 2016; Maeda *et al.*, 2019). In contrast, Co culturing Wnt16 deficient osteoblasts and osteoclasts with $1\alpha,25(OH)_2D_3$ resulted in increased osteoclast formation (Kobayashi *et al.*, 2016).

Another Wnt ligand, Wnt3a, was found to diminish osteoclast formation in wild type mice compared to OPG deficient mice (Kobayashi *et al.*, 2016). Wnt4a has been reported to increase osteoblast differentiation by activating non canonical Wnt signalling in mice (Kobayashi *et al.*, 2016). Overexpression of Wnt4 within mice, specifically within osteoblasts, was shown to increase bone mass and reduce the number of osteoclasts (Kobayashi *et al.*, 2016; Maeda *et al.*, 2019) It was identified that Wnt4 surpresses RANKL associated osteoclast precursor differentiation (Kobayashi *et al.*, 2016; Maeda *et al.*, 2019). This evidence from these investigations suggests Wnt signalling is important in controlling osteoclast differentiation.

1.6 Preliminary data

Previous work has revealed heterozygous and homozygous adipocyte specific KO of *Tcf7l2* within mice (labelled Adipo *Tcf7l2*-KO in figures 20 and 21) resulted in a tendency for lowered osteocalcin gene expression within the femur, and lower osteocalcin content within plasma, when compared with WT mice (Fig. 20; Nguyen-Tu, da Silva Xavier, unpublished). Adipocyte specific *Tcf7l2* KO mice also had abnormal trabecular network structure when compared with WT mice (Fig. 21; Nguyen-Tu, da Silva Xavier, unpublished). This suggests that loss of *Tcf7l2* gene expression in adipocytes leads to defects in bone function/metabolism, which is associated with lowered osteocalcin secretion, suggesting an impairment in the function of the osteoblasts. Lowered osteocalcin secretion can then impact on pancreatic beta cell function and energy homeostasis in this mouse model and partially account for the phenotype observed in mice lacking *Tcf7l2* in adipocytes (Nguyen-Tu *et al.*, 2021).

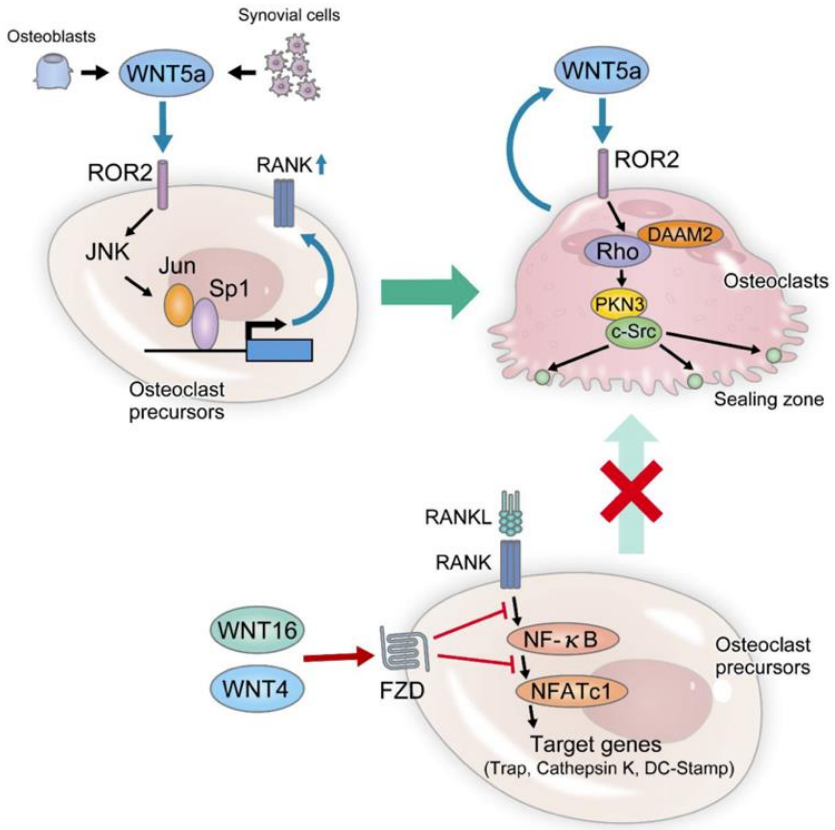

Figure 19- Role of Wnt signalling in osteoclast differentiation and function. Wnt5a has been found to initiate RANK within osteoclasts, thereby facilitating osteoclast differentiation. Wnt5a has also been seen to stimulate actin ring development within osteoclasts, which enables osteoclasts to begin bone resorption. Wnt4 and Wnt16 have been found to inhibit RANKL/RANK associated signaling, thereby inhibiting expression of genes responsible for osteoclast differentiation. DAAM2: dishevelled associated activator of morphogenesis, c-src: Proto-oncogene tyrosine-protein kinase Src,NF-ΚB: Nuclear factor kappa B, NFATc1- Nuclear factor of activated Tcells 1, JNK: Jun N-terminal kinase, Sp1: Simian virus 40 promoter factor 1 , PKN3: protein kinase N3, ROR2: receptor tyrosine kinase-like orphan receptor 2. (figure from Maeda, K., Kobayashi, Y., Koide, M., et al. (2019) The Regulation of Bone Metabolism and Disorders by Wnt Signaling. *International Journal of Molecular Sciences*, 20 (22): 5525. doi:10.3390/ijms20225525.)

Summary

It is clear T2D is a worldwide problem, as cases of T2D are predicted to increase (Olokoba, Obateru and Olokoba, 2012; Trikkalinou *et al*. 2017). As discussed earlier, ongoing T2D results in impaired control of whole body metabolism and serious complications. T2D has also been linked to increased risk of fractures, increased bone porosity (Pritchard *et al*. 2012; Pritchard *et*

al. 2013; Patsch *et al*. 2013; Picke *et al*. 2019), decreased bone strength (Howard *et al*. 1996; P. Garnero *et al* 2006; Poundarik *et al*. 2015; Picke *et al*. 2019), reduced osteoblasts numbers (Mizokami *et al*. 2013; Picke *et al*. 2019), increased osteoblast apoptosis (Picke *et al*. 2019) and mesenchymal stem cells (MSC) committing to adipocyte lineage rather than osteoblast lineage (Picke *et al*. 2019). T2D is a polygenic disorder and the gene *Tcf7l2* was found to have the highest odds ratio within an Icelandic cohort. Since then, *Tcf7l2* has been shown to have the highest association with T2D in cohorts around the world (Humphries, *et al*. 2006; Grant, *et al*. 2006; Sladek *et al*. 2007; Herder, *et al*., 2008; Sanghera, *et al*. 2008; Cho, *et al*. 2009; Cauchi, 2012; Long, *et al*. 2012; Mahajan, *et al*. 2018). This thesis will aim to address is whether there is a link between TCF7L2 and the increased bone fracture risk seen in T2D patients.

1.7 Aims and hypothesis.

Based on our preliminary data, I hypothesize that adipose tissue specific knockout of *Tcf7l2* (ATCF7L2-KO) within mice will result in altered osteoblast function, which may be due to functional impairment and/or loss of osteoblast cell mass. This may impact negatively impact osteoclast cell mass and number, as osteoblasts and osteoclast cell mass are regulated in tandem (see section 1.3.1 and 1.3.2). Thus, I will measure osteoblast and osteoclast cell mass in paraffin embedded sections of fixed femurs from ATCF7L2-KO mice (femurs from the mice used within the investigation conducted by (Nguyen-Tu *et al.*, 2021). Which have been maintained on a normal chow diet or high fat diet to assess the impact adipocyte-specific loss of *Tcf7l2* expression on bone cell mass, and any potential effects of high fat diet.

I further hypothesise that homozygous carriers of the *TCF7L2* risk allele will have impaired osteoblast function. Thus, I will measure human osteoblast function from genotyped osteoblasts to establish if there is any association between TCF7L2 SNP rs7903146 (the type 2 diabetes risk variant) and osteoblast function from osteoblasts isolated from patients undergoing hip replacement surgery.

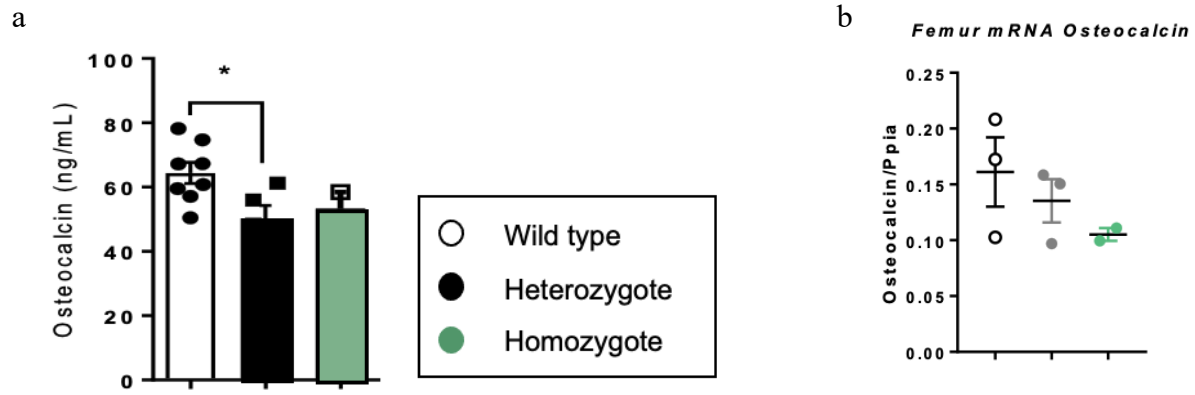

Figure 20- Adipocyte knockout of TCF7L2 results in reduced plasma osteocalcin levels (a) and reduced Osteocalcin expression(b). (a) Preliminary data indicates that heterozygous and homozygous knockout of *Tcf7l2* within adipose tissue within C57BL/6J mice results in a decrease in osteocalcin secretion. A significant difference was observed when comparing the concentration of osteocalcin within the plasma of heterozygous knockout (black bar) mice compared to wild type mice (white bar). (b) Mice with homozygous (green) and heterozygous (grey) adipose tissue specific knock out of TCF7L2 tended to have reduced osteocalcin (Nguyen-Tu, Da Silva Xavier, unpublished).

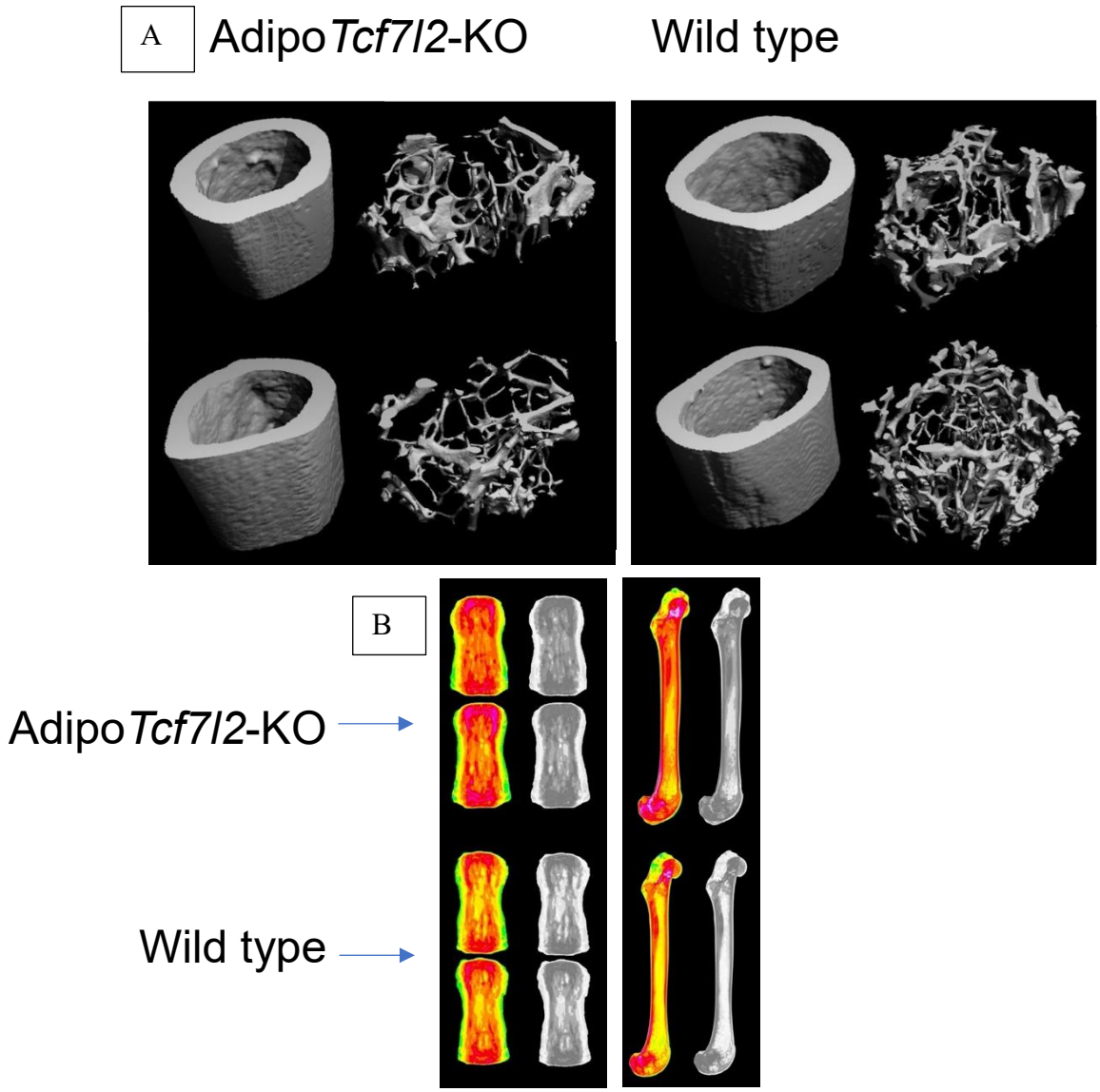

Figure 21- Adipocyte-specific knockout of *Tcf7l2* (labelled Adipo *Tcf7l2*-KO) led to an abnormal trabecular network (A) and increased bone mineralization compared to wild type mice (B). (Nguyen-Tu, Da Silva Xavier, unpublished).

Chapter 2
Methods

2. Methods

2.1.1 Mouse models

Mouse hind limbs used in this study were taken from adipocyte-specific TCF7L2 knockout mice which were sacrificed at the end of the procedures described in the published research paper by Nguyen-Tu and colleagues (Nguyen-Tu et al. 2021). To achieve tissue-selective ablation of *Tcf7l2* alleles, the researchers crossed mice in which exon 1 of *Tcf7l2* was flanked by *LoxP* sites (Da Silva Xavier, et al. 2012) with mice expressing *Cre* recombinase under the control of the *Adipoq* promoter (Eguchi, J., Wang, X., Yu, S., et al. 2011) produce deletion of a single (ATCF7L2-KO(hom)) or two *Tcf7l2* alleles (ATCF7L2-KO(het)). Animals were housed in a pathogen-free facility with 12 h light–dark cycle with free access to a standard mouse chow (RM-1; Special Diet Services, UK) diet and water. High-fat diet (HFD) cohorts were placed on a high-sucrose, high-fat diet (D12331; Research Diets, New Brunswick, NJ, USA) for 12 weeks from 7 weeks of age. Mice were also fed a NC diet for 12 weeks.

2.1.2 Bone section preparation.

Mouse hind limbs were removed from ATCF7L2-KO(het), ATCF7L2-KO(hom) and WT mice that were used in the experiment by Nguyen-Tu and colleagues (Nguyen-Tu et al. 2021). Mouse hind limbs from ATCF7L2-KO(het), ATCF7L2-KO(hom) and WT mice were stored in absolute ethanol. Hind limbs were then removed from the ethanol and the excess fat and muscle was removed using surgical equipment to expose the bone. The bone was then decalcified in 0.196g/ml of EDTA solution (pH8.0) for 4 days and then prepared for paraffin embedding using the following protocol:

Step 1- 50% ethanol for 2 days
Step 2- 70% ethanol for 2 days
Step 3- 95% ethanol (95% ethanol/5% methanol) for 2 days
Step 4- First absolute ethanol for 2 days
Step 5- Second absolute ethanol for 2 days
Step 6- First clearing agent (National Diagnostics Histo-clear) for 2 days
Step 7- Second First clearing agent (National Diagnostics Histo-clear) for 2 days
Step 8- First wax (Paraplast X-tra) at 58°C for 2 hours.
Step9- Second wax (Paraplast X-tra) at 58°C 2 hours.

Bone samples were then embedded using a Leica EG1150 H tissue embedder (catalogue number EG1150 H supplied by Leica Microsystems, Milton Keynes, UK) and tissue slices were cut using a Leica RM2125 RTS microtome (Catalogue number RM2125 supplied by Leica Microsystems, Milton Keynes, UK). Briefly, blocks to be sectioned were placed face down on an ice block for 10 minutes. A fresh blade was placed on the microtome; blades were replaced after approximately every 10 blocks or when sectioning became problematic. The block was inserted into the microtome, so the wax block faced the blade and was aligned in the vertical plane. The microtome was set to cut 10 µM sections in order to plane the block; then 5 µM longitudinal sections were taken, with the sectioning blade angled at 5°. Paraffin sections were placed on Super frost plus glass slides (supplied by Fischer scientific, Product code 10149870)

and incubated at 65°C in a Hybaid Hybridization oven (Hybaid, Basingstoke, U.K.) for 2-5minutes until the wax just started to melt. The slides were then stored overnight at room temperature.

2.1.3 Hematoxylin and Eosin staining

To remove wax from slides before staining, slides were placed into National Diagnostics Histo-clear (supplied by scientific laboratory supplies, Nottingham, England) for 20 minutes. Then slides were rehydrated in 100%,95% and 70% ethanol sequentially for 5 minutes at each ethanol concentration. The slides were washed with distilled water for 1 minute to remove any excess ethanol, and then stained using a Hematoxylin and Eosin staining kit (Vector Laboratories, catalogue number H-3502, supplied by 2bscientific, Bicester, England), according to manufacturer's instructions. Vectashield antifade mounting media (Vector Laboratories, Catalogue number H-1000-10, supplied by 2bscientific, Bicester, England) was used to mount coverslips to the sections and slides were left to dry before imaging.

2.1.4 Brightfield microscopy

Images were acquired using the Olympus BX53 Upright Microscope (supplied by Olympus, catalogue number BX53, Stanstead, England) with an Olympus sc50 camera (supplied by Olympus, catalogue number unavailable since product has been discontinued, Stanstead, England) at 20x magnification. The Images were taken using the manufacturer's software Cellsens (supplied by Olympus, Stanstead, England). For non-sampling, data was collected from all the bone images for each slide. Whereas for the sampling set a random number generator was used to randomly select 10 images to collect data.

2.1.5 Bone image data analysis

Images were analysed using ImageJ (as described in Schneider, Rasband and Eliceiri, 2012) measurements of osteoblast area, osteoclast area and total bone area were recorded. Measurements were originally taken in pixels^2, however the measurements were converted to μm^2 within ImageJ. The cell area data and bone area measurements collected from the images were used to calculate average osteoblast area, average osteoclast area, total osteoblast area, total osteoclast area, total osteoblast number, total osteoclast number, total osteoblast area/total bone area, total osteoclast area/total bone area, total osteoblast number/total bone area and total osteoclast number/total bone area using excel.

2.1.6 Statistical analysis of mosue data

SPPSS was used for statistical analysis and data for mice. The data values of ATCF7L2-KO(hom), ATCF7L2-KO(het) and WT mice, within the same sampling group, were compared with each other using a one way ANOVA with Tukey's multiple comparison post hoc test. The means values corresponding to each mouse genotype compared to each other depending on which sampling group were compared for results for each of the mice were compared with each sampling group were compared with A p value of <0.05 was considered statistically significant.

2.1.7 Culture of human osteoblasts

Osteoblasts were kindly provided by Dr. Morten Hansen and Dr. Morten Frost, our collaborators in Denmark Morten S. Hansen (1-Molecular Endocrinology Laboratory (KMEB), Department of Endocrinology, Odense
University Hospital, Odense, Denmark; 2- Clinical Institute, Faculty of Health Sciences, University of Southern Denmark, Odense, Denmark) and Morten Frost (1- Molecular Endocrinology Laboratory (KMEB), Department of Endocrinology, Odense
University Hospital, Odense, Denmark; 2- Clinical Institute, Faculty of Health Sciences, University of Southern Denmark, Odense, Denmark; 3- Department of Orthopedics, Odense University Hospital, Odense, Denmark). Briefly, primary human osteoblast cells were obtained from bone specimens from patients receiving hip replacement surgery due to osteoarthritis (as described in Pirapaharan *et al*. 2019) under ethics number S-2011-0114. The bone from these patients was cut into small pieces (~5 mm in diameter) and cleaned in PBS. Five bone pieces were placed in each well of a 12-well plate containing Dulbecco's modified Eagle medium (DMEM, Gibco), 10% FBS (Sigma), 2mM L-glutamine (Gibco), 50 µg/mL ascorbic acid (Sigma), 10 mM β-glycerophosphate (Sigma) and 10^{-8} M dexamethasone (Sigma). To prevent the bone pieces from moving, a metal grid was placed on top of the bone slices, and samples incubated for fourteen days, with a single media change at day seven. On day fourteen, metal grids were removed, cells expanded to larger flasks, with media changes twice weekly, until the osteoblast lineage cells reached near confluency after a total of ~35 days. Osteoblasts cultures were then shipped to the University of Birmingham

Once osteoblasts cultures had been received cells were cultured in osteoblast media at 37^{o}C and 5% CO_2 for two days using a CO_2 incubator (supplied by PHC, catalogue number MCO-170AICD-PE, Loughborough, England). Supernatant was removed and stored at -80^{o}C. Osteoblasts were washed 3x with 10 ml of PBS and the cell pellet was collected by centrifugation at 8000xg (centrifuge manufacturer) for 1 minute to collect the cell pellet. The supernatant was discarded and the cell pellet was used for DNA, RNA and protein isolation with the AllPrep DNA/RNA/Protein Mini Kit (supplied by Qiagen, catalogue number 80004, Manchester, England) as per the manufacturer's protocol. RNA and protein samples were kept frozen at -70^{o}C, before being used for genotyping and ELISA experiments. Whereas, DNA samples were collected and stored at -21^{o}C.

2.1.8 Genotyping of human osteoblasts

The SNP genotyping experiments for the rs7903146 SNP was carried out using a TaqMan™ SNP Genotyping Assay (supplied by Thermofisher Scientific, catalogue number 4351374, Loughborough, England). The SNP genotyping was performed on 10 ng of genomic DNA as per manufacturers protocol, two technical replicates were to identify the genotype of the participants for genotyping experiments. On ThermosFisher cloud the Gneotyping_Pre_PCR_Post system template was used and standard run protocols were used for the investigation. Genotyping reactions were run using ThermoFisher's QuantStudio 5 qPCR machine (supplied by ThermoFisher, catalogue number A34322, Loughborough, England).

2.1.9 Primers for real-time PCR using SYBR green

PCR primers for *OST* and *GAPDH* generated using the Primer 3 software were selected based on the primer sequences that satisfied the most of the following criteria:
1. 18 nucleotide long
2. c. 50% GC content
3. No significant GC stretches
4. Aim for 3' end of transcripts
5. Avoid sequence complementarity to avoid hairpins
6. Ensure 3´ end contain no more than two G and/or C
bases.
7. T_m of primers aim between 58-60 C, for all target genes with Tm within 1 C of each other.

The following custom primers were selected for the RNA real time PCR reactions and ordered from Invitrogen by Thermo Fisher scientific:

OST forward Primer sequence- CTC ACA CTC CTC GCC CTA T

OST Reverse Primer sequence- TCT CTT CAC TAC CTC GCT GC

GAPDH Forward primer sequence- TTC ACC ACC ATG GAG AAG GC

GAPDH Reverse primer sequence- TGA TGG CAT GGA CTG TGG TCG TC

Table 4- **Concentration of forward and reverse primer combinations that were used to find the ideal primer concentrations for the RNA PCR reaction**. We performed optimization reactions as per the protocol detailed for the applied biosystems SYBR green RNA to CT 1 step kit using the following primer combinations:

	Reverse primer concentration in nm	
Forward concentration in nm		100
	100	100/100
	200	200/100
	450	450/100

The forward and reverse primer concentration of 100nm/100nm combination was found to have the lowest CT values, This combination of primers was used in subsequent investigations. RNA was extracted using the AllPrep DNA/RNA/Protein Mini Kit (supplied by Qiagen,catalogue number 80004,Manchester, England), RNA concentration was determined using a ND-1000 Nanodrop Spectrophotometer (supplied by ThermofisherScientific/NanoDrop Technologies, discontinued, Product code ND-1000, sold by Marshall Scientific, Hampton,USA). The volume of RNA used in the experiments was dependent on the concentration of the RNA. 10ng of RNA were used for the RNA PCR reactions. Therefore, the volume of RNA solution required was calculated by using the concentration reading from the ND-1000 Nanodrop Spectrophotometer. Real time PCR reactions were carried out using the Applied Biosystems Power SYBR green RNA-to-C_T 1 step kit (supplied by ThermoFisher Scientific, catalogue number 4391178,

Loughborough, England) and SYBR Green PCR Master Mix (supplied by Thermofisher Scientific catalogue number 4309155, Loughborough, England) as per the manufacturer's instructions. (supplied by Qiagen, catalogue number 80004, Manchester, England).The volumes of RNA used in the investigations depended on the concentration of the solutions. A nanoa The PCR reactions were run using a ThermoFisher's QuantStudio 5 qPCR machine (supplied by ThermoFisher, catalogue number A34322, Loughborough, England) using the standard Comparative-Ct-SYBR protocol. No statisitiscal analysis was conducted for RNA PCR data due to our investigation being underpowered.

2.1.10 Measurement Of Human OST from Osteoblast Cell Cultures

OST content within the supernatant samples and protein samples from the osteoblast cell cultures, collected using the AllPrep DNA/RNA/Protein Mini Kit (see section 2.1.7), were measured using the Invitrogen Human OST ELISA kit (supplied by ThermoFisher Scientific. Catalogue number KAQ1381, Loughborough, England) and Biolegend LEGEND MAX Human Uncarboxylated Osteocalcin ELISA kit (supplied by Biolegend, catalogue number 446707, London,England) as per manufacturer's instructions. The supernatant and protein samples collected were stored in a freezer prior to the assay. Absorbance values were read at 450nm using the SpectraMax ABS microplate reader (supplied by Molecular devices part number ABS, Wokingham, England) and the computer software SoftMax Pro 7.1 (supplied by molecular devices, product name SoftMax Pro Standard Software, Wokingham,England). No statisitiscal analysis was conducted due to our investigation being underpowered.

Chapter 3
Results

3.1 Bone image analysis.

Bone image analysis allowed for the calculation of average osteoblast area, average osteoclast area, total number of osteoblasts, total number of osteoclasts, bone area analysed, and hence osteoblast area/total bone area, osteoclast area/total bone area, osteblast number/ total bone area, and osteoclast number/total bone area, which are all common methods used in the literature to provide quantitative assessment of osteoblast and osteoclast populations. As adipocyte-specific knock out of *Tcf7l2* gene expression led to increased plasma osteocalcin content (see figure 21), we hypothesised that bone function may have been affected, e.g. through changes in osteoblast and osteoclast number and morphology. The measurements collected using bone slices from adipocyte-specfic *Tcf7l2* knockout mice were used to assess whether loss of *Tcf7l2* expression in the adipocytes leads to changes in osteoblast and osteoclast populations, and whether alterations in diet had additional impact. As part of the analysis, we also assessed how sampling and the various ways of quantitative assessments of bone cell composition which are commonly used in the literature in this research area could influence how we interpret the data.

We used two methods- with or without sampling- to collect cell area measurements (**as described in methods 2.1.4 Brightfield microscopy)**. The average cell area measurements from all of the mice collected with or without sampling, were then compared to obtain information on whether sampling had an impact on the data and, if not, whether diet and/or genotype had an impact on cell size. The results are shown in figures 10-14/tables 5-13.

3.1.1 Average bone cell area analysis.

Average osteoblast area (Mean of the **Total osteoblast area/ total number of osteoclasts (μm^2/cells) values for each genotype group)** was found to be significantly greater for ATCF7L2-KO(hom) mice compared to ATCF7L2-KO(het) mice (P=0.006) within the NC sampling set (see Table 5 and Figure 22a). Although a significant difference was not observed between the different mice within the NC sampling group and HFD sampling groups, average osteoblast area was also found to be greater for ATCF7L2-KO(hom) mice comapred to ATCF7L2-KO(het) mice and WT mice. This may be due to the noise inherent in the data collected as a result of sampling random bone slice images (please see section 3.1.7 on Power Calculations performed based on the data collected in this project).

Interestingly, average osteoblast area values were the lowest within the HFD sampling group regardless of genotype. It is also important to note that average osteoblast area values were similar for ATCF7L2-KO(het) and WT mice in all sampling groups. This may explain why no significant difference was observed when the average osteoblast area values of the two groups were compared.

Table 6 and figure 22b shows average osteoclast areas **(Mean of the Total osteoblast area/ total number of osteoclasts (μm^2/cells) values for each genotype group)** for each of the mouse sampling groups. Although a significant difference was not observed between the different

mice in each of the any of the sampling groups there are some tendencies for differnces worth mentioning. WT mice within the NC non sampling set had a larger average osteoclast area comapred to ATCF7L2-KO mice. In the NC non sampling group, the average osteoclast area was greater for ATCF7L2-KO(hom) and WT mice compared to ATCF7L2-KO(het) mice. In the HFD sampling group average osteoclast area for ATCF7L2-KO(hom) mice was slightly greater compared to ATCF7L2-KO(het) and WT. These results were not found to be statistically significant and this is possibly due to noise inherent in data collected using the different sampling methods (please see section 3.1.7 regarding G power calculations).

It is important to note that, regardless of genotype, the average osteoclast area values were lower within the NC sampling group and the HFD sampling group compared to the NC non sampling group. This suggests that sampling may have a greater effect on average osteoclast area values as opposed to average osteoblast values. After this, the average total osteoblast area and average total osteoclast area across the bone slices were compared to determine how a HFD and adipocyte specific knockout Of *Tcf7l2* influenced the total area of cells across the bone slices.

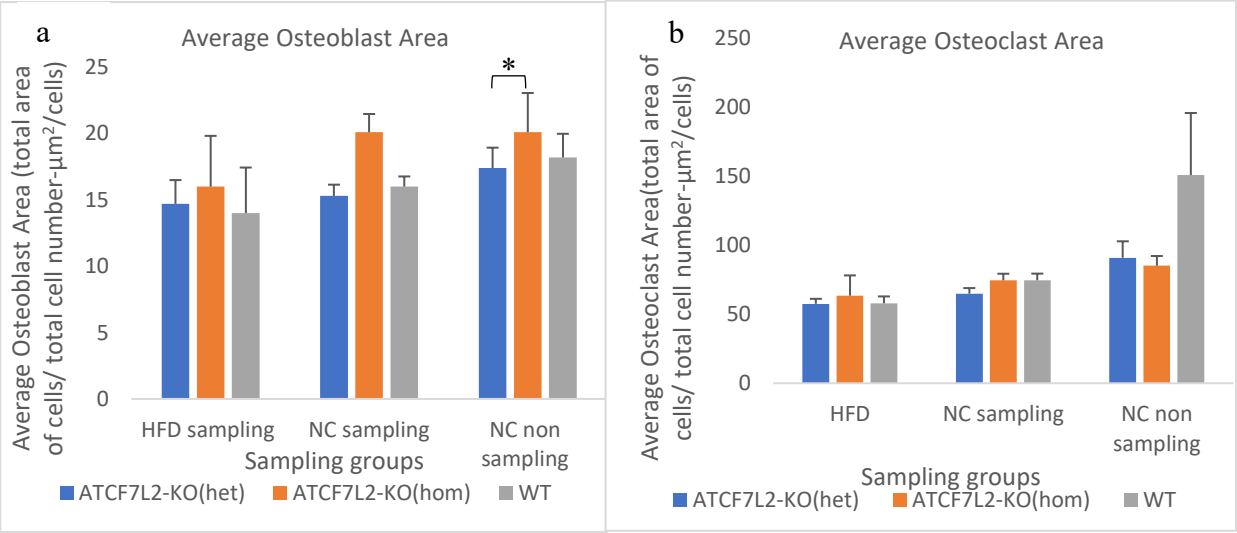

Figure 22- Figure 22- **Assessment of the effect of mouse genotype, diet and sampling on average osteoblast area and average osteoclast area. Average osteoblast (a) and osteoclast (b) area from adipocyte-specific *Tcf7l2* knockout mice and littermate controls**. Error bars shown are SEM. Calculation of average osteoblast area was performed using Excel. Statistical analysis was performed on SPSS using a one-way ANOVA where results yielding a p-value of $p<0.05$ were statistically significant. *, $p<0.05$. HFD, high fat diet; NC, normal chow; ATCF7L2-KO, adipose tissue specific knockout of Tcf7l2 gene; het, heterozygote; hom, homozygote; WT, wild-type littermate control; sampling, sampled images were analysed; non-sampling, all images were analysed. For each mouse 2 technical replicates were used. Number of mice used: NC non sampling: ATCF7L2-KO(het)-5 ,ATCF7L2-KO(hom)- 4 WT- 7. NC sampling: ATCF7L2-KO(het)-9 ATCF7L2-KO(hom)-6 WT-9 HFD sampling: ATCF7L2-KO(het)-3 , ATCF7L2-KO(hom)-3 , WT-2.

Table 5- Assessment of the effect of mouse genotype, diet and sampling on average osteoblast area. Numerical data for Figure 22a. *, p<0.05. HFD, high fat diet; NC, normal chow; ATCF7L2-KO, adipose tissue specific knockout of Tcf7l2 gene; het, heterozygote; hom, homozygote; WT, wild-type littermate control; sampling, sampled images were analysed; non-sampling, all images were analysed.

	Average osteoblast area (μm^2/cells) (3sf) ± standard error (3sf)/ standard deviation for HFD sampling WT (3sf)		
	Sampling group		
Genotype	HFD sampling	NC sampling	NC non sampling
ATCF7L2-KO(het)	14.7 (±1.80)	15.3 (± 0.849)	17.4 (±1.54)
ATCF7L2-KO(hom)	16.0 (± 3.83)	20.1 (± 1.38)	20.1 (±2.96)
WT	14.0 (± 3.44) (std dev)	16.0 (± 0.735)	18.2 (±1.78)

Table 6- Assessment of the effect of mouse genotype, diet and sampling on average osteoclast area. Numerical data for Figure 22b. HFD, high fat diet; NC, normal chow; ATCF7L2-KO, adipose tissue specific knockout of Tcf7l2 gene; het, heterozygote; hom, homozygote; WT, wild-type littermate control; sampling, sampled images were analysed; non-sampling, all images were analysed.

	Average Osteoclast area (μm^2/cells) (3sf) ± standard error (3sf)/ standard deviation for HFD sampling WT (3sf)		
	Sampling group		
Genotype	HFD sampling	NC sampling	NC non sampling
ATCF7L2-KO(het)	57.6 (± 3.65)	65.0 (± 4.04)	91.00 (± 11.9)
ATCF7L2-KO(hom)	63.5 (± 14.7)	74.7 (± 4.74)	85.30(±7.00)
WT	58.0 (± 4.99)	74.7(± 4.82)	151.00 (± 45.0)

3.1.2 Mean Total bone cell area analysis

Figure 23a and table 7 show the average total osteoblast area data for each of the sampling groups **(Total osteoblast area of all bone slices/number of bone slices (μm^2)).** Although a significant difference was not observed between the different mice, In the NC sampling group, the average total osteoblast area was greater for ATCF7L2-KO(hom) mice as opposed to ATCF7L2-KO(het) and WT mice. In addition, within the NC sampling group the average total osteoblast area was found to be greater slightly greater for WT mice compared to ATCF7L2-KO mice.). No statistically significant difference was identified between mice within the HFD sampling group. Average total osteoblast area the greatest for ATCF7L2-KO(het) mice, followed by WT mice and was the lowest for ATCF7L2(hom) mice. The fact that no statistically significant difference was identified when comparing the different mice may be due to the noise inherent

in the data collected (please see section 3.1.7 on Power Calculations performed based on the data collected in this project)

The average total osteoblast area values for mice within the NC sampling and NC non sampling group were greater than the average total osteoblast area values for mice within the HFD sampling group, regardless of genotype. Interestingly, the average total osteoblast area values for mice within the NC non sampling group were greater than that of the NC sampling group, regardless of genotype. This implies that sampling did affect the average total osteoblast area calculated for mice within the NC sampling group.

Figure 23b and table 8 show that average total osteoclast area data for the mice in each of the sampling groups. Although a significant difference was not observed between the different mice in the NC non sampling group, average total osteoclast area was greater for WT mice compared to ATCF7L2-KO(het) and ATCF7L2-KO(hom) mice. The average total osteoclast area was found to be the lowest within ATCF7L2-KO(hom) mice within the NC non sampling group. A statistically significant difference was also not found between the different mice in the NC sampling group. However, the average total osteoclast area was the highest within ATCF7L2-KO(hom) mice as opposed to ATCF7L2(het) and WT mice. The average total osteoclast area values were very low in the HFD sampling group across all genotypes. The fact that no significant difference was identified when comparing the different mice may be due to the noise inherent in the data collected (please see section 3.1.7 on Power Calculations performed based on the data collected in this project)

It is also important to note that the average total osteoclast area values within the NC sampling set are much lower than those within the NC non sampling set and the HFD sampling set, regardless of genotype. Therefore, sampling had an effect on the average total osteoclast area calculated. Next, we calculated the average total number of osteoblasts and osteoclasts in order to determine the influence of a HFD and mouse genotype on bone cell number.

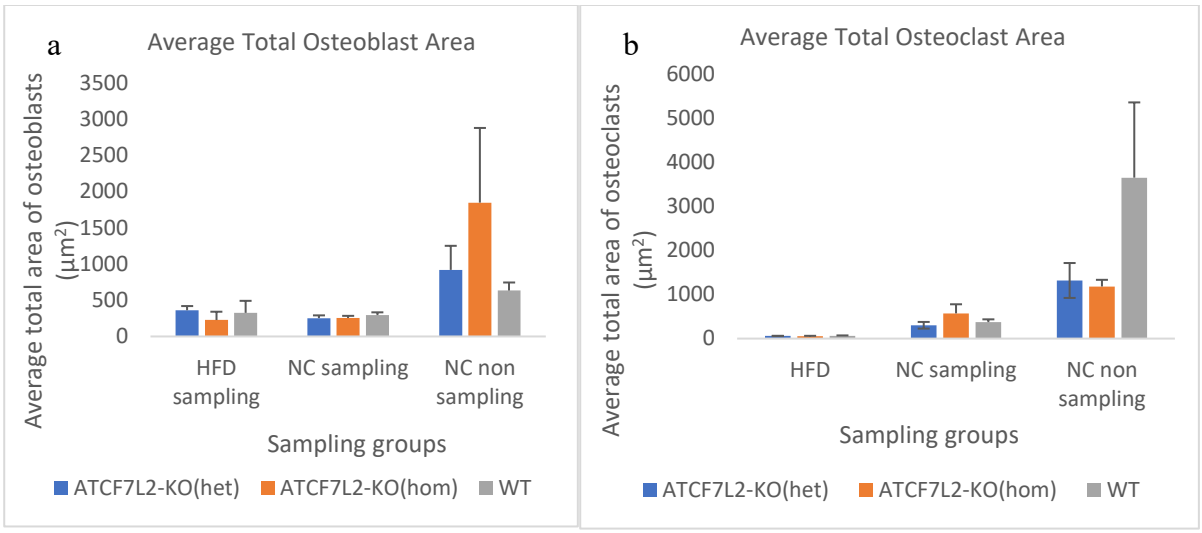

Figure 23- Figure 23- **Assessment of the effect of mouse genotype, diet and sampling on average total osteoblast areas (a) and average total osteoclast areas (b)**.
Error bars shown are SEM. Calculation of average osteoblast area was performed using Excel. Statistical analysis was performed on SPSS using a one-way ANOVA where results yielding a p-value of $p<0.05$ were statistically significant. HFD, high fat diet; NC, normal chow; ATCF7L2-KO, adipose tissue specific knockout of Tcf7l2 gene; het, heterozygote; hom, homozygote; WT, wild-type littermate control; sampling, sampled images were analysed; non-sampling, all images were analysed. For each mouse 2 technical replicates were used. Number of mice used: NC non sampling: ATCF7L2-KO(het)-5 ,ATCF7L2-KO(hom)- 4 WT- 7. NC sampling: ATCF7L2-KO(het)-9 ATCF7L2-KO(hom)-6 WT-9 HFD sampling: ATCF7L2-KO(het)-3 , ATCF7L2-KO(hom)-3 , WT-2.

Table 7- **Assessment of the effect of mouse genotype, diet and sampling on mean total osteoblast area.** Numerical data for Figure 23a. HFD, high fat diet; NC, normal chow; ATCF7L2-KO, adipose tissue specific knockout of Tcf7l2 gene; het, heterozygote; hom, homozygote; WT, wild-type littermate control; sampling, sampled images were analysed; non-sampling, all images were analysed.

	Mean of Total Osteoblast area (μm^2) (3sf) ± standard error (3sf)/ standard deviation for HFD sampling WT (3sf)		
	Sampling group		
Genotype	HFD sampling	NC sampling	NC non sampling
ATCF7L2-KO(het)	362.00 (± 57.8)	253.00(± 38.4)	919.00 (± 332)
ATCF7L2-KO(hom)	227.00 (± 115)	255.00(± 29.7)	1847.00 (±1031)
WT	326.00 (± 166.00)	295.00 (± 38.1)	634.00 (± 111)

Table 8- **Assessment of the effect of mouse genotype, diet and sampling on mean of total osteoclast area.** Numerical data for Figure 23b. HFD, high fat diet; NC, normal chow; ATCF7L2-KO, adipose tissue specific knockout of Tcf7l2 gene; het, heterozygote; hom, homozygote; WT, wild-type littermate control; sampling, sampled images were analysed; non-sampling, all images were analysed.

	Mean of Total Osteoclast area (μm^2) (3sf) ± standard error (3sf)/ standard deviation for HFD sampling WT (3sf)		
	Sampling group		
Genotype	HFD sampling	NC sampling	NC non sampling
ATCF7L2-KO(het)	59.5 (± 4.61)	303.00 (± 75.8)	1321.00 (±397)
ATCF7L2-KO(hom)	55.5 (± 7.52)	573.00 (± 207)	1184.00 (±152)
WT	60.3 (± 12.2) (check)	357.00 (± 62.8)	3657.00 (±1710)

3.1.3 Average total cell number analysis

Figure 24a and table 9 show the data for the average number of osteoblasts for the mice in each of the sampling groups (**Mean of the total number of osteoblasts on all bone slices**). Although a statistically significant difference was not observed between the different mice in the NC non sampling group, ATCF7L2-KO(hom) mice had highest average number of osteoblasts, followed by ATCF7L2-KO(het) mice. WT mice had the lowest average number of osteoblasts within the NC non sampling group.

On the other hand, NC sampling group yielded different results. Although a significant difference was not observed between the different mice in the NC sampling group, WT mice had the largest average number of osteoblasts followed by ATCF7L2-KO(het). ATCF7L2-KO(hom) mice had the lowest average number of osteoblasts within the NC sampling group. However, the average number of osteoblasts for WT mice was only slightly larger than that of ATCF7L2-

KO(hom) and ATCF7L2-KO(het) mice. This may explain why no significant difference was found between the mice within this group. Although a statistically significant difference was not observed between the different mice in the HFD sampling group, the average number of osteoblasts was the greatest within ATCF7L2-KO(hom) mice followed by WT mice. In the HFD sampling group, ATCF7L2-KO(hom) mice had the lowest average number of osteoblasts. The lack of a significant difference being detected by One way ANOVA analysis may be due to the noise inherent in the data collected (please see section 3.1.7 on Power Calculations performed based on the data collected in this project). It is important to note the average number of osteoblasts were much lower within the NC sampling group compared to the NC non sampling group and HFD sampling group, regardless of genotype. Therefore, sampling affected the average number of osteoblasts.

Figure 24b and table 9 shows the average number of osteoclasts for the mice in each of the sampling groups (**Mean of the total number of osteoclasts on all bone slices)**. Although a statistically significant difference was not observed between the different mice in the NC non sampling group, WT mice had the highest average number of osteoclasts followed by ATCF7L2-KO(het) mice. ATCF7L2(hom) mice had the lowest average number of osteoclasts. In contrast, within the NC sampling group, ATCF7L2-KO(hom) mice had the greatest average number of osteoclasts compared to ATCF7L2-KO(het) and WT mice. However, these differences were not found to be significant after statistical analysis. Again, the average number of osteoclasts values for mice within the NC non sampling group were greater than that of mice within the NC sampling group, regardless of genotype. Finally, the average number of osteoclasts within the HFD sampling were the lowest values recorded. The average number of osteoclasts ranged from 2.3 to 3 cells and no significant difference was found when the average number of osteoclasts were compared. These results were not found to be significant after statistical analysis and this is may due to noise inherent in data collected using the different sampling methods (please see section 3.1.7 regarding G power calculations). Next, Osteoclast area was normalized to bone area to determine how genotype affected the area of bone that was occupied by osteoclasts.

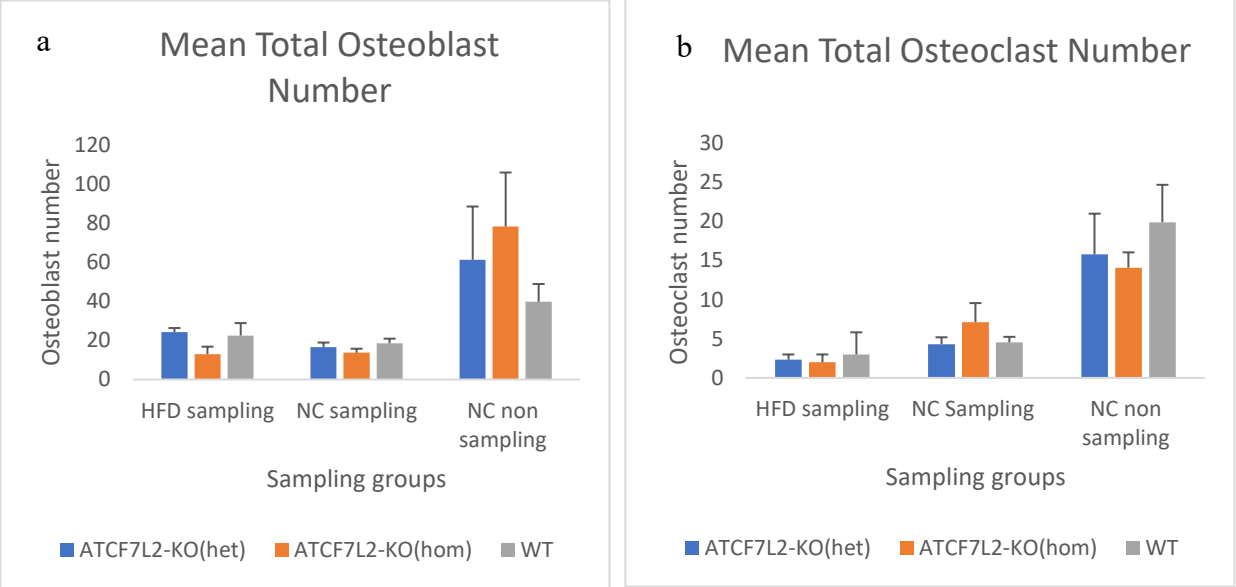

Figure 24- **Assessment of the effect of mouse genotype, diet and sampling on mean total osteoblast number (a) and mean total osteoclast number (b).** Error bars shown are SEM. Calculation of average osteoblast area was performed using Excel. Statistical analysis was performed on SPSS using a one-way ANOVA where results yielding a p-value of $p<0.05$ were statistically significant. HFD, high fat diet; NC, normal chow; ATCF7L2-KO, adipose tissue specific knockout of Tcf7l2 gene; het, heterozygote; hom, homozygote; WT, wild-type littermate control; sampling, sampled images were analysed; non-sampling, all images were analysed. For each mouse 2 technical replicates were used. Number of mice used: NC non sampling: ATCF7L2-KO(het)-5 ,ATCF7L2-KO(hom)- 4 WT- 7. NC sampling: ATCF7L2-KO(het)-9 ATCF7L2-KO(hom)-6 WT-9 HFD sampling: ATCF7L2-KO(het)-3 , ATCF7L2-KO(hom)-3 , WT-2.

Table 9**. Assessment of the effect of mouse genotype, diet and sampling on mean total osteoblast number and mean total osteoclast number.** Numerical data for Figure 24a and b. HFD, high fat diet; NC, normal chow; ATCF7L2-KO, adipose tissue specific knockout of Tcf7l2 gene; het, heterozygote; hom, homozygote; WT, wild-type littermate control; sampling, sampled images were analysed; non-sampling, all images were analysed.

	Mean Total Osteoblast number per bone slice (cell number) (3sf) ± standard error (3sf)/ standard deviation for HFD sampling WT (3sf)		
	Sampling group		
Genotype	HFD sampling	NC sampling	NC non sampling
ATCF7L2-KO(het)	24.3 (± 2.03)	16.5(± 2.41)	61.3(± 27.2)
ATCF7L2-KO(hom)	13.0 (± 3.79)	13.7 (± 2.04)	78.3(± 27.6)
WT	22.5 (± 6.36)	18.5(± 2.40)	39.8(± 9.05)
	Mean Total Osteoclast per bone slice (cell number) (3sf) ± standard error (3sf)/ standard deviation for HFD sampling WT (3sf)		
	Sampling group		
Genotype	HFD sampling	NC sampling	NC non sampling
ATCF7L2-KO(het)	2.33 (± 0.667)	4.3 (± 0.895)	15.8(± 5.21)
ATCF7L2-KO(hom)	2 (± 1.00)	7.13 (± 2.44)	14.1(± 1.96)
WT	3 (± 2.83)	4.54 (± 0.713)	19.9(± 4.79)

Mean osteoclast area normalized to total bone area analysis

Osteoclast area was normalized to bone area and the data Is shown in figure 25/table 10 **(Mean of the total osteoclast area on each slide/total bone area on each slide values).** Although a significant difference was not observed between the different mice in the NC non sampling group, WT had a greater mean osteoclast area to total bone area ratio compared to adipose tissue specific *TCF7L2* knockout mice. In addition, mean Osteoclast area to total bone area ratio was higher for ATCF7L2-KO(hom) mice compared to ATCF7L2-KO(het) mice. Although a statistically significant difference was not observed between the different mice In the NC sampling group, the osteoclast area to total bone area ratio was greatest for ATCF7L2-KO(hom) mice, followed by WT mice and ATCF7L2-KO(het) had the lowest osteoclast area to total bone area ratio. Although a significant difference was not observed between the different mice In the HFD sampling group, WT mice had a greater osteoclast area to total bone area ratio than ATCF7L2-KO(het) and ATCF7L2-KO(hom) mice. Out of the two knockout mice, ATCF7L2- KO(het)

had a greater osteoclast area to total bone area ratio than ATCF7L2-KO(hom) mice. These results were not found to be significant after statistical analysis and this is may due to noise inherent in data collected using the different sampling methods (please see section 3.1.7 regarding G power calculations). Next, osteoclast number: total bone area ratios were calculated in order to determine the influence of genotype on the number of osteoclasts across the entire bone sections.

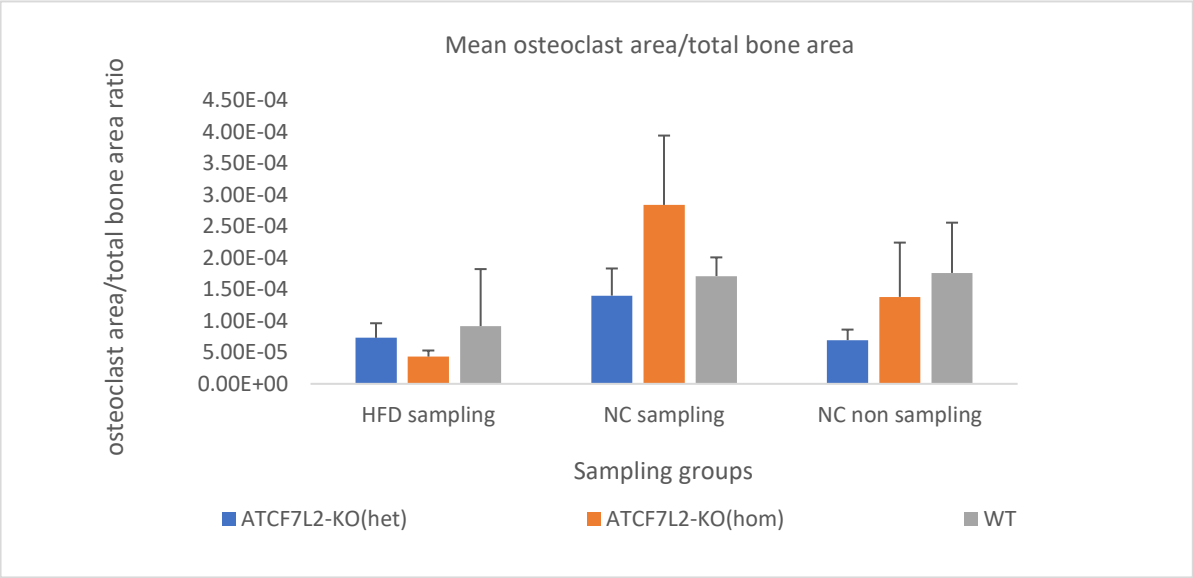

Figure 25- **Assessment of the effect of mouse genotype, diet and sampling on mean total osteoclast area/total bone area.** Error bars shown are SEM. Calculation of average osteoblast area was performed using Excel. Statistical analysis was performed on SPSS using a one-way ANOVA where results yielding a p-value of $p<0.05$ were statistically significant. HFD, high fat diet; NC, normal chow; ATCF7L2-KO, adipose tissue specific knockout of Tcf7l2 gene; het, heterozygote; hom, homozygote; WT, wild-type littermate control; sampling, sampled images were analysed; non-sampling, all images were analysed. For each mouse 2 technical replicates were used. Number of mice used: NC non sampling: ATCF7L2-KO(het)-5 ,ATCF7L2-KO(hom)- 4 WT- 7. NC sampling: ATCF7L2-KO(het)-9 ATCF7L2-KO(hom)-6 WT-9 HFD sampling: ATCF7L2-KO(het)-3 , ATCF7L2-KO(hom)-3 , WT-2.

Table 10- Assessment of the effect of mouse genotype, diet and sampling on mean total osteoclast area/total bone area. Numerical data for Figure 25. HFD, high fat diet; NC, normal chow; ATCF7L2-KO, adipose tissue specific knockout of Tcf7l2 gene; het, heterozygote; hom, homozygote; WT, wild-type littermate control; sampling, sampled images were analysed; non-sampling, all images were analysed.

	Mean Osteoclast area/total bone area ratios(3sf) ± standard error (3sf)/ standard error for HFD sampling WT (3sf)		
	Sampling group		
Genotype	HFD sampling	NC sampling	NC non sampling
ATCF7L2-KO(het)	7.30E-05 ± 2.31E-05	0.00014 ± 4.31E-05	6.92895E-05 ± 1.68E-05
ATCF7L2-KO(hom)	4.32E-05 ± 9.70E-06	0.000284 ± 0.000110	0.000137971 ± 8.61E-05
WT	9.16E-05± 9.05E-05	0.000171 ± 2.97E-05	0.000175705 ± 7.98E-05

3.1.4 Mean osteoclast number normalised to total bone area analysis

Figure 26/table 10 show the data for mean osteoclast number: total bone area ratio values **(mean of the total osteoclast number for each slide/total bone area of each slide values)** for each mouse genotype within the sampling groups. Although a statiscally significant difference was not observed between the different mice in the NC non sampling group in the NC non sampling group, ATCF7L2-KO(hom) mice had the highest mean osteoclast number: bone area ratio. WT mice had the second highest mean osteoclast number: total bone area ratio and the ATCF7L2-KO(het) mthe smallest mean osteoclast number: bone area ratio value.

Mean osteoclast number: bone area ratio values were found to be higher for mice within the NC sampling group compared with those mice within the NC non sampling group, regardless of genotype.

Although a statistically significant difference was not observed between the different mice in the NC sampling group ATCF7L2-KO(hom) mice had the largest mean osteoclast number: bone area ratio. However, within this sampling group, the mean osteoclast number: bone area ratio value was slightly higher for ATCF7L2-KO(het) mice compared to WT mice.

Although a statistically significant difference was not observed between the different mice in the HFD group, the mean osteoclast number: bone area ratio value was the smallest for ATCF7L2-KO(het) mice. The mean osteoclast number: bone area ratio was larger within WT

mice compared to ATCF7L2-KO mice. A statistically significant difference was not found and this may be due to noise inherent in data collected (please see section 3.1.7 regarding G power calculations) The mean osteoblast area: bone area ratio and osteoblast number: bone area ratio was also calculated to determine how genotype influences these parameters.

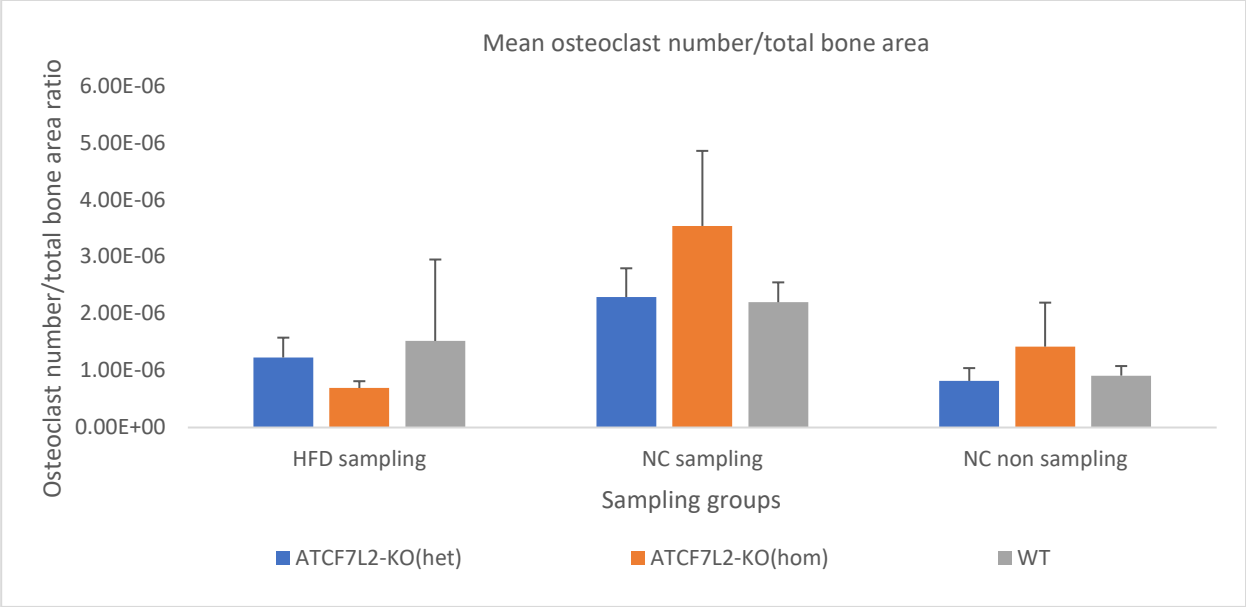

Figure 26- **Assessment of the effect of mouse genotype, diet and sampling on mean total osteoclast number/total bone area**. Error bars shown are SEM. Calculation of average osteoblast area was performed using Excel. Statistical analysis was performed on SPSS using a one-way ANOVA where results yielding a p-value of $p<0.05$ were statistically significantHFD, high fat diet; NC, normal chow; ATCF7L2-KO, adipose tissue specific knockout of Tcf7l2 gene; het, heterozygote; hom, homozygote; WT, wild-type littermate control; sampling, sampled images were analysed; non-sampling, all images were analysed. For each mouse 2 technical replicates were used. Number of mice used: NC non sampling: ATCF7L2-KO(het)-5 ,ATCF7L2-KO(hom)- 4 WT- 7. NC sampling: ATCF7L2-KO(het)-9 ATCF7L2-KO(hom)-6 WT-9 HFD sampling: ATCF7L2-KO(het)-3 , ATCF7L2-KO(hom)-3 , WT-2.

Table 11- Assessment of the effect of mouse genotype, diet and sampling on mean osteoclast number/total bone area. Numerical data for Figure 26. HFD, high fat diet; NC, normal chow; ATCF7L2-KO, adipose tissue specific knockout of Tcf7l2 gene; het, heterozygote; hom, homozygote; WT, wild-type littermate control; sampling, sampled images were analysed; non-sampling, all images were analysed.

	Mean Osteoclast number/total bone area ratio (3sf) ± standard error (3sf)/ standard error for HFD sampling WT (3sf)		
	Sampling group		
Genotype	HFD sampling	NC sampling	NC non sampling
ATCF7L2-KO(het)	1.23E-06 (± 3.49E-07)	2.29E-06 ± 5.90E-07	8.18152E-07 ± 2.25E-07
ATCF7L2-KO(hom)	6.94E-07± 1.19E-07	3.54E-06 ± 1.32E-06	1.42E-06 ± 7.73E-07
WT	1.52E-06± 1.43E-06	2.20E-06± 3.49E-07	9.11E-07 ± 1.68E-07

3.1.5 Osteoblast area: total bone area ratio analysis

Figure 27 and table 12 shows the mean osteoblast area: total bone area ratio values **(Mean of the total osteoblast area for each slide/total bone area of each slide values)** for the different sampling groups and mouse genotypes. Although a statistically significant difference was not observed between the different mice the within the NC non sampling group, mean osteoblast area: total bone area ratio to be higher for ATCF7L2-KO(hom) mice, followed by ATCF7L2-KO(het) mice.

Although a statistically significant difference was not observed between the different mice in the within the NC sampling set, WT mice had a larger mean osteoblast area: total bone area ratio value compared to ATCF7L2-KO mice. The mean osteoblast area: total bone area ratio was to be higher for ATCF7L2-KO(hom) mice compared with ATCF7L2-KO(het) mice. Mean osteoblast number: total bone area ratios were then calculated to determine how genotype influences the number of osteoblasts across bone slices.

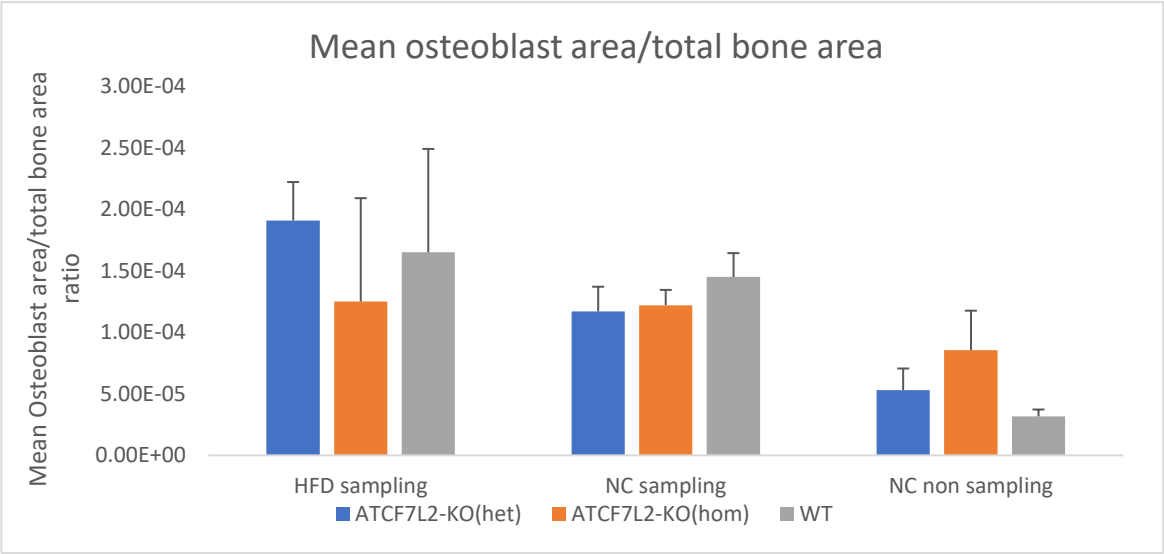

Figure 27- **Assessment of the effect of mouse genotype, diet and sampling on mean total osteoblast number/total bone area**

Error bars shown are SEM. Calculation of average osteoblast area was performed using Excel. Statistical analysis was performed on SPSS using a one-way ANOVA where results yielding a p-value of $p<0.05$ were statistically significant. HFD, high fat diet; NC, normal chow; ATCF7L2-KO, adipose tissue specific knockout of Tcf7l2 gene; het, heterozygote; hom, homozygote; WT, wild-type littermate control; sampling, sampled images were analysed; non-sampling, all images were analysed. For each mouse 2 technical replicates were used. Number of mice used: NC non sampling: ATCF7L2-KO(het)-5 ,ATCF7L2-KO(hom)- 4 WT- 7. NC sampling: ATCF7L2-KO(het)-9 ATCF7L2-KO(hom)-6 WT-9 HFD sampling: ATCF7L2-KO(het)-3 , ATCF7L2-KO(hom)-3 , WT-2.

Table 12- **Assessment of the effect of mouse genotype, diet and sampling on mean total osteoblast area/total bone area.** Numerical data for Figure 27. HFD, high fat diet; NC, normal chow; ATCF7L2-KO, adipose tissue specific knockout of Tcf7l2 gene; het, heterozygote; hom, homozygote; WT, wild-type littermate control; sampling, sampled images were analysed; non-sampling, all images were analysed.

	Mean Osteoblast area/total bone area (cells/μm^2) (3sf) ± standard error (3sf)/ standard deviation for HFD sampling WT (3sf)		
	Sampling group		
Genotype	HFD sampling	NC sampling	NC non sampling
ATCF7L2-KO(het)	0.000191 (± 3.12E-05)	0.000117 (± 2.01E-05)	5.31E-05 (± 1.75E-05)
ATCF7L2-KO(hom)	0.000125 (±8.41E-05)	0.000122 (± 1.25E-5)	8.55E-05 (± 3.21E-05)
WT	0.000165 (± 8.41E-05)	0.000145 (± 1.94E-05)	3.18E-05 (± 5.46E-06)

3.1.6 Mean osteoblast number: total bone area ratio analysis

Figure 28 and table 13 show the mean osteoblast number: total bone area ratio values **(Mean of the total osteoblast number for each slide/total bone area of each slide values)** for the different sampling groups and mouse genotypes. Although a statistically significant difference was not observed between the different mice in the NC non sampling group, ATCFL2-KO mice had a higher mean osteoblast number: total bone area values compared to the WT mice. ATCF7L2-KO(hom) mice had a slightly higher mean osteoblast number: total bone area ratio than ATCF7L2-KO(het) mice.

Although a statistically significant difference was not observed between mice of different genotype, in contrast to the NC non sampling results, WT mice had a higher mean osteoblast number: total bone area ratio compared to WT mice. Mean osteoblast number: total bone area ratio values ,within the NC sampling set, was found to be higher than that of mice within the NC non sampling group. Although a staistically significant difference was not observed between the different mice in the HFD sampling group, ATCF7L2-KO(het) had a higher mean osteoblast number: total bone area ratio, followed by WT mice. However, a statistically significant difference was not found and this may be due to noise inherent in data collected (please see section please see section 3.1.7 regarding G power calculations). It is important to note that mean osteoblast number: total bone area ratio values for WT and ATCF7L2-KO (het) mice, within the HFD sampling group, were greater than both the NC groups.

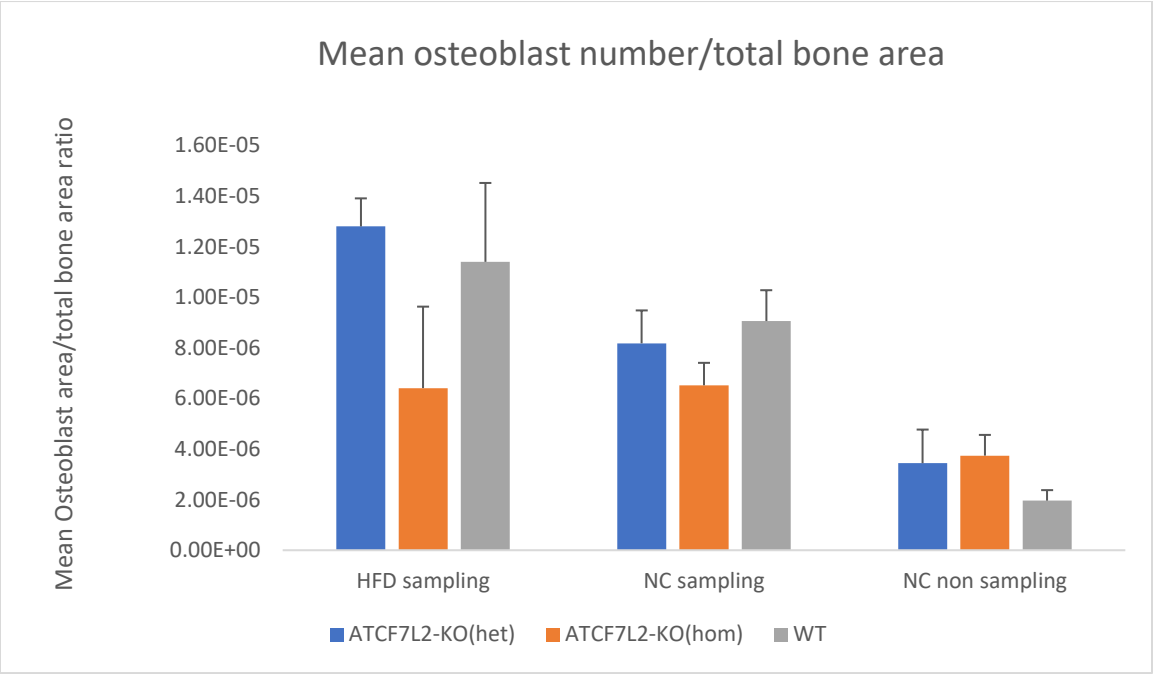

Figure 28- **Assessment of the effect of mouse genotype, diet and sampling on mean total osteoblast number/total bone area.** Error bars shown are SEM. Calculation of average osteoblast area was performed using Excel. Statistical analysis was performed on SPSS using a one-way ANOVA where results yielding a p-value of $p<0.05$ were statistically significant. HFD, high fat diet; NC, normal chow; ATCF7L2-KO, adipose tissue specific knockout of Tcf7l2 gene; het, heterozygote; hom, homozygote; WT, wild-type littermate control; sampling, sampled images were analysed; non-sampling, all images were analysed. For each mouse 2 technical replicates were used. Number of mice used: NC non sampling: ATCF7L2-KO(het)-5 ,ATCF7L2-KO(hom)- 4 WT- 7. NC sampling: ATCF7L2-KO(het)-9 ATCF7L2-KO(hom)-6 WT-9 HFD sampling: ATCF7L2-KO(het)-3 , ATCF7L2-KO(hom)-3 , WT-2.

Table 13- **Assessment of the effect of mouse genotype, diet and sampling on mean total osteoblast number/total bone area.** Numerical data for Figure 28. HFD, high fat diet; NC, normal chow; ATCF7L2-KO, adipose tissue specific knockout of Tcf7l2 gene; het, heterozygote; hom, homozygote; WT, wild-type littermate control; sampling, sampled images were analysed; non-sampling, all images were analysed.

	Mean Osteoblast number/total bone area (cells/μm^2) (3sf) ± standard error (3sf)/ standard error for HFD sampling WT (3sf)		
	Sampling group		
Genotype	HFD sampling	NC sampling	NC non sampling
ATCF7L2-KO(het)	1.28E-05 (± 1.11E-06)	8.18E-06 (± 1.30E-06)	3.44E-06 (± 1.33E-06)
ATCF7L2-KO(hom)	6.41E-06 (± 3.22E-06)	6.52E-06 (± 8.88E-07)	3.74E-06 (± 8.19E-07)
WT	1.14E-05 (±3.21E-06)	9.06E-06 (±1.22E-06)	1.96E-06 (± 4.16E-07)

3.1.7 G power calculation

A G power calculation was carried out (please see table 14) using the mean osteoblast area/ bone area and osteoclast area/ bone area ratios to determine the sample size of mice required to observe a significant difference between adipose tissue specific homozygous knockout of *Tcf7l2* within mice compared to WT mice. The sample size for both the sampling and non sampling sets were calculated. The data reveals the total sample size for osteoblast area/ bone area within the sampling set would require 312 mice in order to determine a significant difference. In addition the osteoclast area/ bone area sampling set would require 186 mice. The osteoblast area/bone area non sampling set would require 980 mice to determine a significant difference. In addition osteoclast area/ bone area non sampling set would require 1972 mice in order to determine a significant difference. Ideally, fewer mice would be sacrificed in order to investigate using sampling vs non sampling. Therefore sampling would be more feasible in future investigations.

Table 14- **G power calculations revealed that the non sampling set of mice require a much larger sample size to observe a significant difference between adipose tissue specific homozygous knockout of TCF7L2 mice vs wild type mice in relation to bone measurements taken.** We used the mean and standard deviation data from the Osteoblast area/ total bone area and Osteoclast area/ total bone area measurements to perform a power calculation using G-power (as described by (Faul *et al.*, 2007); (Faul *et al.*, 2009).

	Sample size 1 (ATCF7L2-KO(hom))	Sample size 2 (Wild type)	Total sample size/total number of mice
Osteoblast area/ bone area sampling set	156	156	312
Osteoblast area/ bone area non sampling set	490	490	980
Osteoclast area/ bone area sampling set	93	93	186
Osteoclast area/ bone area non sampling set	936	936	1972

3.2 Data from human osteoblasts

3.2.1 SNP analysis

SNP analysis was conducted to identify the genotype of five donors using the prevalidated TaqMan™ SNP Genotyping Assay for the rs7903146 variation in *TCF7L2*, which is associated with increased type 2 diabetes risk. The genotyping assay revealed that 4 out of 5 participants were identified as being homozygous carriers of risk allele of the rs7903146 SNP of TCF7L2 (TCF7L2hom) and 1 participant was found to be heterozygous carrier of the risk allele (TCF7L2het) (refer to table 15). None of the samples we received were from partcipants who were homozygous for the non-risk variation of rs7903146. We therefore performed preliminary comparisons of the TCF7L2het carrier with TCF7L2hom carriers because current literature suggests that are at higher risk of T2D than TCF7L2het carriers of the TCF7L2 risk allele (Tong *et al*. 2009; Le Bacquer *et al*. 2012; Assmann *et al*. 2014; Bahaaeldin *et al*. 2020). Identification of the SNP carrier status of the participants was then used to make comparisons in relation to osteocalcin expression and protein content between TCF7L2hom carriers and TCF7L2het carriers of the risk allele through quantitative real-time PCR experiments and ELISA assays, respectively.

Table 15- **Genotype of participants and average recovered DNA concentrations per sample.**

Participant number (p)	genotype	Average DNA (ng/μl) (3sf) ± standard deviation (3sf)
1	homozygous	4.50 ± 0.424
2	heterozygous	4.00 ± 0.424
3	homozygous	2.30 ± 0.404
4	homozygous	2.30 ± 1.13
5	homozygous	1.00 ± 0

3.2.2 Gene expression analysis

To measure *OST* expression, real-time quantitative polymerase chain reactions (rt-PCR) were conducted on RNA samples isolated from the osteoblast cells received from participants using the Applied Biosystems Power SYBR green RNA-to-C_T 1 step kit. *OST* rt-PCR reactions were set up alongside a house keeping gene, *Glyceraldehyde-3-phosphate dehydrogenase* (*GAPDH)*. The comparative cycle threshold (CT) method was used to identify expression of the *OST* and *GAPDH* gene from the RNA samples isolated from the different osteoblast cell cultures, using the AllPrep DNA/RNA/Protein Mini Kit. The comparative CT methods involved calculating the ratio of *OST* expression*: GAPDH* expression.

For the rt-PCR reaction, two technical replicates were used for each participant's RNA sample. Participant 5 had the lowest concentration of extracted DNA and no signal amplification was detected using the RNA isolated from this participant. Therefore, this participant was excluded from the subsequent caculations for gene expression.

Figure 29a shows the spread of *OST* expression readings for the participants. The box plot for TCF7L2hom participants shows that the data was positively skewed. The box plot also shows that the median value for OST expression was greater for the TCF7L2het participant compared to the TCF7L2hom participant (0.0318 vs 0.00325 respectively (3sf)). The interquartile range for the TCF7L2hom plot was 0.0424 compared to 0.0540 for the TCF7L2het plot. Therefore, the spread of the OST expression data is a smaller for the TCF7L2het participants. Our data also indicates that there was variation in *OST* gene expression between those who are TCF7L2hom for the risk allele. Although significance testing could not be conducted based on limited heterozygote sample numbers, the mean *OST* expression for the TCF7L2het participant was to be higher than the mean *OST* expression for the TCF7L2hom participants. More samples are needed to complete this section of work (Please see table 15).

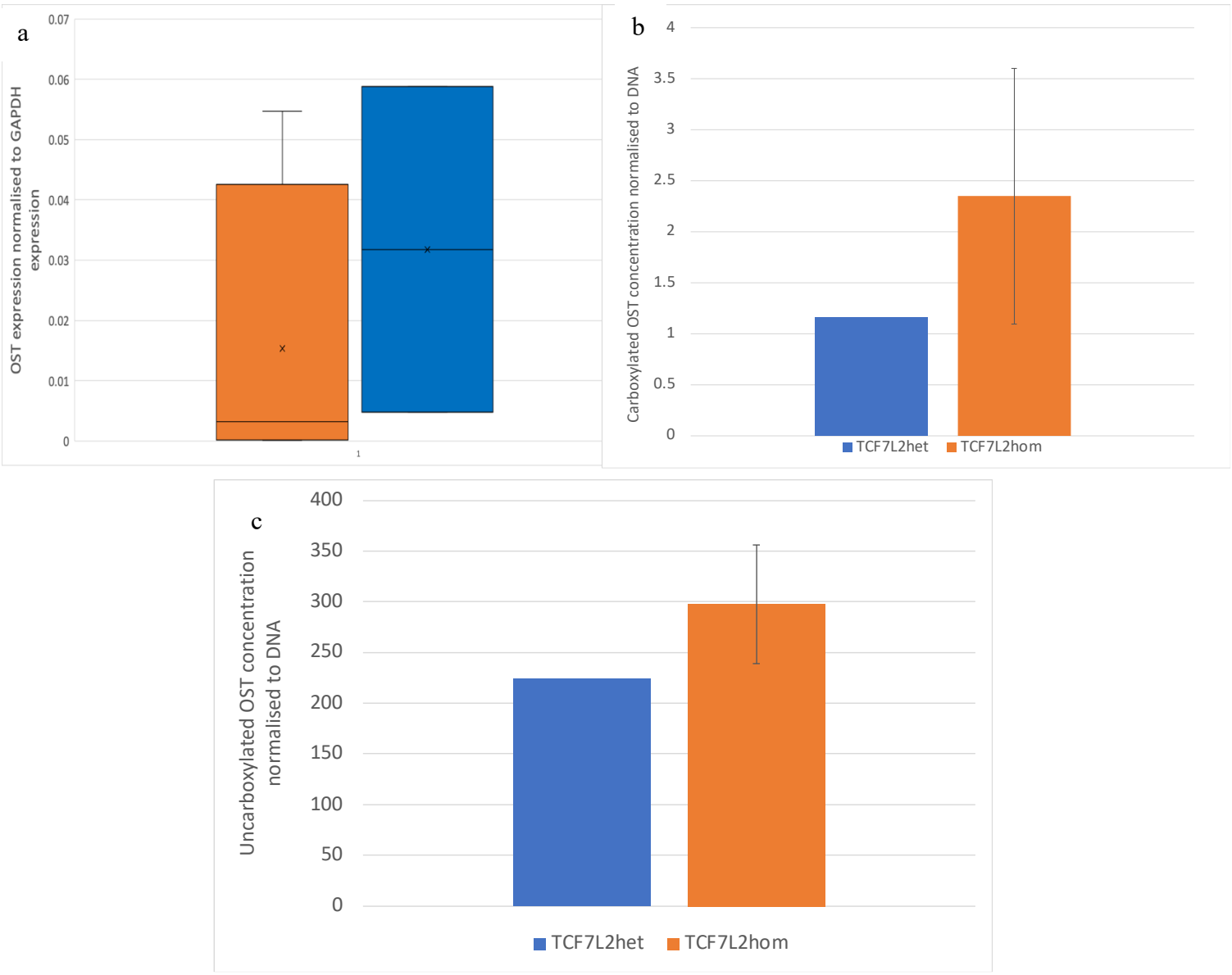

Figure 29- **Gene expression analysis for *OST* (a) and carboxylated (b) and uncarboxylated (c) OST content from patient samples.** (a) The box plot shows the median *OST* expression within the TCF7L2het participant was higher than in TCF7L2hom participants. (b) Mean Carboxylated OST and (C) mean Uncarboxylated OST protein content are shown. Error bars shown are SEM.

Table 16- **The G power calculation output results showed that a minimal sample size of 14 participants of either genotype would be needed to observe a significant difference in *OST* expression.**

Non centrality parameter δ	
Critical t	3.7583532
df	26
Sample size group 1	14
Sample size group 2	14
Total samle size	28
Actual power	0.9511670

3.2.3 Measurement of OST cellular protein content and secreted OST content

Alongside gene expression, OST production and secretion was measured using ELISA assays for secreted and total uncarboxylated OST and carboxylated OST. This was done to determine whether concentrations of these two forms of OST are affected by the *TCF7L2* risk allele within carriers. The AllPrep DNA/RNA/Protein Mini Kit allowed collection of total cellular protein and DNA from each osteoblast preparation. Secreted OST was measured from supernatant that was collected after two days of culture. ELISA assays specific for caboxylated (Invitrogen Human OST ELISA kit) and uncarboxylated (Biolegend LEGEND MAX Human Uncarboxylated Osteocalcin ELISA kit) OST was used to determine concentrations from both forms of OST from the total cellular protein fraction (Table 18) and secreted fraction (Table 19 and table 20), with two technical replicates for each sample. Due to experimental error, the carboxylated OST ELISA was conducted twice. Due to loss of the cellular protein samples, there was very a small enough of the cellular protein samples for participant 1 and participant 3 to use in the second ELISA experiment. Therefore 10x and 100x dilutions were used to obtain results.There was no more cellular protein fraction samples to use for the Uncarboxylated ELISA experiment, therefore only supernatant samples were used.

Due to the small number of samples, we were not able to perform statistical comparisons between samples from the two genotypes. However, we performed power analysis using this preliminary data and g power to determine the minimum sets of human samples that would be needed to adequately power our study (see table 16). The analysis gave the total sample size of 28 which seems achievable if this project were to be extended in the future.

Table 17- **Comparative CT method data for *OST* gene expression from RNA samples.** The TCF7L2hom participants had lower *OST* gene expression values than the TCF7L2het participant. However, more work is needed to confirm is this is in fact true, as only 1 control participant (TCF7L2het) was used in this investigation.

Participant number (p)/genotype of participant	Mean *OST* gene expression (ratio of *OST* expression/ *GAPDH* expression)	*OST* gene expression relative to TCF7L2het control (relative fold change) (3sf) ± standard deviation (3sf)
p1/TCF7L2hom	0.0276	0.868(± 0.0384)
p2/TCF7L2het	0.0317	1(**±** 0.0382)
p3/TCF7L2hom	0.00607	0.191
p4/TCF7L2hom	6.92E-05	0.00218
p5/TCF7L2hom	n/a	n/a

Table 18- Carboxylated OST concentrations protein dilution samples from participant 1 and participant 3 normalised to DNA. This data shows that, after normalisation to DNA, participant 3 had a greater carboxylated OST concentration within the protein sample from participant 1. Data analysis was performed using Excel.

participant number and genotype	Mean carboxylated OST (10x dilution) normalised to DNA± standard deviation (3sf)	Mean OST (100x dilution) normalised to DNA ± standard deviation (3sf)
p1-TCF7L2hom	0.430 (±0.0314)	0.586 (±0.064)
p3- TCF7L2hom	0.881 (±0.0640)	1.04 (±0.0902)

Table 19- **Carboxylated OST concentrations within supernatant samples from participants**. This data shows that, after normalisation to DNA, 3 of the TCF7L2hom participants had greater concentrations of carboxylated OST compared to the TCF7L2het carrier. Data analysis was performed using Excel.

participant number and genotype	Mean carboxylated OST (supernatant) (ng/μl) ± standard deviation (3sf)	Mean carboxylated OST (supernatant) normalised to DNA ± standard deviation (3sf)
p1-TCF7L2hom	4.97 (±0.422)	1.10 (±0.0939)
p2- TCF7L2het	4.63 (±0.143)	1.16 (±0.0357)
p3- TCF7L2hom	4.55 (±0.175)	1.98 (±0.0759)
p4- TCF7L2hom	5.12 (±0.0232)	2.23 (±0.0100)
p5- TCF7L2hom	4.08 (±0.0625)	4.08 (±0.0625)

Table 20– **Uncarboxylated OST concentration found within the supernatant samples**. This data suggests that uncarboxylated OST concentrations within the supernatant samples from TCF7L2het participants were greater than that of the TCF7L2het participant.

Participant number and genotype	Uncarboxylated OST (supernatant) pg/ml ± standard deviation (3sf)	Uncarboxylated OST (Supernantant) normalised to DNA ± standard deviation (3sf)
p1-TCF7L2hom	1780 (±199)	365(±44.2)
p2- TCF7L2het	942 (±67.0)	224 (±16.7)
p3- TCF7L2hom	557 (±0.582)	270 (±0.253)
p4- TCF7L2hom	630 (±146)	258 (±63.7)
p5- TCF7L2hom	n/a	n/a

Chapter 4
Discussion and Conclusion

4.1 Discussion

4.1.1 Overview

An increased bone fracture risk has been associated with T2D and aging (Nicodemus and Folsom 2001; Russo *et al*. 2016; Moayeri *et al*. 2017; Costantini and Conte, 2019; Ntouva *et al*. 2019). In addition, GWAS have repeatedly shown that *Tcf7l2* SNPs are associated with the development of T2D within multiple different populations (Del Bosque-Plata *et al.*, 2021). The *Tcf7l2* rs7903146 SNP has been shown to have the highest association with T2D, and the strong association of these SNP with T2D has been confirmed by other studies (Grant, *et al*. 2006; Nicod *et al*. 2014; Guan *et al*., 2016). Previous unpublished work by Dr. Nguyen-Tu and da Silva Xavier revealed that heterozygous and homozygous ATCF7L2-KO within mice resulted in an abnormal trabecular network structure within ATCF7L2-KO mice when compared with WT mice (please refer to figure 21 within section 1.8). ATCF7L2-KO within mice also lowered osteocalcin content within plasma, when compared with WT mice (see Figure 20 within section 1.7). To further identify the impact on bone, I conducted osteoblast and osteoclast cell analysis. In this investigation I have also tried to assess whether the presence of the T2D risk SNP, rs7903146, for TCF7L2 correlates with the ability for primary human osteoblasts to produce and secrete osteocalcin.

I hypothesised that adipose tissue specific knockout of *Tcf7l2* within mice will result in altered osteoblast and osteoclast function, which may be due to functional impairment and/or loss of cell mass. I also hypothesised that homozygous carriers of the *TCF7L2* risk allele will have impaired osteoblast function.

In order to conduct this investigation, I used bones from the hind limbs of mice who had homozygous or heterozygous adipose tissue specific knockout of *Tcf7l2* and from WT littermate controls. The mouse bones were from the same cohort of mice used in the research paper by Nguyen-Tu et al. (2021). Mice were either fed a HFD or NC diet. To assess cell morphology and number, I performed histochemical analysis from slices from paraffin embedded bones from the mice. For each bone slice I measured osteoblast cell surface area, osteoclast cell surface area and the total bone surface area in the image. In the first instance, analysis was performed on whole bone slices from the NC diet cohort (non-sampling). It took 5 months to manually assess 18 complete bone slices from 18 mice, which made it practically impossible to analyse the bone slices from all the mice within the period of the MSc using this method. Image sampling was needed to allow us to complete the assessment of the HFD cohort, but were aware that this could bias data. We therefore assessed the impact of image sampling (10 random image for each bone slice) on analysis on the NC diet and compared it with the data obtained when whole images were analysed, before applying the sampling technique to the HFD cohort. Power calculations based on the data collected in this study indicate that the differences are so small that large numbers of mice would have been needed for data to achieve statistical significance, using either method of image analysis, indicating that any difference is not likely to be biologically significant.

4.1.2 Osteoblast data analysis

In this current project, long cortical bones from adipocyte-specific *Tcf7l2* knockout mice that have been back-crossed on to a C57BL/6J mice were assessed. Evidence suggests that C57BL/6J mice develop imparied glucose tolerance and insulin secretion when fed a HFD (Fajardo *et al.*, 2014). This impairment in glucose tolerance can be attributed to reduced secretion of insulin and insulin resistance (Fajardo *et al.*, 2014). A HFD seems to negatively affect trabecular bone compartments(Fajardo *et al.*, 2014). This was shown in the preliminary unpublished work by Dr. Nguyen-Tu and Da Silva Xavier related to this investigation (refer to figure 21). Lower trabecular bone volumes within C57BL/6J mice have been found and this has been linked to increased osteoclast activity and possibly due to lower bone formation (Fajardo *et al.*, 2014). However, In this investigation, long cortical bones from C57BL/6J mice were assessed. The effect of a HFD on C57BL/6J mice has revealed decreased femoral strength, bending stiffness and fracture toughness (Ionova-Martin *et al.*, 2010; Ionova-Martin *et al.*, 2011). When C57BL/6J mice were fed a HFD a greater accumulation of AGES were quantified within the femurs of these mice (Fajardo *et al.*, 2014). The writers suggest that that the accumulation of AGES mat explain the decrease in fracture toughness (Fajardo *et al.*, 2014).

T2D has been associated with the development of AGEs and AGEs have been found to affect osteoblast function (Picke *et al*. 2019). AGEs have also been linked to an increased rate of apoptosis of osteoblasts and osteoblast precursor cells (Picke *et al*. 2019). In another investigation, when human osteoblasts were exposed to a high glucose concentration and/or AGEs, a reduction in the expression of the osteoblast specific markers Runx2 and Osterix was identified (Picke *et al*. 2019). Runx2 is a downstream mediator of Wnt signalling within osteoblasts, and as discussed in 1.5.5, Wnt signaling is critical for osteoblast differentiation and function. Therefore, T2D could negatively affect osteoblast differentiation and function via impaired Wnt signalling.

In addition to hyperglycaemia, fatty acids and inflammation may also negatively influence osteoblast function too (Picke *et al*. 2019). Non esterified fatty acids and saturated fatty acids have been shown to induce osteoblast apoptosis and reduce osteoblast differentiation (Hardouin, Rharass and Lucas, 2016). As discussed in section 1.5.5, MSCs have the ability to develop into osteoblasts or adipocytes within bone. This depends on the balance between Wnt signalling and PPARγ signalling within bone (Maeda *et al.*, 2019). It is important to note that T2D has been found to induce bone marrow adiposity (Picke *et al*. 2019. This is due to reduced osteoblastogensis and increased adipogenesis, as a result of increased PPARγ signalling (Picke *et al*. 2019).

As mentioned in section 1.5.4, ATCF7L2-KO within mice has been linked to impaired effects on metabolism. ATCF7L2-KO within mice has been linked to impaired glucose tolerance, impaired GSIS, hyperinsulinemia, impaired incretin effect and insulin stimulated endogenous glucose production. Human carriers of the *Tcf7l2* rs7903146 SNP (heterozygous-C/T, homozygous-T/T) were found to be associated with a reduced insulin secretion during an early insulin response to an OGTT compared with controls (carriers of CC allele) (Lyssenko *et al*. 2007). A significant

decrease in insulin secretion was found after measurement by disposition index and arginine stimulated insulin secretion between CT/TT carriers vs CC carriers (Lyssenko *et al*. 2007). A reduced Incretin effect was confirmed within this investigation as reduced insulin secretion was observed after OGTT within CT/TT carriers compared to CC carriers (Lyssenko *et al*.2007). Using this information, adipose tissue specific knockout of *Tcf7l2* within mice may be associated with impaired glucose control. Since AGEs have been associated with osteoblast development, ATCF7L2-KO within mice may result in impaired osteoblast differentiation via exacerbating insulin resistance. The increase in glucose concentrations within mice then inhibits osteoblast differentiation.

In a previous investigation, impaired glucose tolerance was idenfied within ATCF7L2-KO(het) and ATCF7L2-KO(hom) mice after being fed a NC diet for ATCF7L2-KO(het) mice glucose intolerance was identifed at 16 weeks by IPGTT (Nguyen-Tu *et al.*, 2021). ATCF7L2-KO(hom) mice displayed impaired oral glucose tolerance at 16 weeks of age (Nguyen-Tu *et al.*, 2021). Another study in which *Tcf7l2* expresssion was silenced in mature mouse adipocytes also resulted in glucose intolerance when the mice were fed a NC diet and HFD (Chen *et al.*, 2018). Therefore, I expected worse outcomes for ATCF7L2-KO(hom) mice, when fed a HFD, because *Tcf7l2* gene expression completely knocked out within the adipose tissue of these mice. These mice were also found to have reduced glucose tolerance after IPGTT and impaired GSIS after oral glucose challenge when compared with control mice (Nguyen-Tu *et al.*, 2021). Mice with ATCF7L2-KO would therefore be more susceptible to impaired glucose control and the development of hyperglycaemia compared to WT mice.

When 8 week old female C57BL/6 mice were fed a HFD, a significant increase in bone marrow adiposity was found compared to aged matched C57BL/6 mice fed a regular diet (Styner *et al.*, 2014). Bone marrow adiposity was 2.6 fold higher within mice fed a HFD compared to those fed regular diet (Styner *et al.*, 2014). The authors suggest that the increase bone marrow adiposity might stimulate stimulation marrow MSCs to differentiate into adipocytes (Styner *et al.*, 2014). The authors also suggest an alternative explanation, they suggest lipid content of pre-existing bone marrow adipocytes could increase (Styner *et al.*, 2014). If bone marrow adiposity does indeed increase within C57BL/6 mice, this would be detrimental to osteoblasts when mice are fed a HFD (Styner *et al.*, 2014). Genetic expression testing using adipocytes from mice who have had adipose tissue specific knockout of Tcf7l2 and WT mice reveled that knockout of Tcf7l2 within adipose tissue was linked reduced expression of lipolytic genes and increased expression of lipogenic genes (Geoghegan *et al.*, 2019). After a 24 hour fast, an increase in free fatty acids was observed in knockout mice and WT mice (Geoghegan *et al.*, 2019). In addition, the release of free fatty acids was lower within knockout mice compared to WT mice after conducting in vivo lipolysis testing (Geoghegan *et al.*, 2019). In another investigation, homozygous adipocyte specific knockout of *Tcf7l2* within C57BL/6J mice revealed that plasma levels of circulating non-esterified fatty acids was significantly increased compared with age and sex matched controls. As mentioned earlier non esterified fatty acids and saturated fatty acids have been shown to induce osteoblast apoptosis and reduce osteoblast differentiation (Hardouin, Rharass and Lucas, 2016). Since we used the legs from the mice used the study conducted by Nguyen-Tu *et*

al., 2021, the excess release of non-esterified fatty acids within ATCF7L2-KO(hom) may negatively affect the osteoblasts area and number within ATCF7L2-KO(hom) mice.

I hypothesised that adipose tissue specific knockout of *Tcf7l2* within mice will result in altered osteoblast function, which may be due to functional impairment and/or loss of osteoblast cell mass. Using the findings from literature mentioned above, I anticipated that data representing osteoblast area and osteoblast number would be lower within ATCF7L2(het)-KO mice and ATCF7L2-KO(hom) mice compared to WT mice. In addition, I also expected that data representing osteoblast area and osteoblast number would be lower for ATCF7L2-KO(het) mice and ATCF7L2-KO(hom) mice when fed a NC diet and HFD. A significant difference was only detected by, one way ANOVA analysis, when the average osteoblast area for mice within the NC non sampling group were compared. I found that the average osteoblast area values for ATCF7L2-KO(hom) mice were significantly greater compared to ATCF7L2-KO(het) and WT mice in each of the sampling groups (refer to figure 22a/table 5). This was unexpected because glucose metabolism is supposedly impaired within these mice, which would in turn impair osteoblast diffrentiation and survival.

No significant difference was detected by one way ANOVA analysis when the data representing the different mouse genotypes groups were compared. Therefore, I can not make any valid conlcusions and suggest that further work be conducted to confirm the results found. A g power calculation was conducted and the results are shown in table 14. This data revealed that the non-sampling set of mice require a much larger sample size to observe a significant difference between ATCF7L2-KO(hom) mice compared to WT mice. The total sample size required to observe a significant difference is 312 mice (156 mice per genotype group) for the sampling set. However, for the non-sampling set required 980 mice (490 mice per genotype group). This implies that it would be more feasible to only conduct image sampling in further investigations. However, non-sampling allows for data to be representative of entire bone slices. Therefore, a larger quantity and more accurate data can be collected from non-sampling groups. In addition to this, there was differences in the data for mice within the NC sampling group and for those within the NC non sampling group. I was not able to conduct image analysis of all the images taken of bones from mice fed a HFD in this investigation. This would have allowed for the addition of a HFD non sampling group. Therefore, as of yet this investigation is underpowered and I suggest the use of more mice in future work. I also suggest the use of non-sampling and sampling methodology in future work.

Despite no significant difference being found for any of the other results, there are still some trends worth discussing. In the NC non sampling group, data representing osteoblast area and osteoblast number was greater within ATCF7L2-KO(hom) mice comapred to ATCF7L2-KO(het) and WT mice (See figures 23a, 24a, 27 and 28. See tables 5,7,9, 12 and 13). Again, this was unexpected because glucose metabolism is supposedly impaired within these mice, which would in turn impair osteoblast diffrentiation and survival. The fact that no signficant difference was identified means we cannot conclude that ATCF7L2-KO(hom) mice have greater osteoblast area and osteoblast number when fed a NC diet.

On the other hand, data representing osteoblast area and osteoblast number for mice within the NC non sampling group, except for average osteoblast area, is greater for WT mice compared to ATCF7L2-KO mice (See figures 23a, 24a, 27 and 28. See tables 5,7,9, 12 and 13). In addition, mean total osteoblast area, mean total osteoblast number, mean osteoblast number: total bone area values are lower within ATCF7L2-KO(hom) mice compared to ATCF7L2-KO(het) mice and WT mice. This data suggests the total number of osteoblasts and osteoblast cell mass is decreased within ATCF7L2-KO(hom) mice. This data was expected since ATCF7L2-KO within mice results in impaired glucose homeostasis, and would produce a negative effect on osteoblasts. The average total osteoblast area, mean total osteoblast number, the mean osteoblast area: total bone area ratio and the mean osteoblast number: total bone area ratio values are smaller for ATCF7L2-KO(hom) mice compared to ATCF7L2-KO(het) and WT mice (See figures 23a, 24a, 27 and 28. See tables 5,7,9, 12 and 13). This suggests that osteoblast number, osteoblast area and osteoblast cell mass is decreased within ATCF7L2-KO(hom) when exposed to a HFD. Therefore the link between impaired glucose control and lipid metabolism within ATCF7L2-KO(hom) mice and osteoblast differentiation/function may explain these results. Next, I will discuss the data collected related to osteoclast area and number.

4.1.3 Osteoclast data analysis

Evidence in literature regarding the effect of T2D on osteoclasts is controversial(Picke *et al*. 2019). Authors have suggested T2D results in a positive effect on osteoclasts, whereas others report a negative influence of T2D on osteoclasts (Picke *et al*. 2019). In TallyHo mice and ZDF rats, the serum markers for osteoclast activity, CTX and TRAP, were found to be increased (Picke *et al*. 2019). Histological numbers of osteoclasts were also found to be increased within these models (Picke *et al*. 2019). Other studies have also reported increases in bone resorption parameters (Hamann *et al.*, 2013; Won *et al.*, 2011; Xu *et al.*, 2014). As discussed in section 1.1.1, T2D results in increased inflammation (Graves, 2008). Humans with T2D and periodontitis have increased levels of the pro inflammatory mediators, TNF-α, IL-1β and IL-6. These mediators are linked with ongoing inflammation and induction of dyslipidemia (Jiao, Xiao and Graves, 2015). An increase in TNF-α has also been associated with increased bone marrow adiposity within T2D patients. These adipocytes have been shown to have greater RANKL: OPG ratio when treated TNF-α (Kobayashi *et al.*, 2000). TNFα can also stimulate osteoclastogenesis independently of RANKL/OPG axis (Kobayashi *et al.*, 2000).

Increased production of AGEs may also positively influence osteoclasts. AGES bind to their receptor, RAGE, which can be found on osteoclasts (Catalfamo *et al.*, 2013; Xie *et al.*, 2013). RAGE initiates signalling that enables increased expression of RANKL, thereby enhancing osteoclastogenesis (Catalfamo *et al.*, 2013; Xie *et al.*, 2013). RAGE has also been linked to decreasing OPG expression, thereby increasing the ratio of RANKL/OPG and osteoclast formation (Jiao, Xiao and Graves, 2015). As discussed in section 1.1.1, T2D induces oxidative stress. The development of ROS, because of oxidative stress, has been shown to increase RANKL expression (Jiao, Xiao and Graves, 2015). ROS may also increase RAGE expression which further increases osteoclastogenesis (Jiao, Xiao and Graves, 2015). The increase in saturated

fatty acids, associated with T2D, has been also shown to increase osteoclast survival (Picke *et al*. 2019).

Despite this evidence, some authors have found opposing results. Hyperglycaemia was first reported to decrease osteoclast differentiation and activity of osteoclasts by (Wittrant *et al.*, 2008). Since then, other studies have also confirmed this (Park and Lee, 2022). Another investigation revealed that when osteoclast-like Raw264.7 cells are exposed to high glucose, the expression of osteoclast specific genes was decreased (Picke *et al*. 2019). Osteoclasts, from Six-week-old male Sprague Dawley rats fed a HFD, were cultured with high glucose levels and this resulted in reduced osteoclast formation, differentiation and function (Hu *et al.*, 2019). Therefore, T2D may negatively affect osteoclasts differentiation, formation and function

I hypothesised that ATCF7L2-KO would negatively influence osteoclast cell mass and number because osteoblasts and osteoclasts cell mass are regulated in tandem (see section 1.3.1 and 1.3.2). However, no significant difference was detected after one way ANOVA when the mean values for mice within the same sampling group were compared with each other. Therefore, no conclusions can be made regarding whether ATCF7L2-KO within mice results in an increase or decrease in osteoclast number, osteoclast cell area and osteoclast cell mass. More work will be required to detect a significant difference and future work may help with preventing inconsistencies in data collected between sampling groups. A g power calculation was conducted and the results are shown in table 14. This data revealed that the non-sampling set of mice require a much larger sample size to observe a significant difference between ATCF7L2-KO(hom) mice compared to WT mice. The total sample size required to observe a significant difference is 312 mice (156 mice per genotype group) for the sampling set. However, for the non-sampling set required 980 mice (490 mice per genotype group). This implies that it would be more feasible to only involve sampling in further investigations. However, non-sampling allows for data collection to be representative of entire bone slices. Therefore, more accurate data can be collected from non-sampling groups. In addition to this, there was differences in the data shown for mice within the NC sampling group and for those within the NC non sampling group, this made drawing conclusions difficult. I was also not able to conduct image analysis of the bones from HFD mice in this investigation. This would have allowed for the addition of a HFD non sampling group. Therefore, in future work, I would suggest the use of non-sampling and sampling methodology to determine if there are indeed differences between the two methods in relation to data collected.

Despite no significant difference being found for any of the other results, there are still some trends worth discussing. As mentioned above, T2D has been reported to impair osteoclast formation, differentiation and function. The data for the HFD group agrees with literature that suggests T2D induces a negative effect. This is because ATCF7L2-KO(hom) and ATCF7L2-KO(het) mice had lower mean total osteoclast number values and mean osteoclast number: total bone area ratio values than WT mice. This suggests the number of osteoclasts Is lower within ATCF7L2-KO(het) and ATCF7L2-KO(hom) mice. Therefore, reduced number of osteoclasts may be due to hyperglycaemia present within these knockout mice. In this investigation, mean total

osteoclast number and mean osteoclast number total bone area is also lower for ATCF7L2-KO(het) mice vs control mice.

In the investigation conducted by Nguyen et al 2021, ATCF7L2-KO(het) mice were not placed on a HFD. Results from this investigation suggests when ATCF7L2-KO(het) mice were fed a HFD, the effect is similar to that of ATCF7L2-KO(hom) mice. It is important to note, that the mean osteoclast number: total bone area value for ATCF7L2-KO(het) mice was greater than that corresponding to ATCF7L2-KO(hom) mice. This implies that a HFD has a much greater negative effect on ATCF7L2-KO(hom) mice compared to ATCF7L2-KO(het) mice. Impaired glucose tolerance was also reported in ATCF7L2-KO(het) and ATCF7L2(hom) mice when fed a NC diet (Nguyen et al 2021). Therefore, an assumption can be made that glucose control is impaired within ATCF7L2-KO mice even when fed a NC diet. This may explain why the mean total osteoclast number values, within the NC Non sampling group, for ATCF7L2-KO(het) and ATCF7L2-KO(hom) are smaller than WT mice.

The average osteoclast area data, for the NC non sampling group, reveals that WT mice had a greater average osteoclast area than ATCF7L2-KO(het) and ATCF7L2-KO(hom) mice (see figure 22b). This is also true for average total osteoclast and mean osteoclast area: total bone area data (see figure 23b and figure 25). The HFD results for mean osteoclast area: total bone area ratios and mean total osteoclast area (see table 8 and table 10) show that WT mice had greater values than ATCF7L2-KO(hom) mice. This suggests data suggests that osteoclast size and cell mass is lower within ATCF7L2-KO(hom) mice when fed a NC and HFD. This also agrees with literature regarding the negative effect of T2D on osteoclasts.

Despite the findings, in relation to osteoclast number and osteoclast area, there are contradictions in the results. In relation to osteoclast number data, there are differences in the trends shown by the NC non sampling group and the NC non sampling group. To explain these differences, It is also important to relate back to the idea that osteoblasts and osteoclasts are regulated in tandem (see section 1.3.1 and 1.3.2). When ATCF7L2-KO(hom) mice were fed a HFD, these mice exhibited lower mean total osteoblast number and mean osteoblast number: total bone area values than ATCF7L2-KO(het) and WT mice. Osteoblasts have been shown to limit osteoclast differentiation, via decreasing RANKL expression and increasing OPG expression (see section 1.3.1 and 1.3.2).

As suggested earlier, the impaired glucose control within ATCF7L2-KO mice, may result in increased AGE associated impairment of the Wnt signalling pathway via inhibiting RUNX2 activity. Loss of β-catenin has been linked to decreased OPG expression (Regard *et al.*, 2012). Osteoblast specific knockout of β-catenin resulted in increased RANKL expression (Regard *et al.*, 2012). Since β-catenin is involved in downstream Wnt signalling, impaired Wnt associated osteoblasts differentiation may result in reduced osteoblast number. As mentioned earlier, hyperglycaemia, ROS generation and AGE generation has been found to increase RANKL expression within osteoclasts (Jiao, Xiao and Graves, 2015)). Therefore ATCF7L2-KO within mice and hyperglycaemia associated loss of Wnt signaling within osteoblasts may result in an increase in the RANKL/OPG ratio, which could increase osteoclast numbers within ATCF7L2-

KO(hom) mice. Therefore, an increase in the RANKL/OPG ratio may explain why the mean total osteoclast number was found to be greater for ATCF7L2-KO(hom) mice within the NC sampling group. This may also explain why ATCF7L2-KO(hom) mice, in both the NC sampling groups, had a greater mean osteoclast number: total bone area ratio value than ATCF7L2-KO(het) and WT mice.

4.1.4 Human data analysis

I hypothesised that homozygous carriers of the *TCF7L2* risk allele will have impaired osteoblast function. To test this, I used osteoblast cell cultures that were isolated from patients undergoing hip replacement surgery. I conducted genotyping, RT-PCR and ELISA experiments to determine if there is any association between the *Tcf7l2* rs7903146 SNP (the type 2 diabetes risk variant) and osteoblast function.

OST is the most abundant bone matrix protein, therefore it is a useful marker of bone formation and osteoblast function (Tsao *et al.*, 2017). When OST is produced post translational modifications are made, this involves γ-carboxylation at 3 glutamic acid residues (Zoch, Clemens and Riddle, 2016). However, these carboxyl groups can be removed within resorption lacunae created by osteoclasts, this results in the formation of uncarboxylated OST (Zoch *et al*. 2016). Carboxylated OST is secreted into bone matrix where the carboxylated glutamic acid residues enable OST to bind to calcium ions within hydroxyapatite (Delmas *et al.*, 2000). Carboxylated OST is thought to associate with BAp to maintain bone strength and inhibit bone flexibility (Komori, 2020). Whereas uncarboxylated OST has been found to be involved in insulin secretion, insulin secretion, increasing insulin sensitivity, glucose uptake in tissues, beta cell proliferation, testosterone production, spermatogenesis, germ cell survival, adiponectin secretion (Tangseefa *et al*. 2018). Therefore, apart from being marker of bone formation, OST has multiple roles within the body.

It has been identified that baseline serum concentration of both forms of OST were lower in T2D subjects vs control subjects (Díaz-López *et al*. 2013). In addition, those in the lowest tertile for serum carboxylated OST and uncarboxylated OST were associated with a greater risk of diabetes incidence than those in the upper tertile (Díaz-López *et al*. 2013). In elderly men a greater number of metabolic syndrome traits was found to be associated with lower average serum OST presence (Confavreux *et al*. 2014). Whereas an increase in serum OST was linked to a decrease in severe metabolic syndrome (Confavreux *et al*. 2014). Using this information, and evidence that suggests T2D has a negative effect on osteoblasts (Picke *et al.*, 2019), I assumed that TCF7L2hom participants would have reduced OST expression, reduced carboxylated OST release and reduced uncarboxylated OST release than the TCF7L2het participant.

Results showed that median OST expression for TCF7L2hom participants was found to be lower than the TCF7L2het participant (figure 29a). This agrees with the preliminary results described in section 1.7 (figure 20b). However, the mean concentration of carboxylated OST was found to be greater within TCF7L2hom participants compared to the TCF7L2het participant (figure 29b). In addition, the mean concentration of uncarboxylated OST was also greater with TCF7L2hom

participants compared to the TCF7L2het participant (figure 29c). However, no valid conclusions can be drawn from this data as only 1 control participant (TCF7L2het) was used. This was due to a lack of osteoblast cell culture donation because of the COVID-19 pandemic. A g power calculation revealed that total sample size of 28 participants (14 TCF7L2hom participants and 14 TCF7L2het participants) would be required to detect a significant difference in *OST* expression, uncarboxylated OST release and carboxylated OST release. This seems achievable if work was to continue in the future.

In this investigation, TCF7L2hom partcipants were shown to have lower median OST expression compared to the TCF7L2het participant. This would suggest a decrease in osteoblast function. This can be explained by the link between hyperglycaemia, AGES and the negative effect on osteoblasts. As discussed in section 1.5.4, glucose control was found to be impaired within human carriers of the *Tcf7l2* rs7903146 SNP (Lyssenko *et al*.2007). This impaired glucose control would result in hyperglycaemia and AGEs production. AGEs have been linked to apoptosis of osteoblasts, apoptosis of osteoblast precursor cells (Picke *et al*. 2019) and a reduction in the expression of the osteoblast specific markers Runx2 and Osterix (Picke *et al*. 2019). Runx2 is a master regulator of osteoblast development, osteocalcin expression and other osteoblast associated genes (Rutkovskiy, Stensløkken and Vaage, 2016). Therefore, hyperglycaemia within TCF7L2hom participants would result in impaired osteocalcin expression. However, more work Is needed to confirm the effect on the *Tcf7l2* rs7903146 SNP on OST expression within osteoblasts. Since impaired glucose control was also identified in TCF7L2het carriers, osteocalcin expression may be impaired within these participants too (Lyssenko *et al*.2007). Therefore, in future work, I would suggest the involvement of controls who are not carriers of the *Tcf7l2* rs7903146 SNP. This would allow the comparison of OST expression between *Tcf7l2* rs7903146 SNP carriers (TCF7L2hom) and TCF7L2het) and non-carriers.

I expected the protein release to be lower within TCF7L2hom partcipants too, however the release of carboxylated and uncarboxlayed OST was paradoxically greater within TCF7L2hom participants. OST has a calcium dependent alpha helix protein conformation which has gamma carboxyglutamic acid residues (VS *et al.*, 2013). These gamma carboxyglutamic acid residues enable OST to bind to hydroxyapaptite within the bone matrix, this process is essential for bone mineralisation (VS *et al.*, 2013). The increase in carboxylated OST within TCF7L2hom participants may explain why T2D patients have been found to have normal and increased bone mineral density (BMD) (Eckhardt *et al.*, 2020). BMD is used to measure bone mass, bone mass is related to bone strength and the ability of bones to withstand trauma (VS *et al.*, 2013). Since most of the bone strength has been found to arise from BMD, increased carboxylated OST release from osteoblasts within TCF7L2hom patients may protect patients from bone fracture (VS *et al.*, 2013). The observation that OST has also been found to influence BAp orientation parallel to collagen to maintain bone strength and inhibit bone flexibility, may also explain why carboxylated OST was greater within TCF7L2hom participants (Komori, 2020).

The greater secretion of uncarboxylated OST secretion within TCF7L2hom carriers could be linked to the feedback loops that exist between bone and the pancreas and adiponectin, As

discussed earlier. OST is thought to act has a hormone and is important in controlling glucose metabolism (Kanazawa, 2015). The pioneering work by the Karsenty group suggests that OST possibly regulate glucose metabolism through stimulating the release of insulin secretion and adiponectin (Lee, *et al*. 2007). This is because *OST* knockout within mice resulted in glucose intolerance and hyperglycaemia paired with reduced insulin secretion and adiponectin (Lee, *et al*. 2007). Experiments involving knockout of OST receptors on osteoblasts within mice suggests insulin signalling is responsible for the impact of OST on whole body glucose control (Kanazawa, 2015). Insulin possibly stimulates the expression of *OST* which then further influences insulin release from the pancreas forming a feedforward loop (Kanazawa, 2015). Adiponectin receptors are also found on osteoblasts, which is thought to stimulate AMP-activated protein and initiate expression of *OST* (Kanazawa, 2015). Since OST then stimulates adiponectin release from adipose tissues it is possible that there is also a feed forward loop that exists between bone and adipose tissue (Kanazawa, 2015)**.**

However, results from the investigations by the Karsenty group have been disputed by others (Manolagas, 2020; Moriishi and Komori, 2020). No difference in blood glucose levels and HbA1c was found in both sexes at all ages within WT and OST knockout mice (OCN-/-) with a C57BL/6N genetic background (Moriishi *et al*. 2020). Intraperitoneal glucose tolerance tests after being feeding mice with a NC diet or HFD showed that serum glucose and Insulin levels were not different between WT mice and OCN-/- mice regardless of age and sex (Moriishi *et al*. 2020). No difference was also identified in serum glucose levels within mice fed a NC or HFD at 4 and 8 months of age during insulin tolerance tests (Moriishi *et al*. 2020). This data suggests that OST possibly has little to no effect on glucose metabolism. Results from a diabetic mouse model involving KK/TaJcl mice being fed a HFD showed that exercise led to a decrease in body weight, increase in carboxylated OST but no difference in uncarboxylated OST compared to control mice (Moriishi *et al*. 2020).

Therefore, carboxylated OST could be responsible for glucose metabolism after exercise and uncarboxylated OST possibly plays no role in glucose metabolism improvement after exercise (Moriishi *et al*. 2020). CRISPR/Cas9 induced double allele knockout of *Bglap* and *Bglap2* within mice from a C57BL/6;C3H genetic background showed that random fed blood glucose of 5- to 6-month-old female mice was not found to be different between OCN-/- and WT mice with a (Diegel *et al*. 2020). Fasting blood glucose was also not found to be different between 5- to 6-month-old female OCN-/-mice and WT mice (Diegel *et al*. 2020). Finally, fasting blood glucose was not different for males and female OCN-/- and WT mice were 6 months old (Diegel *et al*. 2020). This data goes against results presented by the Karsenty group and suggests OST possibly has no influence on glucose metabolism.

OST is thought to bind to G protein-coupled receptor class C group 6 member A (GPRC6A) (Pi *et al*. 2021). Evidence suggests OST binds to GPRC6A and stimulates the release of insulin and the incretin GLP-1, which then controls glucose metabolism (Pi *et al*. 2021). Global *Gprc6a* knockout and knockout of *Gprc6a* within skeletal muscle myocytes, pancreatic β-cells, liver hepatocytes resulted in aberrant metabolism control (Pi *et al*. 2021). However, other

Gprc6a knockout mouse models have shown no changes in glucose intolerance, insulin resistance and fat metabolism (Pi *et al*. 2021).

Therefore, OST possibly does not act as a hormone through binding to GPRC6A/GPRC6A and possibly has little to no involvement with glucose control. Lack of reproducibility of the results from the Karsenty group experiment involving in OCN-/- mice raises concerns about our speculation that the *Tcf7l2* risk SNP possibly upregulates the osteocalcin-insulin-adiponectin loop of metabolism control. However, differences in phenotypic outcomes OCN-/- and GPRC6A deficient mouse models could be explained by variation in environmental exposure, differences in phenotyping, environmental exposure, diets used, the genetic background used and method of gene targeting (Pi *et al*. 2021). *GPRC6A* deficient mice seem to have a greater susceptibility to when placed on a HFD compared to OCN-/- mice (Pi *et al*. 2021). Investigations have not been conducted using a diet high in carbohydrates and fat within *OST* and *Gprc6a* deficient mice which could help replicate the western human diet. The differences in metabolic defects may be explained by the genetic background used. For example, C57BL/6J have an exon deletion within the gene *Nicotinamide nucleotide transhydrogenase (Nnt)* (Pi *et al*. 2021). *Nnt* encodes an inner mitochondrial membrane protein that enables electron transport during oxidative phosphorylation (Pi *et al*. 2021). Therefore, deletion of *Nnt* could result in impaired aerobic respiration. This mitochondrial dysfunction could help explain the defective insulin release and glucose metabolism within OCN-/- and GPRC6A negative observed within C57BL/6J compared to C57BL/6N mice. The conflicting data collected when using mouse models highlights the importance of our effort to include osteoblasts from humans known to have T2D.

Using the results from the Karsenty group results, being homozygous for the *Tcf7l2* risk SNP could possibly be beneficial, as patients could have better metabolism control. We are unable to conclude whether uncarboxylated OST and carboxylated OST is indeed greater within TCF7L2hom participants compared to TCF7L2het participants. This is because only 1 participant was found to be heterozygous for the *TCF7L2* risk SNP. Therefore, it is possible that uncarboxylated OST and carboxylated OST is not greater within TCF7L2hom patients. In our investigation *OST* expression was lower for TCF7L2hom carriers when compared with the TCF7L2het carrier. However, carboxylated OST and uncarboxylated OST secretion was greater within the TCF7L2hom carriers. If we take into consideration the evidence from the Karsenty group, whereby OST may act as a hormone for whole body glucose control (Lee, *et al*. 2007). This may divert osteoblasts and osteoclasts function away from bone remodelling, and towards metabolism control. Consuming a high carbohydrate high fat diet, obesity and suffering from T2D have all been implicated in having a negative effect on bones (Shapses and Sukumar, 2012; Pritchard *et al*. 2012; Patsch *et al*. 2013; Pritchard *et al*. 2013; Tian and Yu, 2017; Picke *et al*. 2019; Gkastaris *et al*., 2020; Proia *et al*., 2021). Therefore, it is also possible bone cells are unable balance metabolism control and bone remodeling which may lead to improper bone repair and an increased risk of fracture within T2D patients.

If the controls and patients were properly powered, I would assume that there would be an decrease in OST expression, uncarboxylated OST release and carboxylated OST release within

TCF7L2hom carriers compared to controls. This is based on literature that implies T2D has a negative effect on osteoblasts. However, at this point, I have no additional insight and more work is needed.

This work is important as the effect of T2D has been related to increased fracture risk within T2D patients. T2D, hyperglycaemia, impaired lipid metabolism and AGE production have been reported to have negative effects on osteoblast differentiation and function (Picke *et al.*, 2019). However the effect of T2D on osteoclasts is controversial (Picke *et al.*, 2019). TCF7L2 has been implicated as being associated with the strongest risk of T2D development (Del Bosque-Plata *et al.*, 2021). In addition, ATCF7L2-KO within mice has been linked to impaired glucose control and GSIS (Nguyen-Tu *et al*. 2021). This investigation aimed to find out if ATCF7L2-KO within mice affects bone cell number, bone cell area and bone cell mass. I have tried to link the impaired metabolic effects of ATCF7L2-KO within mice to literature explaining how T2D affects bone cells. Identifying a link between *Tcf7l2* and bone cell dysfunction could explain the increased risk of fracture within T2D patients. Human carriers of the *Tcf7l2* rs7903146 SNP have been found to have reduced insulin secretion and a reduced incretin effect than controls (Lyssenko *et al*. 2007). Therefore, the use of human osteoblast cell cultures within this investigation may have implicated the *Tcf7l2* rs7903146 SNP on osteoblast cell dysfunction.

However, future work is needed to address these questions as the data I have collected has not given any definitive answers to my initial hypotheses. as suggested before, In future work, using more mice would help obtain more data to possibly see significant differences in relation to parameters measured. I would also suggest using laser capture microdissection to specifically isolate osteoblasts and osteoclasts from the bone slices. These bone cells could then be subjected to gene expression profile experiments to determine the effect of genotype and diet on specific bone cell markers. This would help identify if ATCF7L2-KO and diet does result in decreased bone cell proliferation and bone cell function. This would help address the speculations I have made regarding the effect of hyperglycemia and AGEs on bone cells. This could also help address controversy within literature surrounding the effect of T2D on bone cells.

Manipulation of bone cell Wnt signalling within ATCF7L2-KO mice may also be interesting. This could involve breeding ATCF7L2-KO mice to also have osteoblast specific knockout of LRP5/6, Frizzled, or β-cat. Comparisons can then be made with those mice that only have ATCF7L2-KO and mice with ATCF7L2-KO and LRP5/6, Frizzled or β-cat knockout. Wnt signalling has also been shown to inhibit osteoclast development (Kobayashi *et al.*, 2016)Maeda *et al.*, 2019). Therefore, it would be worth investigating the effect of manipulating osteoclast Wnt signalling by introducing osteoclast specific knockout of knockout of LRP5/6, Frizzled, or β-cat, within ATCF7L2-KO mice. The knockout of osteoclasts specific genes, such as RANKL, RANK, CSF-1 and DC STAMP, within ATCF7L2-KO mice may also be interesting. The images the two different types of mice could then be used to obtain bone cell data and comparisons could be made. This could help identify whether ATCF7L2-KO within mice affects the differentiation of bone cells The non-canonical pathway has been shown to induce osteoblast differentiation, increase osteoclast differentiation as well as inhibit osteoclast differentiation (Kobayashi *et al.*, 2016;

Maeda *et al.*, 2019). ATCF7L2-KO mice could be engineered to have knockout mutations in receptors and downstream mediators of the non-canonical wnt signalling pathway. This could involve knockout of the frizzled receptor, receptor tyrosine kinase-like orphan receptor 2, Jun N-terminal kinase and Simian virus 40 promoter factor 1 within bone cells of ATCF7L2-KO. Bone cell data of mice with ATCF7L2-KO and ATCF7L2-KO mice with non-canonical Wnt signalling knockout mutations may shed some light on whether ATCF7L2-KO affects non canonical Wnt signalling.

Osteoblast differentiation is also controlled by BMPs, BMP 2 and 4 have been found to induce RUNX2 expression (Rutkovskiy, Stensløkken and Vaage, 2016). BMP 2 and 4 have also shown to work in tandem with RUNX2 to induce RUNX2 associated gene expression (Rutkovskiy, Stensløkken and Vaage, 2016). Since RUNX2 is a downstream regulator of wnt signalling, this may be pathway that enables osteoblast differentiation when Wnt signalling is not possible. Therefore, knockout of BMP2, BMP4 and their receptors (Bone morphogenic protein receptor I and Bone morphogenic protein receptor II) could be introduced within ATCF7L2-KO mice. This could help identify whether ATCF7L2-KO affects other signalling pathways, other than Wnt signalling, involved in bone cell differentiation. Inflammation has been implicated in bone cell function (Rutkovskiy, Stensløkken and Vaage, 2016). For example, TGFβ has been shown to bind to its receptor on osteoblasts and initiate the SMAD pathway which results in RUNX2 inhibition (Rutkovskiy, Stensløkken and Vaage, 2016). On the other hand, IL-11 inhibits DKK1/2, which prevents DKK1/2 inhibition of Wnt signalling (Rutkovskiy, Stensløkken and Vaage, 2016). ELISA experiments involving serum samples from ATCF7L2-KO mice could be used to detect inflammation markers. This could determine the influence of ATCF7L2-KO on inflammation marker release.

For my results involving osteoblast cell cultures from humans, I mentioned that my results are underpowered. The use of more osteoblast samples from TCF7L2hom participants and TCF7L2het participants may reveal more about whether the *Tcf7l2* rs7903146 SNP influences osteoblast function. I think It would also be useful to involve osteoclast cell cultures from participants. Osteoclasts could be isolated from TCF7L2hom and TCF7L2het participants. The expression and production of osteoclast specific genes could then be tested by PCR and ELISA experiments. This could help identify the influence of the *Tcf7l2* rs7903146 SNP on osteoclast activity and function.

4.2 Conclusion

As far as I am aware, this investigation is the is the first to explore the effect of ATCF7L2-KO within mice on bone cell number, bone cell area and bone cell mass. This is also the first investigation that has used human osteoblast cell cultures, from patients who were carriers of the *Tcf7l2* rs7903146 SNP, to investigate osteoblast function. It is evident that T2D is related to an increased risk of bone fractures within patients (Nicodemus and Folsom 2001; Russo *et al*. 2016; Moayeri *et al*. 2017; Costantini and Conte, 2019; Ntouva *et al*. 2019). I hypothesised that ATCF7L2-KO within mice would have resulted in altered osteoblast function, due to functional impairment and/or loss of osteoblast cell mass. I also hypothesised that ATCF7L2-KO may

impact negatively impact osteoclast cell mass and number, as osteoblasts and osteoclast cell mass are regulated in tandem. Finally, I hypothesised that homozygous carriers of the *TCF7L2* risk allele will have impaired osteoblast function. I found that, within the NC non sampling group, average osteoblast area within ATCF7L2-KO(hom) mice was found to be significantly greater than ATCF7L2-KO(het) mice (p=0.006) (see figure 22a/table 5). However, no significant difference was observed for any of the other parameters measured between ATCF7L2-KO(hom), ATCF7L2-KO(het) and WT mice, when mice were in the same sampling group. As for the human osteoblast data, median OST expression was found to be lower within TCF7L2hom participants compared to the TCF7L2het participant. Carboxylated OST and uncarboxylated OST release was found to be greater within TCF7L2hom participants than the TCF7L2het participant. However, data from this investigation is currently underpowered and further work is needed to confirm these results. Further work is also required to obtain more definitive data regarding the influence of ATCF7L2-KO on bone cell function and the influence of the *Tcf7l2* rs7903146 SNP on osteoblast function.

Figure 30- Results from the human osteoblast experiments and future questions to address.

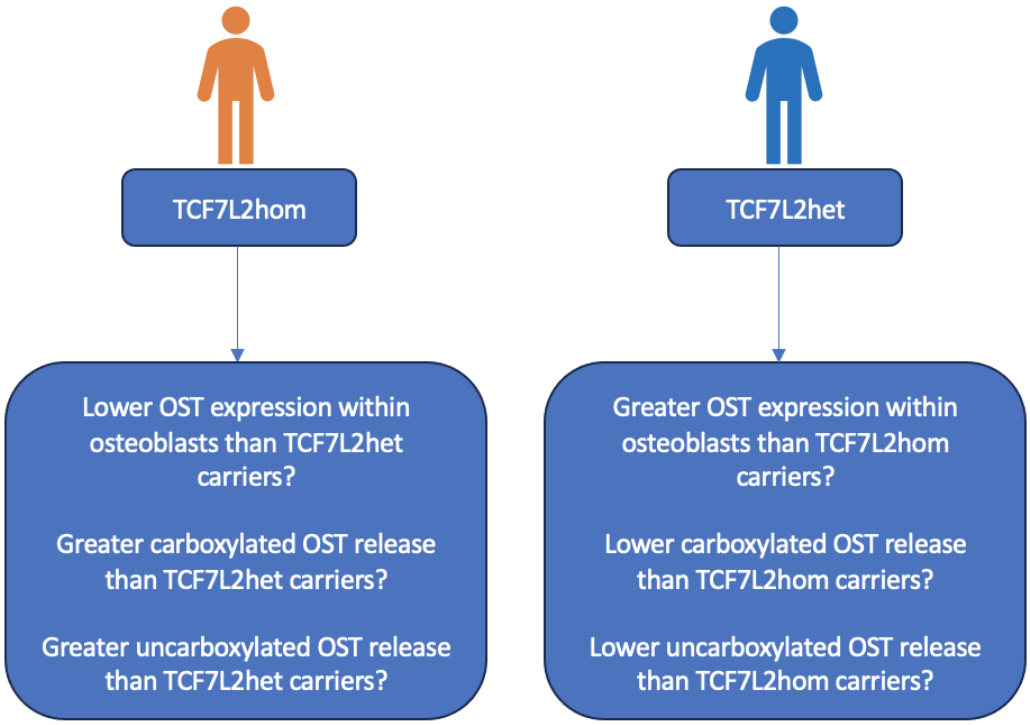

5 Limitations

Upon comparing the results of the NC sampling group and NC non sampling group there appears to be some disagreement in the results shown. Therefore, It is questionable whether sampling group accurately represents the bone images. To confirm this, in the first instance HFD non sampling image analysis needs to be carried out. HFD non sampling will allow a comparison with the HFD sampling data to determine whether there is agreement between the two groups. This raises the question of which sampling group Is the best method for bone analysis.

Our Gpower calculations showed that a fewer total number of mice will be needed to observe a significant difference in the NC sampling group compared to the NC non sampling group. However, non sampling allows you to analyse the entirety of the bone slices and obtain more data. Despite this, the ethical implication on the number of mice needed needs to be taken into consideration. A useful improvement for future work could include analyzing bone slices with immunohistochemistry. This could help specifically target specific bone cells and make cell identification easier. Comparisons with data collected from using images taken with light microscopes can then be conducted to see if there is any discrepancies in cell identification.

An improvement that could have been made to our investigation is obtaining results from ELISA experiments using the protein samples from all the participants. Only 1 uncarboxylated OST result was found using the 100x dilution protein sample from participant 3. This could be explained by a possible loss of OST during the protein isolation using the AllPrep DNA/RNA/Protein Mini Kit. During protein isolation supernatant needed to be discarded and only the protein pellet needed to be resuspended. The protein pellet was difficult to see with the naked eye therefore some of the protein pellet may have been discarded with the supernatant during protein sample isolation. For the carboxylated OST ELISA only results from participants 1 and 3 were able to be obtained. This was due to experimental error within the uncarboxylated OST experiment which led to not enough protein samples from participants 2,4 and 5 left to be used within the carboxylated OST ELISA experiment. Including data from all participants will allow comparisons to be made between the supernatant and protein samples to determine if the protein samples show the same pattern as supernatant samples. The Supernatant and protein samples from Participant 5 were either very low or the absorbance value was lower than the background reading. This could possibly be explained by the cells not looking very healthy under a microscope. The osteoblasts cell cultures were collected and delivered from Denmark which may have led to cellular damage during delivery. This is because is difficult to cells viable for extended periods of time outside their natural environment**.** It is important to observe cells to determine whether the cells should be used within the investigation. If osteoblasts do not look healthy under a microscope it is ideal to discard these cells and not include them within the investigation. However, due to osteoblast samples being limited in this investigation, because of the COVID-19 pandemic, we decided to include the cells from participant 5 in our investigation. Our Gpower calculation indicated that a minimum number of 28 participants (14 TCF7L2hom participants and 14 TCF7L2het participants) would be required to observe a significant difference in OST secretion and production. This seems

likely to be feasible for continuation of this work in the future. Therefore, ideally a greater number of participants would have made observations more valid which will need to be taken into consideration in future investigations.

The *Tcf7l2* risk SNP resides within an intronic region which, at least in islets, is known to lead to changes in the expression of the different transcripts that can result from the *Tcf7l2* gene (Prokunina-Olsson, *et al*. 2009; Nicod *et al*. 2014). However, currently in literature there is no information on the influence of rs7903146 risk SNP on *Tcf7l2* gene transcript levels in osteoblasts. Future work could involve determination of the effect of the rs7903146 risk SNP on the expression of *Tcf7l2* gene transcripts within osteoblasts. The influence of the *Tcf7l2* rs7903146 risk SNP on systemic plasma OST levels within T2D patients may also be worth investigating. Ideally, obtaining osteoblasts from humans who are not carriers of the *Tcf7l2* rs7903146 risk SNP would be used as controls. This may be difficult as the rs7903146 SNP is the most common SNP in the *Tcf7l2* gene (Ding, *et al*. 2018). We could inadvertently be introducing bias into our investigation by obtaining cells during hip replacement surgery from those who are known to be diabetic. Those who are non-diabetic and healthy individuals may be less likely to undergo hip replacement surgery for cells to be taken. Therefore, we are inadvertently going to receive more bone cells from individuals who are TCF7L2hom or TCF7L2het carriers of the *Tcf7l2* rs7903146 risk SNP introducing confirmation bias.

References

Adams, J. D. and Vella, A. (2018) 'What Can Diabetes-Associated Genetic Variation in TCF7L2 Teach Us About the Pathogenesis of Type 2 Diabetes?', Metabolic Syndrome and Related Disorders, 16(8), pp. 383-389.

Ali, O. (2013) 'Genetics of type 2 diabetes', World Journal of Diabetes, 4(4), pp. 114.

Alsmadi, O., Al-Rubeaan, K., Mohamed, G., Alkayal, F., Al-Saud, H., Al-Saud, N. A., Al-Daghri, N., Mohammad, S. and Meyer, B. F. (2008) 'Weak or no association of TCF7L2 variants with Type 2 diabetes risk in an Arab population', BMC Medical Genetics, 9(1), pp. 72.

Anello, M., Lupi, R., Spampinato, D., Piro, S., Masini, M., Boggi, U., Del Prato, S., Rabuazzo, A. M., Purrello, F. and Marchetti, P. (2005) 'Functional and morphological alterations of mitochondria in pancreatic beta cells from type 2 diabetic patients', Diabetologia, 48(2), pp. 282-289.

Araki, E., Oyadomari, S. and Mori, M. (2003) 'Endoplasmic Reticulum Stress and Diabetes Mellitus.', Internal Medicine, 42(1), pp. 7-14.

Argilés, J. M., Campos, N., Lopez-Pedrosa, J. M., Rueda, R. and Rodriguez-Mañas, L. (2016) 'Skeletal Muscle Regulates Metabolism via Interorgan Crosstalk: Roles in Health and Disease', Journal of the American Medical Directors Association, 17(9), pp. 789-796.

Aronson, D. and Rayfield, E. J. (2002) Cardiovascular Diabetology, 1(1), pp. 1.

Assaad-Khalil, S., Elebrashy, I., Afify, Y., Abdelmordy, B., Zakaria, W., Aboushady, R., Zanaty, S., Basiouny, E., Ibrahim, A., Sallam, R. and Anan, I. (2017) 'The Financial Burden of Diabetes Mellitus Type 1 And Type 2 In Egypt', Value in Health, 20(9), pp. A477.

Assmann, T. S., Duarte, G. C. K., Rheinheimer, J., Cruz, L. A., Canani, L. H. and Crispim, D. (2014) 'The TCF7L2 rs7903146 (C/T) polymorphism is associated with risk to type 2 diabetes mellitus in Southern-Brazil', Arquivos Brasileiros de Endocrinologia & Metabologia, 58(9), pp. 918-925.

Aubrey, B. J., Kelly, G. L., Janic, A., Herold, M. J. and Strasser, A. (2018) 'How does p53 induce apoptosis and how does this relate to p53-mediated tumour suppression?', Cell Death & Differentiation, 25(1), pp. 104-113.

Babij, P., Zhao, W., Small, C., Kharode, Y., Yaworsky, P. J., Bouxsein, M. L., Reddy, P. S., Bodine, P. V., Robinson, J. A., Bhat, B., Marzolf, J., Moran, R. A. and Bex, F. (2003) 'High Bone Mass in Mice Expressing a Mutant LRP5 Gene', Journal of Bone and Mineral Research, 18(6), pp. 960-974.

Bahaaeldin, A. M., Seif, A. A., Hamed, A. I. and Kabiel, W. A. Y. (2020) 'Transcription Factor 7-Like-2 (TCF7L2) rs7903146 (C/T) Polymorphism in Patients with Type 2 Diabetes Mellitus', Dubai Diabetes and Endocrinology Journal, 26(3), pp. 112-118.

Bao, Q., Chen, S., Qin, H., Feng, J., Liu, H., Liu, D., Li, A., Shen, Y., Zhao, Y., Li, J. and Zong, Z. (2017) 'An appropriate Wnt/β-catenin expression level during the remodeling phase is required for improved bone fracture healing in mice', Scientific Reports, 7(1).

Bennett, C. N., Longo, K. A., Wright, W. S., Suva, L. J., Lane, T. F., Hankenson, K. D. and Macdougald, O. A. (2005) 'Regulation of osteoblastogenesis and bone mass by Wnt10b', Proceedings of the National Academy of Sciences, 102(9), pp. 3324-3329.

Berbudi , A., Rahmadika , N., Tjahjadi , A. I. and Ruslami, R. (2020) 'Type 2 Diabetes and its Impact on the Immune System', Current Diabetes Reviews, 16(5), pp. 442–449.

Boskey, A. L. and Coleman, R. (2010) 'Aging and Bone', Journal of Dental Research, 89(12), pp. 1333-1348.

Boucher, J., Kleinridders, A. and Kahn, C. R. (2014) 'Insulin Receptor Signaling in Normal and Insulin-Resistant States', Cold Spring Harbor Perspectives in Biology, 6(1), pp. a009191-a009191.

Boyce, B. F. and Xing, L. (2008) 'Functions of RANKL/RANK/OPG in bone modeling and remodeling', Archives of Biochemistry and Biophysics, 473(2), pp. 139-146.

Boyden, L. M., Mao, J., Belsky, J., Mitzner, L., Farhi, A., Mitnick, M. A., Wu, D., Insogna, K. and Lifton, R. P. (2002) 'High Bone Density Due to a Mutation in LDL-Receptor–Related Protein 5', New England Journal of Medicine, 346(20), pp. 1513-1521.

Boyle, W. J., Simonet, W. S. and Lacey, D. L. (2003) 'Osteoclast differentiation and activation', Nature, 423, pp. 337–342

Brown, J. E. (2012) 'Dysregulated adipokines in the pathogenesis of type 2 diabetes and vascular disease', The British Journal of Diabetes & Vascular Disease, 12(5), pp. 249-254.

Cannon, A., Handelsman, Y., Heile, M. and Shannon, M. (2018) 'Burden of Illness in Type 2 Diabetes Mellitus', Journal of Managed Care & Specialty Pharmacy, 24(9-a Suppl), pp. S5-S13.

Carey, I. M., Critchley, J. A., Dewilde, S., Harris, T., Hosking, F. J. and Cook, D. G. (2018) 'Risk of Infection in Type 1 and Type 2 Diabetes Compared With the General Population: A Matched Cohort Study', Diabetes Care, 41(3), pp. 513-521.

Castillo-Armengol, J., Fajas, L. and Lopez-Mejia, I. C. (2019) 'Inter-organ communication: a gatekeeper for metabolic health', EMBO reports, 20(9).

Catalfamo, D., Britten, T., Storch, D., Calderon, N., Sorenson, H. and Wallet, S. (2013) 'Hyperglycemia induced and intrinsic alterations in type 2 diabetes-derived osteoclast function', Oral Diseases, 19(3), pp. 303-312.

Cauchi, S. E., I. El Achhab, Y. Mtiraoui, N. Chaieb, L. Salah, D. Nejjari, C. Labrune, Y. Yengo, L. Beury, D. Vaxillaire, M. Mahjoub, T. Chikri, M. Froguel, P. (2012) 'European genetic variants associated with type 2 diabetes in North African Arabs', Diabetes & Metabolism, 38(4), pp. 316-323.

Cerf, M. E. (2013) 'Beta Cell Dysfunction and Insulin Resistance', Frontiers in Endocrinology, 4(37).

Chang, Y.-C., Chang, T.-J., Jiang, Y.-D., Kuo, S.-S., Lee, K.-C., Chiu, K. C. and Chuang, L.-M. (2007) 'Association Study of the Genetic Polymorphisms of the Transcription Factor 7-Like 2 (TCF7L2) Gene and Type 2 Diabetes in the Chinese Population', Diabetes, 56(10), pp. 2631-2637.

Chen, L., Magliano, D. and Zimmet, P. (2011) 'The worldwide epidemiology of type 2 diabetes mellitus—present and future perspectives', Nature Reviews Endocrinoglogy, 8, pp. 228-236.

Chen, X., Ayala, I., Shannon, C., Fourcaudot, M., Acharya, N. K., Jenkinson, C. P., Heikkinen, S. and Norton, L. (2018) 'The Diabetes Gene and Wnt Pathway Effector TCF7L2 Regulates Adipocyte Development and Function', Diabetes, 67(4), pp. 554-568.

Chen-zhou Wu, Yi-hang Yuan, Hang-hang Liu, Shen-sui Li, Bo-wen Zhang, Wen Chen, Zi-jian An, Si-yu Chen, Yong-zhi Wu, Bo Han, Li, C.-j. and Li, L.-j.

Cheng, C. Y. Y., Chu, J. Y. S. and Chow, B. K. C. (2011) 'Central and Peripheral Administration of Secretin Inhibits Food Intake in Mice through the Activation of the Melanocortin System', Neuropsychopharmacology, 36(2), pp. 459-471.

Cho, Y. M., Kim, T. H., Lim, S., Choi, S. H., Shin, H. D., Lee, H. K., Park, K. S. and Jang, H. C. (2009) 'Type 2 diabetes-associated genetic variants discovered in the recent genome-wide association studies are related to gestational diabetes mellitus in the Korean population', Diabetologia, 52(2), pp. 253-261.

Choe, S. S., Huh, J. Y., In, J. H., Kim, J. I. and Ki m, J. B. (2016) 'Adipose Tissue Remodeling: Its Role in Energy Metabolism and Metabolic Disorders', frontiers in Endocrinology, 7(30).

Clarke, B. (2008) 'Normal Bone Anatomy and Physiology', Clinical Journal of the American Society of Nephrology, 3(Supplement 3), pp. S131-S139.

Clement, K., Hercberg, S., Passinge, B., Galan, P., Varroud-Vial, M., Shuldiner, A., Beamer, B., Charpentier, G., Guy-Grand, B., Froguel, P. and Vaisse, C. (2000) 'The Pro115Gln and Pro12Ala

PPAR gamma gene mutations in obesity and type 2 diabetes', International Journal of Obesity, 24(3), pp. 391-393.

Confavreux, C. B., Szulc, P., Casey, R., Varennes, A., Goudable, J. and Chapurlat, R. D. (2014) 'Lower serum osteocalcin is associated with more severe metabolic syndrome in elderly men from the MINOS cohort', European Journal of Endocrinology, 171(2), pp. 275-283.

Costantini, S. and Conte, C. (2019) 'Bone health in diabetes and prediabetes', World Journal of Diabetes, 10(8), pp. 421-445.

Cropano, C., Santoro, N., Groop, L., Dalla Man, C., Cobelli, C., Galderisi, A., Kursawe, R., Pierpont, B., Goffredo, M. and Caprio, S. (2017) 'The rs7903146 Variant in the TCF7L2 Gene Increases the Risk of Prediabetes/Type 2 Diabetes in Obese Adolescents by Impairing β-Cell Function and Hepatic Insulin Sensitivity', Diabetes Care, 40(8), pp. 1082-1089.

D el Bosque-Plata, L., Martínez-Martínez, E., Ángel Espinoza-Camacho, M., Gragnoli and Claudia (2021) 'The Role of TCF7L2 in Type 2 Diabetes', Perspectives In Diabetes, 70(6), pp. 1220–1228.

Da Silva Xavier, G., Bellomo, E. A., Mcginty, J. A., French, P. M. and Rutter, G. A. (2013) 'Animal Models of GWAS-Identified Type 2 Diabetes Genes', Journal of Diabetes Research, 2013, pp. 1-12.

Da Silva Xavier, G., Loder, M. K., Mcdonald, A., Tarasov, A. I., Carzaniga, R., Kronenberger, K., Barg, S. and Rutter, G. A. (2009) 'TCF7L2 Regulates Late Events in Insulin Secretion From Pancreatic Islet -Cells', Diabetes, 58(4), pp. 894-905.

Da Silva Xavier, G., Mondragon, A., Sun, G., Chen, L., Mcginty, J. A., French, P. M. and Rutter, G. A. (2012) 'Abnormal glucose tolerance and insulin secretion in pancreas-specific Tcf7l2-null mice', Diabetologia, 55(10), pp. 2667-2676.

Dallas, S. L., Prideaux, M. and Bonewald, L. F. (2013) 'The Osteocyte: An Endocrine Cell … and More', Endocrine Reviews, 34(5), pp. 658-690.

de la Monte, S. M. (2012) 'Contributions of Brain Insulin Resistance and Deficiency in Amyloid-Related Neurodegeneration in Alzheimer's Disease', Drugs, 72, pp. 49-66.

Defronzo, R. A. and Tripathy, D. (2009) 'Skeletal Muscle Insulin Resistance Is the Primary Defect in Type 2 Diabetes', Diabetes Care, 32(suppl_2), pp. S157-S163.

Delmas, P. D., Eastell , R., Garnero, P., Seibel, M. J. and Stepan, J. (2000) 'The Use of Biochemical Markers of Bone Turnover in Osteoporosis', Osteoporosis Inrernational foundation, 6, pp. 2-17.

Dianna J Magliano, Edward J Boyko (Co-chair), Beverley, Balkau, Noel Barengo, E. B., Abdul Basit, Dominika, Bhata, C. B., Gillian Booth, Bertrand Cariou, Juliana, Chan, H. C., Lei Chen, Tawanda Chivese, Dana Dabalea,, Hema Divakar, D. D., Bruce B Duncan, Michael Fang, Ghazal, Fazli, C. F., Kathryn Foti, Laercio Franco, Edward Gregg,, Leonor Guariguata, A. G., Anthony Hanley, Jessica L Harding,, William H Herman, C. H., Cecilia Høgfeldt, Elbert Huang,, Adam Hulman, S. J., Alicia J Jenkins, Seung Jin Han, Calvin, Ke, E. L. K., Shihchen Kuo, Jean Lawrence, Dinky Levitt,, Xia Li, L. L., Paz Lopez-Doriga Ruez, Andrea Luk,, Ronald C Ma, J. M., Louise Maple-Brown, Jean-Claude, Mbanya, N. M., Fernando Mijares Diaz, Hiliary Monteith,, Ayesha Motala, E. N., Graham D Ogle, Katherine, Ogurstova, R. O., Bige Ozkan, Emily Papadimos, Chris, Patterson, M. P., Cate Pihoker, Justin Porter, Camille Powe,, Ambady Ramachandran, G. R., Mary Rooney, Julian Sacre,, Elizabeth Selvin, B. S., Jonathan E Shaw, David Simmons,, Caroline Stein, J. S., Olive Tang, Justin Echouffo, Tcheugui, J. V., Amelia Wallace, Pandora L Wander,, Donald Warne, M. W., Sarah Wild, Jencia Wong, Yuting, Xie, X. Y., Lili Yuen, Philip Zeitler, Ping Zhang, Sui Zhang, and Xinge Zhang, Z. Z.

Diegel, C. R., Hann, S., Ayturk, U. M., Hu, J. C. W., Lim, K.-E., Droscha, C. J., Madaj, Z. B., Foxa, G. E., Izaguirre, I., Transgenics Core, V. V. A., Paracha, N., Pidhaynyy, B., Dowd, T. L., Robling, A. G., Warman, M. L. and Williams, B. O. (2020) 'An osteocalcin-deficient mouse strain without endocrine abnormalities', PLOS Genetics, 16(5), pp. e1008361.

Ding, W., Xu, L., Zhang, L., Han, Z., Jiang, Q., Wang, Z. and Jin, S. (2018) 'Meta-analysis of association between TCF7L2 polymorphism rs7903146 and type 2 diabetes mellitus', BMC Medical Genetics, 19(1).

Dlasková , A., Spacek , T., Santorová , J., Plecitá-Hlavatá , L., Berková , Z., Saudek , F., Lessard , M., Bewersdorf , J. and Jezek, P. (2010) '4Pi microscopy reveals an impaired three-dimensional mitochondrial network of pancreatic islet beta-cells, an experimental model of type-2 diabetes', Biochimica et biophysica acta, 1797(6-7), pp. 1327-1341.

Donath, M. Y., Ehses, J. A., Maedler, K., Schumann, D. M., Ellingsgaard, H., Eppler, E. and Reinecke, M. (2005) 'Mechanisms of -Cell Death in Type 2 Diabetes', Diabetes, 54(Supplement 2), pp. S108-S113.

Dou, H., Ma, E., Yin, L., Jin, Y. and Wang, H. (2013) 'The Association between Gene Polymorphism of TCF7L2 and Type 2 Diabetes in Chinese Han Population: A Meta-Analysis', PLoS ONE, 8(3), pp. e59495.

Dröse, S. and Brandt, U. (2012) Molecular Mechanisms of Superoxide Production by the Mitochondrial Respiratory Chain. Advances in Experimental Medicine and Biology New York: Springer.

Ducy, P., Desbois, C., Boyce, B., Pinero, G., Story, B., Dunstan, C., Smith, E., Bonadio, J., Goldstein, S., Gundberg, C., Bradley, A. and Karsenty, G. (1996) 'Increased bone formation in osteocalcin-deficient mice', Nature, 382(6590), pp. 448-452.

Dunmore, S. J. and Brown, J. E. P. (2013) 'The role of adipokines in β-cell failure of type 2 diabetes', Journal of Endocrinology, 216(1), pp. T37-T45.

Díaz-López, A., Bulló, M., Juanola-Falgarona, M., Martínez-González, M. A., Estruch, R., Covas, M.-I., Arós, F. and Salas-Salvadó, J. (2013) 'Reduced Serum Concentrations of Carboxylated and Undercarboxylated Osteocalcin Are Associated With Risk of Developing Type 2 Diabetes Mellitus in a High Cardiovascular Risk Population: A Nested Case-Control Study', The Journal of Clinical Endocrinology & Metabolism, 98(11), pp. 4524-4531.

Eckhardt, B. A., Rowsey, J. L., Thicke, B. S., Fraser, D. G., O'Grady, K. L., Bondar, O. P., Hines, J. M., Singh, R. J., Thoreson, A. R., Rakshit, K., Lagnado, A. B., Passos, J. F., Vella, A., Matveyenko, A. V., Khosla, S., Monroe, D. G. and Farr, J. N. (2020) 'Accelerated osteocyte senescence and skeletal fragility in mice with type 2 diabetes', JCI Insight, 5(9).

Eguchi, J., Wang, X., Yu, S., Kershaw, E., Erin, Chiu, C., Patricia, Dushay, J., Estall, L., Jennifer, Klein, U., Maratos-Flier, E. and Rosen, D., Evan (2011) 'Transcriptional Control of Adipose Lipid Handling by IRF4', Cell Metabolism, 13(3), pp. 249-259.

Erion , D. M., Park , H.-J. and Lee, H.-Y. (2016) 'The role of lipids in the pathogenesis and treatment of type 2 diabetes and associated co-morbidities', BMB Reports, 49(3), pp. 139–148.

Fajardo, R. J., Karim, L., Calley, V. I. and Bouxsein, M. L. (2014) 'A Review of Rodent Models of Type 2 Diabetic Skeletal Fragility', Journal of Bone and Mineral Research, 29(5), pp. 1025-1040.

Faul, F., Erdfelder, E., Buchner, A. and Lang, A.-G. (2009) 'Statistical power analyses using G*Power 3.1: Tests for correlation and regression analyses', Behavior Research Methods, 41(4), pp. 1149-1160.

Faul, F., Erdfelder, E., Lang, A.-G. and Buchner, A. (2007) 'G*Power 3: A flexible statistical power analysis program for the social, behavioral, and biomedical sciences', Behavior Research Methods, 39(2), pp. 175-191.

Feldman, M., Friedman, L. S., Brandt, L. J., Chung, R. T., Rubin, D. T. and Wilcox, C. M. (2021) Sleisenger and Fordtran's gastrointestinal and liver disease: pathophysiology, diagnosis, management . Elsevier health sciences.

Ferron, M., Mckee, M. D., Levine, R. L., Ducy, P. and Karsenty, G. (2012) 'Intermittent injections of osteocalcin improve glucose metabolism and prevent type 2 diabetes in mice', Bone, 50(2), pp. 568-575.

Firdous, P., Nissar, K., Ali , S., Ganai, B. A., Shabir, U., Hassan, T. and Masoodi, S. R. (2018) 'Genetic Testing of Maturity-Onset Diabetes of the Young Current Status and Future Perspectives', Frontiers In Endocrinology.

Florencio-Silva, R., Sasso, G. R. D. S., Sasso-Cerri, E., Simões, M. J. and Cerri, P. S. (2015) 'Biology of Bone Tissue: Structure, Function, and Factors That Influence Bone Cells', BioMed Research International, 2015, pp. 1-17.

Fonseca, V. A. (2009) 'Defining and Characterizing the Progression of Type 2 Diabetes', Diabetes Care, 32(suppl_2), pp. S151-S156.

Franks, P. W., Rolandsson, O., Debenham, S. L., Fawcett, K. A., Payne, F., Dina, C., Froguel, P., Mohlke, K. L., Willer, C., Olsson, T., Wareham, N. J., Hallmans, G., Barroso, I. and Sandhu, M. S. (2008) 'Replication of the association between variants in WFS1 and risk of type 2 diabetes in European populations', Diabetologia, 51(3), pp. 458-463.

Fu , Z., Gilbert , E. R. and Liu, D. (2013) 'Regulation of Insulin Synthesis and Secretion and Pancreatic Beta-Cell Dysfunction in Diabetes', Current Diabetes Reviews, 9(1), pp. 25-53.

Furuta, H., Furuta, M., Sanke, T., Ekawa, K., Hanabusa, T., Nishi, M., Sasaki, H. and Nanjo, K. (2002) 'Nonsense and Missense Mutations in the Human Hepatocyte Nuclear Factor-1β Gene (TCF2) and Their Relation to Type 2 Diabetes in Japanese', The Journal of Clinical Endocrinology & Metabolism, 87(8), pp. 3859-3863.

Galicia-Garcia, U., Benito-Vicente, A., Jebari, S., Larrea-Sebal, A., Siddiqi, H., Uribe, K. B., Ostolaza, H. and Martín, C. (2020) 'Pathophysiology of Type 2 Diabetes Mellitus', International Journal of Molecular Sciences, 21(17), pp. 6275.

Ganasegeran, K., Hor, C. P., Jamil, M. F. A., Loh, H. C., Noor, J. M., Hamid, N. A., Suppiah, P. D., Abdul Manaf, M. R., Ch'Ng, A. S. H. and Looi, I. (2020) 'A Systematic Review of the Economic Burden of Type 2 Diabetes in Malaysia', International Journal of Environmental Research and Public Health, 17(16), pp. 5723.

Geoghegan, G., Simcox, J., Seldin, M. M., Parnell, T. J., Stubben, C., Just, S., Begaye, L., Lusis, A. J. and Villanueva, C. J. (2019) 'Targeted deletion of Tcf7l2 in adipocytes promotes adipocyte hypertrophy and impaired glucose metabolism', Molecular Metabolism, 24, pp. 44-63.

Giacco, F. and Brownlee, M. (2010) 'Oxidative stress and diabetic complications', Circulation research, 107(9), pp. 1058-1070.

Gkastaris , K., Goulis , D. G., Potoupnis , M., Anastasilakis , A. D. and Kapetanos, G. (2020) 'Obesity, osteoporosis and bone metabolism', International Society of Musculoskeletal and Neuronal Interactions, 20(3).

Gloyn, A. L., Braun, M. and Rorsman, P. (2009) 'Type 2 Diabetes Susceptibility Gene TCF7L2 and Its Role in -Cell Function', Diabetes, 58(4), pp. 800-802.

Gloyn, A. L., Weedon, M. N., Owen, K. R., Turner, M. J., Knight, B. A., Hitman, G., Walker, M., Levy, J. C., Sampson, M., Halford, S., Mccarthy, M. I., Hattersley, A. T. and Frayling, T. M. (2003) 'Large-Scale Association Studies of Variants in Genes Encoding the Pancreatic -Cell KATP Channel Subunits Kir6.2 (KCNJ11) and SUR1 (ABCC8) Confirm That the KCNJ11 E23K Variant Is Associated With Type 2 Diabetes', Diabetes, 52(2), pp. 568-572.

Gong, Y., Slee, R. B., Fukai, N., Rawadi, G., Roman-Roman, S., Reginato, A. M., Wang, H., Cundy, T., Glorieux, F. H., Lev, D., Zacharin, M., Oexle, K., Marcelino, J., Suwairi, W., Heeger, S., Sabatakos, G., Apte, S., Adkins, W. N., Allgrove, J., Arslan-Kirchner, M., Batch, J. A., Beighton, P., Black, G. C. M., Boles, R. G., Boon, L. M., Borrone, C., Brunner, H. G., Carle, G. F., Dallapiccola, B., De Paepe, A., Floege, B., Halfhide, M. L., Hall, B., Hennekam, R. C., Hirose, T., Jans, A., Jüppner, H., Kim, C. A., Keppler-Noreuil, K., Kohlschuetter, A., Lacombe, D., Lambert, M., Lemyre, E., Letteboer, T., Peltonen, L., Ramesar, R. S., Romanengo, M., Somer, H., Steichen-Gersdorf, E., Steinmann, B., Sullivan, B., Superti-Furga, A., Swoboda, W., Van Den Boogaard, M.-J., Van Hul, W., Vikkula, M., Votruba, M., Zabel, B., Garcia, T., Baron, R., Olsen, B. R. and Warman, M. L. (2001) 'LDL Receptor-Related Protein 5 (LRP5) Affects Bone Accrual and Eye Development', Cell, 107(4), pp. 513-523.

Grant , S. F. A. (2019) 'The TCF7L2 Locus: A Genetic Window Into the Pathogenesis of Type 1 and Type 2 Diabetes', Diabetes Care, 42(9), pp. 1624–1629.

Grant, S. F. A., Thorleifsson, G., Reynisdottir, I., Benediktsson, R., Manolescu, A., Sainz, J., Helgason, A., Stefansson, H., Emilsson, V., Helgadottir, A., Styrkarsdottir, U., Magnusson, K. P., Walters, G. B., Palsdottir, E., Jonsdottir, T., Gudmundsdottir, T., Gylfason, A., Saemundsdottir, J., Wilensky, R. L., Reilly, M. P., Rader, D. J., Bagger, Y., Christiansen, C., Gudnason, V., Sigurdsson, G., Thorsteinsdottir, U., Gulcher, J. R., Kong, A. and Stefansson, K. (2006) 'Variant of transcription factor 7-like 2 (TCF7L2) gene confers risk of type 2 diabetes', Nature Genetics, 38(3), pp. 320-323.

Graves, D., T (2008) 'Diabetic complications and dysregulated innate immunity', Frontiers in Bioscience, 13(13), pp. 1227.

Guan, Y., Yan, L. H., Liu, X. Y., Zhu, X. Y., Wang, S. Z. and Chen , L. M. (2016) 'Correlation of the TCF7L2 (rs7903146) polymorphism with an enhanced risk of type 2 diabetes mellitus: a meta-analysis', Genetic and Molecular Research.

Guilherme, A., Virbasius, J. V., Puri, V. and Czech, M. P. (2008) 'Adipocyte dysfunctions linking obesity to insulin resistance and type 2 diabetes', Nature Reviews Molecular Cell Biology, 9(5), pp. 367-377.

Guo, T., Hanson, R. L., Traurig, M., Li Muller, Y., Ma, L., Mack, J., Kobes, S., Knowler, W. C., Bogardus, C. and Baier, L. J. (2007) 'TCF7L2 Is Not a Major Susceptibility Gene for Type 2 Diabetes in Pima Indians: Analysis of 3,501 Individuals', Diabetes, 56(12), pp. 3082-3088.

Gutierrez-Aguilar, R. and Woods, S. C. (2011) 'Nutrition and L and K-enteroendocrine cells', Current Opinion in Endocrinology, Diabetes & Obesity, 18(1), pp. 35-41.

Haeusler, R. A., Mcgraw, T. E. and Accili, D. (2018) 'Biochemical and cellular properties of insulin receptor signalling', Nature Reviews Molecular Cell Biology, 19(1), pp. 31-44.

Hamann , C., Goettsch , C., Mettelsiefen , J., Henkenjohann , V., Rauner , M., Hempel , U., Bernhardt , R., Fratzl-Zelman , N., Roschger , P., Rammelt , S., Peter Günther , K., Hofbauer and C., L. (2011) 'Delayed bone regeneration and low bone mass in a rat model of insulin-resistant type 2 diabetes mellitus is due to impaired osteoblast function', American Journal Of Physiology.

Hamann, C., Rauner, M., Höhna, Y., Bernhardt, R., Mettelsiefen, J., Goettsch, C., Günther, K.-P., Stolina, M., Han, C.-Y., Asuncion, F. J., Ominsky, M. S. and Hofbauer, L. C. (2013) 'Sclerostin antibody treatment improves bone mass, bone strength, and bone defect regeneration in rats with type 2 diabetes mellitus', Journal of Bone and Mineral Research, 28(3), pp. 627-638.

Harding, H. P. and Ron, D. (2002) 'Endoplasmic Reticulum Stress and the Development of Diabetes: A Review', Diabetes, 51(Supplement 3), pp. S455-S461.

Hardouin, P., Rharass, T. and Lucas, S. (2016) 'Bone Marrow Adipose Tissue: To Be or Not To Be a Typical Adipose Tissue?', Frontiers In Endocrinology, 7(85).

Hattersley, A. T. (2007) 'Prime suspect: the TCF7L2 gene and type 2 diabetes risk', Journal of Clinical Investigation, 117(8), pp. 2077-2079.

Hauschka, P. V., Lian, J. B. and Gallop, P. M. (1975) 'Direct identification of the calcium-binding amino acid, gamma-carboxyglutamate, in mineralized tissue.', Proceedings of the National Academy of Sciences, 72(10), pp. 3925-3929.

Herder , C., Rathmann , W., Strassburger , K., Finner , H., Grallert , H., Huth , C., Meisinger , C., Gieger , C., Martin , S., Giani , G., Scherbaum , W. A., Wichmann , H.-E. and Illig, T. (2008) 'Variants of the PPARG, IGF2BP2, CDKAL1, HHEX, and TCF7L2 genes confer risk of type 2 diabetes independently of BMI in the German KORA studies', Hormone and metabolic research, 40(10).

Hex, N., Barlett, C., Wright, D., Taylor, M. and Varley, D. (2012) 'Estimating the current and future costs of Type 1 and

Type 2 diabetes in the UK, including direct health costs

and indirect societal and productivity costs', Diabetic Medicine, 29(7), pp. 855-862.

Holmen, S. L., Giambernardi, T. A., Zylstra, C. R., Buckner-Berghuis, B. D., Resau, J. H., Hess, J. F., Glatt, V., Bouxsein, M. L., Ai, M., Warman, M. L. and Williams, B. O. (2004) 'Decreased BMD and Limb Deformities in Mice Carrying Mutations in Both Lrp5 and Lrp6', Journal of Bone and Mineral Research, 19(12), pp. 2033-2040.

Houschyar , K. S., Tapking , C., Borrelli, M. R., Popp , D., Duscher , D., Maan , Z. N., Chelliah , M. P., Li , J., Harati , K., Christoph, Susanne Rein , Dominik Pförringer , Georg Reumuth , Grieb, G., Sylvain Mouraret , Mehran Dadras , Wagner, J. M., Jungul Y. Cha , Frank Siemers , Marcus Lehnhardt and 1, B. B.

Houschyar , K. S., Tapking , C., Borrelli, M. R., Popp , D., Duscher , D., Maan , Z. N., Chelliah , M. P., Li , J., Harati , K., Wallner, C., Rein , S., Pförringer , D., Reumuth , G., Grieb, G., Mouraret , S., Dadras , M., Wagner, J. M., Cha , J. Y., Siemers , F., Lehnhardt , M. and Behr, B. (2018) 'Wnt Pathway in Bone Repair and Regeneration – What Do We Know So Far', Frontiers in cell and developmental biology, 6(170).

Howard, E. W., Benton, R., Ahern-Moore, J. and Tomasek, J. J. (1996) 'Cellular Contraction of Collagen Lattices Is Inhibited by Nonenzymatic Glycation', Experimental Cell Research, 228(1), pp. 132-137.

Hu , Z., Ma, C., Liang, Y., Zou, S. and Liu, X. (2019) 'Osteoclasts in bone regeneration under type 2 diabetes mellitus', Acta Biomaterialia, 84(15), pp. 402-413.

Huang, X., Liu, G., Guo, J. and Su, Z. (2018a) 'The PI3K/AKT pathway in obesity and type 2 diabetes', International Journal of Biological Sciences, 14(11), pp. 1483-1496.

Huang, Z.-Q., Liao, Y.-Q., Huang, R.-Z., Chen, J.-P. and Sun, H.-L. (2018b) 'Possible role of TCF7L2 in the pathogenesis of type 2 diabetes mellitus', Biotechnology & Biotechnological Equipment, 32(4), pp. 830-834.

Huang, Z.-Q., Liao, Y.-Q., Huang, R.-Z., Chen, J.-P. and Sun, H.-L. (2018c) 'Possible role of TCF7L2 in the pathogenesis of type 2 diabetes mellitus', Biotechnology & Biotechnological Equipment, 32(4), pp. 830-834.

Humphries, S. E., Gable, D., Cooper, J. A., Ireland, H., Stephens, J. W., Hurel, S. J., Li, K. W., Palmen, J., Miller, M. A., Cappuccio, F. P., Elkeles, R., Godsland, I., Miller, G. J. and Talmud, P. J. (2006) 'Common variants in the TCF7L2 gene and predisposition to type 2 diabetes in UK European Whites, Indian Asians and Afro-Caribbean men and women', Journal of Molecular Medicine, 84(12), pp. 1005-1014.

Hygum, K., Starup-Linde, J., Harsløf, T., Vestergaard, P. and Langdahl, B. L. (2017) 'MECHANISMS IN ENDOCRINOLOGY: Diabetes mellitus, a state of low bone turnover – a systematic review and meta-analysis', European Journal of Endocrinology, 176(3), pp. R137-R157.

Ichiro Hino , S., Tanji , C., Nakayama , K. I. and Kikuchi, A. (2005) 'Phosphorylation of β-Catenin by Cyclic AMP-Dependent Protein Kinase Stabilizes β-Catenin through Inhibition of Its Ubiquitination', Molecular and cellular biology.

Ionova-Martin, S. S., Do, S. H., Barth, H. D., Szadkowska, M., Porter, A. E., Ager, J. W., Ager, J. W., Alliston, T., Vaisse, C. and Ritchie, R. O. (2010) 'Reduced size-independent mechanical properties of cortical bone in high-fat diet-induced obesity', Bone, 46(1), pp. 217-225.

Ionova-Martin, S. S., Wade, J. M., Tang, S., Shahnazari, M., Ager, J. W., Lane, N. E., Yao, W., Alliston, T., Vaisse, C. and Ritchie, R. O. (2011) 'Changes in cortical bone response to high-fat diet from adolescence to adulthood in mice', Osteoporosis International, 22(8), pp. 2283-2293.

Ip, W., Chiang, Y.-T. A. and Jin, T. (2012) 'The involvement of the wnt signaling pathway and TCF7L2 in diabetes mellitus: The current understanding, dispute, and perspective', Cell & Bioscience, 2(1), pp. 28.

Ip, W., Shao, W., Song, Z., Chen, Z., Wheeler, M. B. and Jin, T. (2015) 'Liver-Specific Expression of Dominant-Negative Transcription Factor 7-Like 2 Causes Progressive Impairment in Glucose Homeostasis', Diabetes, 64(6), pp. 1923-1932.

Ip , W. S., Weijuan, Chiang , Y.-t. A., Jin and Tianru (2012) 'The Wnt signaling pathway effector TCF7L2 is upregulated by insulin and represses hepatic gluconeogenesis', American Journal of physiology.

Jansson, H., Lindholm, E., Lindh, C., Groop, L. and Bratthall, G. (2006) 'Type 2 diabetes and risk for periodontal disease: a role for dental health awareness', Journal of Clinical Periodontology, 33(6), pp. 408-414.

Jiao, H., Xiao, E. and Graves, D. T. (2015) 'Diabetes and Its Effect on Bone and Fracture Healing', Current Osteoporosis Reports, 13(5), pp. 327-335.

Jin, T. (2008) 'The WNT signalling pathway and diabetes mellitus', Diabetologia, 51(10), pp. 1771-1780.

Jin, T. (2016) 'Current Understanding on Role of the Wnt Signaling Pathway Effector TCF7L2 in Glucose Homeostasis', Endocrine Reviews, 37(3), pp. 254-277.

Jin, T. and Liu, L. (2008) 'Minireview: The Wnt Signaling Pathway Effector TCF7L2 and Type 2 Diabetes Mellitus', Molecular Endocrinology, 22(11), pp. 2383-2392.

Jitrapakdee, S., Vidal-Puig, A. and Wallace, J. C. (2006) 'Anaplerotic roles of pyruvate carboxylase in mammalian tissues', Cellular and Molecular Life Sciences, 63, pp. 843-854.

Kanazawa, I. (2015) 'Osteocalcin as a hormone regulating glucose metabolism', World Journal of Diabetes, 6(18), pp. 1345.

Katakami, N. (2018) 'Mechanism of Development of Atherosclerosis and Cardiovascular Disease in Diabetes Mellitus', Journal of Atherosclerosis and Thrombosis, 25(1), pp. 27-39.

Kato, M., Patel, M. S., Levasseur, R., Lobov, I., Chang, B. H.-J., Glass, D. A., Hartmann, C., Li, L., Hwang, T.-H., Brayton, C. F., Lang, R. A., Karsenty, G. and Chan, L. (2002) 'Cbfa1-independent decrease in osteoblast proliferation, osteopenia, and persistent embryonic eye vascularization in mice deficient in Lrp5, a Wnt coreceptor', Journal of Cell Biology, 157(2), pp. 303-314.

Khosrow S. Houschyar , *, Christian Tapking , 3, Mimi R. Borrelli and Daniel Popp , 5 Dominik Duscher , 6 Zeshaan N. Maan , 4 Malcolm P. Chelliah , 4 Jingtao Li , 7 Kamran Harati , 1 Christoph Wallner , 1 Susanne Rein , 8 Dominik Pförringer , 9 Georg Reumuth , 10 Gerrit Grieb , 11 Sylvain Mouraret , 4, 12 Mehran Dadras , 1 Johannes M. Wagner , 1 Jungul Y. Cha , 13 Frank Siemers , 10 Marcus Lehnhardt , 1 and Björn Behr 1.

Kim, J.-M., Lin, C., Stavre, Z., Greenblatt, M. B. and Shim, J.-H. (2020) 'Osteoblast-Osteoclast Communication and Bone Homeostasis', Cells, 9(9), pp. 2073.

Klec, C., Ziomek, G., Pichler, M., Malli, R. and Graier, W. F. (2019) 'Calcium Signaling in ß-cell Physiology and Pathology: A Revisit', International Journal of Molecular Sciences, 20(24), pp. 6110.

Kobayashi, K., Takahashi, N., Jimi, E., Udagawa, N., Takami, M., Kotake, S., Nakagawa, N., Kinosaki, M., Yamaguchi, K., Shima, N., Yasuda, H., Morinaga, T., Higashio, K., Martin, T. J. and Suda, T. (2000) 'Tumor Necrosis Factor α Stimulates Osteoclast Differentiation by a Mechanism Independent of the Odf/Rankl–Rank Interaction', Journal of Experimental Medicine, 191(2), pp. 275-286.

Kobayashi , Y., Uehara , S., Udagawa , N. and Takahashi, N. (2016) 'Regulation of bone metabolism by Wnt signals', The Journal Of Biochemistry, 159(4), pp. 387–392.

Kolb, H., Kempf, K., Röhling, M., Lenzen-Schulte, M., Schloot, N. C. and Martin, S. (2021) 'Ketone bodies: from enemy to friend and guardian angel', BMC Medicine, 19(1).

Komatsu, D. E., Mary, M. N., Schroeder, R. J., Robling, A. G., Turner, C. H. and Warden, S. J. (2010) 'Modulation of Wnt signaling influences fracture repair', Journal of Orthopaedic Research, 28(7), pp. 928-936.

Komiya, Y. and Habas, R. (2008) 'Wnt signal transduction pathways', Organogenesis, 4(2), pp. 68-75.

Komori, T. (2006) 'Regulation of osteoblast differentiation by transcription factors', Journal of Cellular Biochemistry, 99(5), pp. 1233-1239.

Komori , T. (2020) 'What is the function of osteocalcin?', Journal of Oral Biosciences, 62(3), pp. 223-227.

Kooner, J. S., Saleheen, D., Sim, X., Sehmi, J., Zhang, W., Frossard, P., Been, L. F., Chia, K.-S., Dimas, A. S., Hassanali, N., Jafar, T., Jowett, J. B. M., Li, X., Radha, V., Rees, S. D., Takeuchi, F., Young, R., Aung, T., Basit, A., Chidambaram, M., Das, D., Grundberg, E., Hedman, Å. K., Hydrie, Z. I., Islam, M., Khor, C.-C., Kowlessur, S., Kristensen, M. M., Liju, S., Lim, W.-Y., Matthews, D. R., Liu, J., Morris, A. P., Nica, A. C., Pinidiyapathirage, J. M., Prokopenko, I., Rasheed, A., Samuel, M., Shah, N., Shera, A. S., Small, K. S., Suo, C., Wickremasinghe, A. R., Wong, T. Y., Yang, M., Zhang, F., Abecasis, G. R., Barnett, A. H., Caulfield, M., Deloukas, P., Frayling, T. M., Froguel, P., Kato, N., Katulanda, P., Kelly, M. A., Liang, J., Mohan, V., Sanghera, D. K., Scott, J., Seielstad, M., Zimmet, P. Z., Elliott, P., Teo, Y. Y., Mccarthy, M. I., Danesh, J., Tai, E. S. and Chambers, J. C. (2011) 'Genome-wide association study in individuals of South Asian ancestry identifies six new type 2 diabetes susceptibility loci', Nature Genetics, 43(10), pp. 984-989.

Krishnan, V. (2006) 'Regulation of bone mass by Wnt signaling', Journal of Clinical Investigation, 116(5), pp. 1202-1209.

La Sala, L., Prattichizzo, F. and Ceriello, A. (2019) 'The link between diabetes and atherosclerosis', European Journal of Preventive Cardiology, 26(2_suppl), pp. 15-24.

Laouali, N., El Fatouhi, D., Aguayo, G., Balkau, B., Boutron-Ruault, M.-C., Bonnet, F. and Fagherazzi, G. (2021) 'Type 2 diabetes and its characteristics are associated with poor oral health: findings from 60,590 senior women from the E3N study', BMC Oral Health, 21(1).

Le, B., Nurcombe, V., Cool, S., Van Blitterswijk, C., De Boer, J. and Lapointe, V. (2017) 'The Components of Bone and What They Can Teach Us about Regeneration', Materials, 11(1), pp. 14.

Le Bacquer, O., Kerr-Conte, J., Gargani, S., Delalleau, N., Huyvaert, M., Gmyr, V., Froguel, P., Neve, B. and Pattou, F. (2012) 'TCF7L2 rs7903146 impairs islet function and morphology in non-diabetic individuals', Diabetologia, 55(10), pp. 2677-2681.

Le Fur, S., Le Stunff, C. and Bougneres, P. (2002) 'Increased Insulin Resistance in Obese Children Who Have Both 972 IRS-1 and 1057 IRS-2 Polymorphisms', Diabetes, 51(Supplement 3), pp. S304-S307.

Lee , N. K., Sowa , H., Hinoi , E., Ferron, M., Deok Ahn , J., Confavreux , C., Dacquin , R., Mee , P. J., McKee , M. D., Jung , D. Y., Zhang , Z., Kim , J. K., Mauvais-Jarvis , F., Ducy , P. and Karsenty, G. (2007) 'Endocrine regulation of energy metabolism by the skeleton', Cell, 130(3), pp. 456-469.

Lee, S., Lee, C. E., Elias, C. F. and Elmquist, J. K. (2009) 'Expression of the diabetes-associated geneTCF7L2in adult mouse brain', The Journal of Comparative Neurology, 517(6), pp. 925-939.

Libby, P., Buring, J. E., Badimon , L., Hansson , G. K., Deanfield , J., Bittencourt , M. S., Tokgözoğlu, L. and Lewis, E. F. (2019) 'Atherosclerosis', Nature Reviews Disease Primers, 5(56).

Lin, Y., Li, P., Cai, L., Zhang, B., Tang, X., Zhang, X., Li, Y., Xian, Y., Yang, Y., Wang, L., Lu, F., Liu, X., Rao, S., Chen, M., Ma, S., Shi, Y., Bao, M., Wu, J., Yang, Y., Yang, J. and Yang, Z. (2010) 'Association study of genetic variants in eight genes/loci with type 2 diabetes in a Han Chinese population', BMC Medical Genetics, 11(1), pp. 97.

Lin, Y. and Sun, Z. (2010) 'Current views on type 2 diabetes', Journal of Endocrinology, 204(1), pp. 1-11.

Lipiec, M. A., Bem, J., Koziński, K., Chakraborty, C., Urban-Ciećko, J., Zajkowski, T., Dąbrowski, M., Szewczyk, Ł. M., Toval, A., Ferran, J. L., Nagalski, A. and Wiśniewska, M. B. (2020) 'TCF7L2 regulates postmitotic differentiation programs and excitability patterns in the thalamus', Development, 147(16), pp. dev190181.

Long, J., Edwards, T., Signorello, L. B., Cai, Q., Zheng, W., Shu, X.-O. and Blot, W. J. (2012) 'Evaluation of Genome-wide Association Study-identified Type 2 Diabetes Loci in African Americans', American Journal of Epidemiology, 176(11), pp. 995-1001.

Looker, A. C., Eberhardt, M. S. and Saydah, S. H. (2016) 'Diabetes and fracture risk in older U.S. adults', Bone, 82, pp. 9-15.

Loria, P., Lonardo, A. and Anania, F. (2013) 'Liver and diabetes. A vicious circle', Hepatology Research, 43(1), pp. 51-64.

LOWELL , B. B. and SHULMAN , G. I. (2005) 'Mitochondrial Dysfunction and Type 2 Diabetes', Science, 307(5708), pp. 384-387.

Luo, L. and Liu, M. (2016) 'Adipose tissue in control of metabolism', Journal of Endocrinology, 231(3), pp. R77-R99.

Lyssenko, V., Lupi, R., Marchetti, P., Del Guerra, S., Orho-Melander, M., Almgren, P., Sjögren, M., Ling, C., Eriksson, K.-F., Lethagen, Y.-L., Mancarella, R., Berglund, G., Tuomi, T., Nilsson, P., Del Prato, S. and Groop, L. (2007a) 'Mechanisms by which common variants in the TCF7L2 gene increase risk of type 2 diabetes', Journal of Clinical Investigation, 117(8), pp. 2155-2163.

Lyssenko, V., Lupi, R., Marchetti, P., Del Guerra, S., Orho-Melander, M., Almgren, P., Sjögren, M., Ling, C., Eriksson, K.-F., Lethagen, ט.-L., Mancarella, R., Berglund, G., Tuomi, T., Nilsson, P., Del Prato, S. and Groop, L. (2007b) 'Mechanisms by which common variants in the TCF7L2 gene increase risk of type 2 diabetes', The Journal of clinical investigation., 117.

Maeda, K., Kobayashi, Y., Koide, M., Uehara, S., Okamoto, M., Ishihara, A., Kayama, T., Saito, M. and Marumo, K. (2019) 'The Regulation of Bone Metabolism and Disorders by Wnt Signaling', International Journal of Molecular Sciences, 20(22), pp. 5525.

Mahajan, A. and Taliun, D. and Thurner, M. and Robertson, N. R. and Torres, J. M. and Rayner, N. W. and Payne, A. J. and Steinthorsdottir, V. and Scott, R. A. and Grarup, N. and Cook, J. P. and Schmidt, E. M. and Wuttke, M. and Sarnowski, C. and Mägi, R. and Nano, J. and Gieger, C. and Trompet, S. and Lecoeur, C. and Preuss, M. H. and Prins, B. P. and Guo, X. and Bielak, L. F. and Below, J. E. and Bowden, D. W. and Chambers, J. C. and Kim, Y. J. and Ng, M. C. Y. and Petty, L. E. and Sim, X. and Zhang, W. and Bennett, A. J. and Bork-Jensen, J. and Brummett, C. M. and Canouil, M. and Ec Kardt, K.-U. and Fischer, K. and Kardia, S. L. R. and Kronenberg, F. and Läll, K. and Liu, C.-T. and Locke, A. E. and Luan, J. A. and Ntalla, I. and Nylander, V. and Schönherr, S. and Schurmann, C. and Yengo, L. and Bottinger, E. P. and Brandslund, I. and Christensen, C. and Dedoussis, G. and Florez, J. C. and Ford, I. and Franco, O. H. and Frayling, T. M. and Giedraitis, V. and Hackinger, S. and Hattersley, A. T. and Herder, C. and Ikram, M. A. and Ingelsson, M. and Jørgensen, M. E. and Jørgensen, T. and Kriebel, J. and Kuusisto, J. and Ligthart, S. and Lindgren, C. M. and Linneberg, A. and Lyssenko, V. and Mamakou, V. and Meitinger, T. and Mohlke, K. L. and Morris, A. D. and Nadkarni, G. and Pankow, J. S. and Peters, A. and Sattar, N. and Stančáková, A. and Strauch, K. and Taylor, K. D. and Thorand, B. and Thorleifsson, G. and Thorsteinsdottir, U. and Tuomilehto, J. and Witte, D. R. and Dupuis, J. and Peyser, P. A. and Zeggini, E. and Loos, R. J. F. and Froguel, P. and Ingelsson, E. and Lind, L. and Groop, L. and Laakso, M. and Collins, F. S. and Jukema, J. W. and Palmer, C. N. A. and Grallert, H. and Metspalu, A. and Dehghan, A. and Köttgen, A. and Abecasis, G. R. and Meigs, J. B. and Rotter, J. I. and Marchini, J. and Pedersen, O. and Hansen, T. and Langenberg, C. and Wareham, N. J. and Stefansson, K. and Gloyn, A. L. and Morris, A. P. and Boehnke, M. and Mccarthy, M. I. (2018) 'Fine-mapping type 2 diabetes loci to single-variant resolution using high-density imputation and islet-specific epigenome maps', Nature Genetics, 50(11), pp. 1505-1513.

Manna, P. and Jain, S. K. (2015) 'Obesity, Oxidative Stress, Adipose Tissue Dysfunction, and the Associated Health Risks: Causes and Therapeutic Strategies', Metabolic syndrome and related disorders, 1(13), pp. 423-444.

Manolagas, S. C. (2020) 'Osteocalcin promotes bone mineralization but is not a hormone', PLOS Genetics, 16(6), pp. e1008714.

Manolagas, S. C. and Almeida, M. (2007) 'Gone with the Wnts: β-Catenin, T-Cell Factor, Forkhead Box O, and Oxidative Stress in Age-Dependent Diseases of Bone, Lipid, and Glucose Metabolism', Molecular Endocrinology, 21(11), pp. 2605-2614.

Martos-Rodríguez, C. J., Albarrán-Juárez, J., Morales-Cano, D., Caballero, A., Macgrogan, D., De La Pompa, J. L., Carramolino, L. and Bentzon, J. F. (2021) 'Fibrous Caps in Atherosclerosis Form by Notch-Dependent Mechanisms Common to Arterial Media Development', Arteriosclerosis, Thrombosis, and Vascular Biology, 41(9).

Marín-Peñalver , J. J., Martín-Timón , I., Sevillano-Collantes , C. and Javier del Cañizo-Gómez, F. (2016) 'Update on the treatment of type 2 diabetes mellitus', World journal of diabetes, 7(17), pp. 354–395.

Miyamoto, T. (2015) 'Mechanism Underlying Post-menopausal Osteoporosis: HIF1α is Required for Osteoclast Activation by Estrogen Deficiency', The Keio Journal of Medicine, 64(3), pp. 44-47.

Miyata, T., Kawai , R., Taketomi , S. and Sprague, S. M. (1996) 'Possible involvement of advanced glycation end-products in bone resorption', Nephrology Dialysis Transplantation, 11(5), pp. 54–57.

Mizokami, A., Yasutake, Y., Gao, J., Matsuda, M., Takahashi, I., Takeuchi, H. and Hirata, M. (2013) 'Osteocalcin Induces Release of Glucagon-Like Peptide-1 and Thereby Stimulates Insulin Secretion in Mice', PLoS ONE, 8(2), pp. e57375.

Moayeri, A., Mohamadpour, M., Mousavi, S., Shirzadpour, E., Mohamadpour, S. and Amraei, M. (2017) 'Fracture risk in patients with type 2 diabetes mellitus and possible risk factors: a systematic review and meta-analysis', Therapeutics and Clinical Risk Management, Volume 13, pp. 455-468.

Mohamed , J., Nafizah, A. H. N., Zariyantey , A. H. and Budin, S. B. (2016) 'Mechanisms of Diabetes-Induced Liver Damage', Sultan Qaboos University Medical Journal, 16(2).

Moreira, P. I., Santos, M. S., Moreno, A. N. M., SeiçA, R. and Oliveira, C. R. (2003) 'Increased Vulnerability of Brain Mitochondria in Diabetic (Goto-Kakizaki) Rats With Aging and Amyloid-β Exposure', Diabetes, 52(6), pp. 1449-1456.

Moriishi, T. and Komori, T. (2020) 'Lack of reproducibility in osteocalcin-deficient mice', PLOS Genetics, 16(6), pp. e1008939.

Moriishi, T., Ozasa, R., Ishimoto, T., Nakano, T., Hasegawa, T., Miyazaki, T., Liu, W., Fukuyama, R., Wang, Y., Komori, H., Qin, X., Amizuka, N. and Komori, T. (2020) 'Osteocalcin is necessary for the alignment of apatite crystallites, but not glucose metabolism, testosterone synthesis, or muscle mass', PLOS Genetics, 16(5), pp. e1008586.

Moucheraud, C., Lenz, C., Latkovic, M. and Wirtz, V. J. (2019) 'The costs of diabetes treatment in low- and middle-income countries: a systematic review', BMJ Global Health, 4(1), pp. e001258.

Movassat , J. a., Delangre , E. i., Liu , J., Gu, Y. and Janel, N. (2019) 'Hypothesis and Theory: Circulating Alzheimer's-Related Biomarkers in Type 2 Diabetes. Insight From the Goto-Kakizaki Rat', Frontiers in Neurology.

Muller, L. M. A. J., Gorter, K. J., Hak, E., Goudzwaard, W. L., Schellevis, F. G., Hoepelman, A. I. M. and Rutten, G. E. H. M. (2005) 'Increased Risk of Common Infections in Patients with Type 1 and Type 2 Diabetes Mellitus', Clinical Infectious Diseases, 41(3), pp. 281-288.

Murphy, M. P. and Levine, H. (2010) 'Alzheimer's Disease and the Amyloid-β Peptide', Journal of Alzheimer's Disease, 19(1), pp. 311-323.

Murray and Coleman (2019) 'Impact of Diabetes Mellitus on Bone Health', International Journal of Molecular Sciences, 20(19), pp. 4873.

Murray, K. D., Choudary, P. V. and Jones, E. G. (2007) 'Nucleus- and cell-specific gene expression in monkey thalamus', Proceedings of the National Academy of Sciences, 104(6), pp. 1989-1994.

Napoli, N., Strollo, R., Paladini, A., Briganti, S. I., Pozzilli, P. and Epstein, S. (2014a) 'The Alliance of Mesenchymal Stem Cells, Bone, and Diabetes', International Journal of Endocrinology, 2014, pp. 1-26.

Napoli, N., Strotmeyer, E. S., Ensrud, K. E., Sellmeyer, D. E., Bauer, D. C., Hoffman, A. R., Dam, T.-T. L., Barrett-Connor, E., Palermo, L., Orwoll, E. S., Cummings, S. R., Black, D. M. and Schwartz, A. V. (2014b) 'Fracture risk in diabetic elderly men: the MrOS study', Diabetologia, 57(10), pp. 2057-2065.

Nguyen-Tu, M.-S., Martinez-Sanchez, A., Leclerc, I., Rutter, G. A. and Da Silva Xavier, G. (2021) 'Adipocyte-specific deletion of Tcf7l2 induces dysregulated lipid metabolism and impairs glucose tolerance in mice', Diabetologia, 64(1), pp. 129-141.

Nicod, N., Pradas-Juni, M. and Gomis, R. (2014) 'Role of the single nucleotide polymorphism rs7903146 of TCF7L2 in inducing nonsense-mediated decay', SpringerPlus, 3(1), pp. 41.

Nicodemus, K. K. and Folsom, A. R. (2001) 'Type 1 and Type 2 Diabetes and Incident Hip Fractures in Postmenopausal Women', Diabetes Care, 24(7), pp. 1192-1197.

Nkonge, K. M., Nkonge, D. K. and Nkonge, T. N. (2020) 'The epidemiology, molecular pathogenesis, diagnosis, and treatment of maturity-onset diabetes of the young (MODY)', Clinical Diabetes and Endocrinology, 6(1).

Norton, L., Fourcaudot, M., Abdul-Ghani, M. A., Winnier, D., Mehta, F. F., Jenkinson, C. P. and Defronzo, R. A. (2011) 'Chromatin occupancy of transcription factor 7-like 2 (TCF7L2) and its role in hepatic glucose metabolism', Diabetologia, 54(12), pp. 3132-3142.

Ntouva, A., Toulis, K. A., Keerthy, D., Adderley, N. J., Hanif, W., Thayakaran, R., Gokhale, K., Thomas, G. N., Khunti, K., Tahrani, A. A. and Nirantharakumar, K. (2019) 'Hypoglycaemia is associated with increased risk of fractures in patients with type 2 diabetes mellitus: a cohort study', European Journal of Endocrinology, 180(1), pp. 51-58.

O'Brien, F. J., Brennan, O., Kennedy, O. D. and Lee, T. C. (2005) 'Microcracks in cortical bone: how do they affect bone biology?', Current Osteoporosis Reports, 3(2), pp. 39-45.

Oftadeh, R., Perez-Viloria, M., Villa-Camacho, J. C., Vaziri, A. and Nazarian, A. (2015) 'Biomechanics and Mechanobiology of Trabecular Bone: A Review', Journal of Biomechanical Engineering, 137(1), pp. 010802.

Oftadeh , R., Perez-Viloria , M., Villa-Camacho , J. C., Vaziri , A. and Nazarian, A. (2015) 'Biomechanics and Mechanobiology of Trabecular Bone: A Review', Journal of biomechanical engineering, 137(1).

Oh, K.-J., Park, J., Kim, S. S., Oh, H., Choi, C. S. and Koo, S.-H. (2012) 'TCF7L2 Modulates Glucose Homeostasis by Regulating CREB- and FoxO1-Dependent Transcriptional Pathway in the Liver', PLoS Genetics, 8(9), pp. e1002986.

Okoronkwo, I. L., Ekpemiro, J. N., Okwor, E. U., Okpala, P. U. and Adeyemo, F. O. (2015) 'Economic burden and catastrophic cost among people living with type2 diabetes mellitus attending a tertiary health institution in south-east zone, Nigeria', BMC Research Notes, 8(1).

Olzmann, J. A. and Carvalho, P. (2019) 'Dynamics and functions of lipid droplets', Nature Reviews Molecular Cell Biology, 20(3), pp. 137-155.

Ott, M., Susan (2018) 'Cortical or Trabecular Bone: What’s the Difference?', American Journal of Nephrology, 47(6), pp. 373-375.

Owen, K. and Hattersley, A. T. (2001) 'Maturity-onset diabetes of the young: from clinical description to molecular genetic characterization', Best Practice & Research Clinical Endocrinology & Metabolism, 15(3), pp. 309-323.

Palmer, A. K., Gustafson, B., Kirkland, J. L. and Smith, U. (2019) 'Cellular senescence: at the nexus between ageing and diabetes', Diabetologia, 62(10), pp. 1835-1841.

Palmer, A. K., Tchkonia, T., Lebrasseur, N. K., Chini, E. N., Xu, M. and Kirkland, J. L. (2015) 'Cellular Senescence in Type 2 Diabetes: A Therapeutic Opportunity', Diabetes, 64(7), pp. 2289-2298.

Papatheodorou, K., Banach, M., Bekiari, E., Rizzo, M. and Edmonds, M. (2018) 'Complications of Diabetes 2017', Journal of Diabetes Research, 2018, pp. 1-4.

Park, S.-M. and Lee, J.-H. (2022) 'Effects of Type 2 Diabetes Mellitus on Osteoclast Differentiation, Activity, and Cortical Bone Formation in POSTmenopausal MRONJ Patients', Journal of Clinical Medicine, 11(9), pp. 2377.

Patel, S., Alam, A., Pant, R. i. and Chattopadhyay, S. (2019) 'Wnt Signaling and Its Significance Within the Tumor Microenvironment: Novel Therapeutic Insights', Frontiers In Immunology.

Patsch, J. M., Burghardt, A. J., Yap, S. P., Baum, T., Schwartz, A. V., Joseph, G. B. and Link, T. M. (2013) 'Increased cortical porosity in type 2 diabetic postmenopausal women with fragility fractures', Journal of Bone and Mineral Research, 28(2), pp. 313-324.

Peila, R., Rodriguez, B. L. and Launer, L. J. (2002) 'Type 2 Diabetes, APOE Gene, and the Risk for Dementia and Related Pathologies', Diabetes, 51(4), pp. 1256-1262.

Pi, M., Nishimoto, S. K. and Darryl Quarles, L. (2021) 'Explaining Divergent Observations Regarding Osteocalcin/GPRC6A Endocrine Signaling', Endocrinology, 162(4).

Picke, A.-K., Campbell, G., Napoli, N., Hofbauer, L. C. and Rauner, M. (2019) 'Update on the impact of type 2 diabetes mellitus on bone metabolism and material properties', Endocrine Connections, 8(3), pp. R55-R70.

Pierelli, G., Stanzione, R., Forte, M., Migliarino, S., Perelli, M., Volpe, M. and Rubattu, S. (2017) 'Uncoupling Protein 2: A Key Player and a Potential Therapeutic Target in Vascular Diseases', Oxidative Medicine and Cellular Longevity, 2017, pp. 1-11.

Pinti, M. V., Fink, G. K., Hathaway, Q. A., Durr, A. J., Kunovac, A. and Hollander, J. M. (2019) 'Mitochondrial dysfunction in type 2 diabetes mellitus: an organ-based analysis', American Journal of Physiology-Endocrinology and Metabolism, 316(2), pp. E268-E285.

Pirapaharan, D. C., Olesen, J. B., Andersen, T. L., Christensen, S. B., Kjærsgaard-Andersen, P., Delaisse, J.-M. and Søe, K. (2019) 'Catabolic activity of osteoblast-lineage cells contributes to osteoclastic bone resorption in vitro', Journal of Cell Science, 132(10), pp. jcs229351.

Ponzetti, M. and Rucci, N. (2021) 'Osteoblast Differentiation and Signaling: Established Concepts and Emerging Topics', International Journal of Molecular Sciences, 22(13), pp. 6651.

Poundarik, A. A., Wu, P.-C., Evis, Z., Sroga, G. E., Ural, A., Rubin, M. and Vashishth, D. (2015) 'A direct role of collagen glycation in bone fracture', Journal of the Mechanical Behavior of Biomedical Materials, 52, pp. 120-130.

Poznyak, A., Grechko, A. V., Poggio, P., Myasoedova, V. A., Alfieri, V. and Orekhov, A. N. (2020) 'The Diabetes Mellitus–Atherosclerosis Connection: The Role of Lipid and Glucose Metabolism and Chronic Inflammation', International Journal of Molecular Sciences, 21(5), pp. 1835.

Prattichizzo, F., De Nigris, V., La Sala, L., Procopio, A. D., Olivieri, F. and Ceriello, A. (2016) '"Inflammaging" as a Druggable Target: A Senescence-Associated Secretory Phenotype—Centered View of Type 2 Diabetes', Oxidative Medicine and Cellular Longevity, 2016, pp. 1-10.

Preshaw, P. M., Alba, A. L., Herrera, D., Jepsen, S., Konstantinidis, A., Makrilakis, K. and Taylor, R. (2012) 'Periodontitis and diabetes: a two-way relationship', Diabetologia, 55(1), pp. 21-31.

Price, P. A., Otsuka, A. A., Poser, J. W., Kristaponis, J. and Raman, N. (1976) 'Characterization of a gamma-carboxyglutamic acid-containing protein from bone.', Proceedings of the National Academy of Sciences, 73(5), pp. 1447-1451.

Pritchard, J. M., Giangregorio, L. M., Atkinson, S. A., Beattie, K. A., Inglis, D., Ioannidis, G., Gerstein, H., Punthakee, Z., Adachi, J. D. and Papaioannou, A. (2013) 'Changes in trabecular bone microarchitecture in postmenopausal women with and without type 2 diabetes: a two year longitudinal study', BMC Musculoskeletal Disorders, 14(1), pp. 114.

Pritchard, J. M., Giangregorio, L. M., Atkinson, S. A., Beattie, K. A., Inglis, D., Ioannidis, G., Punthakee, Z., Adachi, J. D. and Papaioannou, A. (2012) 'Association of larger holes in the trabecular bone at the distal radius in postmenopausal women with type 2 diabetes mellitus compared to controls', Arthritis Care & Research, 64(1), pp. 83-91.

Qin, Y., Guan, J. and Zhang, C. (2014) 'Mesenchymal stem cells: mechanisms and role in bone regeneration', Postgraduate Medical Journal, 90(1069), pp. 643-647.

Ralston , S. H. (2013) 'Bone structure and metabolism', Medicine, 41(10), pp. 581-585.

Ralston, S. H. (2013) 'Bone structure and metabolism', medicine.

Rathinavelu, S., Guidry-Elizondo, C. and Banu, J. (2018) 'Molecular Modulation of Osteoblasts and Osteoclasts in Type 2 Diabetes', Journal of Diabetic Research.

Rebolledo, O. R. and Actis Dato, S. M. (2005) 'Postprandial hyperglycemia and hyperlipidemia-generated glycoxidative stress: its contribution to the pathogenesis of diabetes complications', Eur opean Rev iew for Med ical and Pharmacol ogical Sci ences, 9, pp. 191-208.

Regard, J. B., Zhong, Z., Williams, B. O. and Yang, Y. (2012) 'Wnt Signaling in Bone Development and Disease: Making Stronger Bone with Wnts', Cold Spring Harbor Perspectives in Biology, 4(12), pp. a007997-a007997.

Rehman, K. and Akash, M. S. H. (2016) 'Mechanisms of inflammatory responses and development of insulin resistance: how are they interlinked?', Journal of Biomedical Science, 23(1).

Ren, Q., Han, X. Y., Wang, F., Zhang, X. Y., Han, L. C., Luo, Y. Y., Zhou, X. H. and Ji, L. N. (2008) 'Exon sequencing and association analysis of polymorphisms in TCF7L2 with type 2 diabetes in a Chinese population', Diabetologia, 51(7), pp. 1146-1152.

Rhodes, C. J. (2005) 'Type 2 Diabetes-a Matter of ß-Cell Life and Death?', Science, 307(5708), pp. 380-384.

Ringel, J., Engeli, S., Distler, A. and Sharma, A. M. (1999) 'Pro12Ala Missense Mutation of the Peroxisome Proliferator Activated Receptor γ and Diabetes Mellitus', Biochemical and Biophysical Research Communications, 254(2), pp. 450-453.

Risch, N. and Merikangas, K. (1996) 'The Future of Genetic Studies of Complex Human Diseases', Science, 273(5281), pp. 1516-1517.

Roden, M. and Shulman, G. I. (2019) 'The integrative biology of type 2 diabetes', Nature, 576(7785), pp. 51-60.

Ronveaux, C. C., Tomé , D. and Raybould , H. E. (2015) 'Glucagon-like peptide 1 interacts with ghrelin and leptin to regulate glucose metabolism and food intake through vagal afferent neuron signaling', The Journal Of Nutrition, 145(4), pp. 672-680.

Roux, S. and Orcel, P. (2000) 'Bone loss: Factors that regulate osteoclast differentiation - an update', Arthritis Research & Therapy, 2(6), pp. 451.

Rui, L. (2014) 'Energy Metabolism in the Liver', Comprehensive Physiology, pp. 177-197.

Russo, G. T., Giandalia, A., Romeo, E. L., Nunziata, M., Muscianisi, M., Ruffo, M. C., Catalano, A. and Cucinotta, D. (2016) 'Fracture Risk in Type 2 Diabetes: Current Perspectives and Gender Differences', International Journal of Endocrinology, 2016, pp. 1-11.

Rutkovskiy, A., Stensløkken, K.-O. and Vaage, I. J. (2016) 'Osteoblast Differentiation at a Glance', Medical Science Monitor Basic Research, 22, pp. 95-106.

Röder, P. V., Wu, B., Liu, Y. and Han, W. (2016a) 'Pancreatic regulation of glucose homeostasis', Experimental & Molecular Medicine, 48(3), pp. e219-e219.

Röder, P. V., Wu, B., Liu, Y., Han, W. and xmlns:xlink="http://www.w3.org/1999/xlink">, s. a.-h. t. c. u.-i. f. f. h. r. i. w. u. x. h. g.-i.-e. (2016b) 'Pancreatic regulation of glucose homeostasis', Experimental & Molecular Medicine, 48(219).

Saadi, H., Nagelkerke, N., Carruthers, S. G., Benedict, S., Abdulkhalek, S., Reed, R., Lukic, M. and Nicholls, M. G. (2008) 'Association of TCF7L2 polymorphism with diabetes mellitus, metabolic syndrome, and markers of beta cell function and insulin resistance in a population-based sample of Emirati subjects', Diabetes Research and Clinical Practice, 80(3), pp. 392-398.

Sacks, D. B. and Mcdonald, J. M. (1996) 'The Pathogenesis of Type II Diabetes Mellitus:A Polygenic Disease', American Journal of Clinical Pathology, 105(2), pp. 149-156.

Sami, W., Ansari, T., Butt , N. S. and Ab Hamid, M. R. (2017) 'Effect of diet on type 2 diabetes mellitus: A review', International Journal Of Health Sciences, 11(2), pp. 65-71.

Sanches, C. P., Vianna, A. G. D. and Barreto, F. D. C. (2017) 'The impact of type 2 diabetes on bone metabolism', Diabetology & Metabolic Syndrome, 9(1).

Sandhu, M. S., Weedon, M. N., Fawcett, K. A., Wasson, J., Debenham, S. L., Daly, A., Lango, H., Frayling, T. M., Neumann, R. J., Sherva, R., Blech, I., Pharoah, P. D., Palmer, C. N. A., Kimber, C., Tavendale, R., Morris, A. D., Mccarthy, M. I., Walker, M., Hitman, G., Glaser, B., Permutt, M. A., Hattersley, A. T., Wareham, N. J. and Barroso, I. (2007) 'Common variants in WFS1 confer risk of type 2 diabetes', Nature Genetics, 39(8), pp. 951-953.

Sanghera, D. K., Ortega, L., Han, S., Singh, J., Ralhan, S. K., Wander, G. S., Mehra, N. K., Mulvihill, J. J., Ferrell, R. E., Nath, S. K. and Kamboh, M. I. (2008) 'Impact of nine common type 2 diabetes risk polymorphisms in Asian Indian Sikhs: PPARG2 (Pro12Ala), IGF2BP2, TCF7L2 and FTOvariants confer a significant risk', BMC Medical Genetics, 9(1), pp. 59.

SAXENA, R., VOIGHT, B. F., LYSSENKO, V., BURTT, N. L. P., DE BAKKER, P. I. W., CHEN, H., ROIX, J. J., KATHIRESAN, S., HIRSCHHORN, J. N., DALY, M. J., HUGHES, T. E., GROOP, L., ALTSHULER, D., ALMGREN, P., FLOREZ, J. C., MEYEr, J., ARDLIE, K., BENGTSSON BOSTRÖM, K., ISOMAA, B., LETTRE, G., LINDBLAD, U., LYON, H. N., MELANDER, O., NEWTON-CHEH, C., NILSSON, P., ORHO-MELANDER, M., RÅSTAM, L., SPELIOTES, E. K., TASKINEN, M.-R., TUOMI, T., GUIDUCCI, C., BERGLUND, A., CARLSON, J., GIANNINY, L., HACKETT, R., HALL, L., HOLMKVIST, J., LAURILA, E., SJÖGREN, M., STERNER, M., SURTI, A., SVENSSON, M., SVENSSON, M., TEWHEY, R., BLUMENSTIEL, B., PARKIN, M., DEFELICE, M., BARRY, R., BRODEUR, W., CAMARATA, J., CHIA, N., FAVA, M., GIBBONS, J., HANDSAKER, B., HEALY, C., NGUYEN, K., GATES, C., SOUGNEZ, C., GAGE, D., NIZZARI, M., GABRIEL, S. B., CHIRN, G.-W., MA, Q., PARIKH, H., RICHARDSON, D., RICKE, D. and PURCELL, S. (2007) 'Genome-Wide Association Analysis Identifies Loci for Type 2 Diabetes and Triglyceride Levels', 316, (5829), pp. 1331-1336.

Schleicher, E. and Friess, U. (2007) 'Oxidative stress, AGE, and atherosclerosis', Kidney International, 72, pp. S17-S26.

Schmid, A. I., Szendroedi, J., Chmelik, M., Krššák, M., Moser, E. and Roden, M. (2011) 'Liver ATP Synthesis Is Lower and Relates to Insulin Sensitivity in Patients With Type 2 Diabetes', Diabetes Care, 34(2), pp. 448-453.

Schneider, C. A., Rasband, W. S. and Eliceiri, K. W. (2012) 'NIH Image to ImageJ: 25 years of image analysis', Nature Methods, 9(7), pp. 671-675.

Shahbazi , J., Lock, R. and Liu, T. (2013) 'Tumor Protein 53-Induced Nuclear Protein 1 Enhances p53 Function and Represses Tumorigenesis', Frontiers in Genetics, 4(80).

Shao, W., Wang, D., Chiang, Y.-T., Ip, W., Zhu, L., Xu, F., Columbus, J., Belsham, D. D., Irwin, D. M., Zhang, H., Wen, X., Wang, Q. and Jin, T. (2013a) 'The Wnt Signaling Pathway Effector TCF7L2 Controls Gut and Brain Proglucagon Gene Expression and Glucose Homeostasis', Diabetes, 62(3), pp. 789-800.

Shao, W., Wang, D., Chiang, Y.-T., Ip, W., Zhu, L., Xu, F., Columbus, J., Belsham, D. D., Irwin, D. M., Zhang, H., Wen, X., Wang, Q. and Jin, T. (2013b) 'The Wnt Signaling Pathway Effector TCF7L2 Controls Gut and Brain Proglucagon Gene Expression and Glucose Homeostasis', Diabetes, 62(3), pp. 789-800.

Shapses, S. A. and Sukumar, D. (2012) 'Bone Metabolism in Obesity and Weight Loss', Annual Review of Nutrition, 32(1), pp. 287-309.

Shu, L., Beier, E., Sheu, T., Zhang, H., Zuscik, M. J., Puzas, E. J., Boyce, B. F., Mooney, R. A. and Xing, L. (2015) 'High-Fat Diet Causes Bone Loss in Young Mice by Promoting Osteoclastogenesis Through Alteration of the Bone Marrow Environment', Calcified Tissue International, 96(4), pp. 313-323.

Silbernagel, G., Renner, W., Grammer, T. B., Hügl, S. R., Bertram, J., Kleber, M. E., Hoffmann, M. M., Winkelmann, B. R., März, W. and Boehm, B. O. (2011) 'Association of TCF7L2 SNPs with age at onset of type 2 diabetes and proinsulin/insulin ratio but not with glucagon-like peptide 1', Diabetes/Metabolism Research and Reviews, 27(5), pp. 499-505.

Sladek, R., Rocheleau, G., Rung, J., Dina, C., Shen, L., Serre, D., Boutin, P., Vincent, D., Belisle, A., Hadjadj, S., Balkau, B., Heude, B., Charpentier, G., Hudson, T. J., Montpetit, A., Pshezhetsky, A. V., Prentki, M., Posner, B. I., Balding, D. J., Meyre, D., Polychronakos, C. and Froguel, P. (2007) 'A genome-wide association study identifies novel risk loci for type 2 diabetes', Nature, 445(7130), pp. 881-885.

Staa, T. P. v., Dennison, E. M., Leufkens, H. G. M. and Cooper, C. (2001) 'Epidemiology of fractures in England and Wales', Bone, 29(6).

Styner, M., Thompson, W. R., Galior, K., Uzer, G., Wu, X., Kadari, S., Case, N., Xie, Z., Sen, B., Romaine, A., Pagnotti, G. M., Rubin, C. T., Styner, M. A., Horowitz, M. C. and Rubin, J. (2014) 'Bone marrow fat accumulation accelerated by high fat diet is suppressed by exercise', Bone, 64, pp. 39-46.

Sun, X., Yu, W. and Hu, C. (2014) 'Genetics of Type 2 Diabetes: Insights into the Pathogenesis and Its Clinical Application', BioMed Research International, 2014, pp. 1-15.

Syafril, S. (2018) 'Pathophysiology diabetic foot ulcer', IOP Conference Series: Earth and Environmental Science, 125.

Tamura, M. (2010) 'Role of the Wnt signaling pathway in bone and tooth', Frontiers in Bioscience, E2(4), pp. 1405-1413.

Tangseefa, P., Martin, S. K., Fitter, S., Baldock, P. A., Proud, C. G. and Zannettino, A. C. W. (2018) 'Osteocalcin-dependent regulation of glucose metabolism and fertility: Skeletal implications for the development of insulin resistance', Journal of Cellular Physiology, 233(5), pp. 3769-3783.

Thomas, S. and Jaganathan, B. G. (2022) 'Signaling network regulating osteogenesis in mesenchymal stem cells', Journal of cell communication and signaling, 16(1), pp. 47-61.

Tian, L. and Yu, X. (2017) 'Fat, Sugar, and Bone Health: A Complex Relationship', Nutrients, 9(5), pp. 506.

Tong, Y., Lin, Y., Zhang, Y., Yang, J., Zhang, Y., Liu, H. and Zhang, B. (2009) 'Association between TCF7L2gene polymorphisms and susceptibility to Type 2 Diabetes Mellitus: a large Human Genome Epidemiology (HuGE) review and meta-analysis', BMC Medical Genetics, 10(1), pp. 15.

Toshihisa , K. (2020) 'Functions of Osteocalcin in Bone, Pancreas, Testis, and Muscle', International journal of molecular sciences., 21(20), pp. 7513.

Trikkalinou, A., Papazafiropoulou, A. K. and Melidonis, A. (2017) 'Type 2 diabetes and quality of life', World Journal of Diabetes, 8(4), pp. 120.

Tsao, Y.-T., Huang, Y.-J., Wu, H.-H., Liu, Y.-A., Liu, Y.-S. and Lee, O. (2017) 'Osteocalcin Mediates Biomineralization during Osteogenic Maturation in Human Mesenchymal Stromal Cells', International Journal of Molecular Sciences, 18(1), pp. 159.

Urakami, T. (2019) ' Maturity-onset diabetes of the young (MODY): current perspectives on diagnosis and treatment ', Diabetes, Metabolic Syndrome and Obesity: Targets and Therapy, Volume 12, pp. 1047-1056.

Villanueva , C. J., Waki , H., Godio , C., Nielsen , R., Chou , W.-L., Vargas , L., Wroblewski , K., Schmedt , C., Chao , L. C., Boyadjian , R., Mandrup , S., Hevener , A., Saez , E. and Tontonoz, P. (2011) 'TLE3 is a dual function transcriptional coregulator of adipogenesis', Cell Metabolism, 13(4), pp. 413-427.

Visweswaran, M., Pohl, S., Arfuso, F., Newsholme, P., Dilley, R., Pervaiz, S. and Dharmarajan, A. (2015) 'Multi-lineage differentiation of mesenchymal stem cells – To Wnt, or not Wnt', The International Journal of Biochemistry & Cell Biology, 68, pp. 139-147.

VS , K., K, P., Ramesh , M. and Venkatesan, V. (2013) 'The Association of Serum Osteocalcin with the Bone Mineral Density in Post Menopausal Women', Journal of clinical and diagnostic research, 7(5), pp. 814–816.

Walker, J.

Walker , J. (2020) 'Skeletal system 1: the anatomy and physiology of bones', Nursing Times, 116(2), pp. 38-42.

Walker, J. (2020) 'Skeletal system 1: the anatomy and physiology of bones', Nursing Times.

Wang, T., Zhang, X. and Bikle, D. D. (2017) 'Osteogenic Differentiation of Periosteal Cells During Fracture Healing', Journal of Cellular Physiology, 232(5), pp. 913-921.

Wittrant, Y., Gorin, Y., Woodruff, K., Horn, D., Abboud, H. E., Mohan, S. and Abboud-Werner, S. L. (2008) 'High d(+)glucose concentration inhibits RANKL-induced osteoclastogenesis', Bone, 42(6), pp. 1122-1130.

Won, H. Y., Lee, J.-A., Park, Z. S., Song, J. S., Kim, H. Y., Jang, S.-M., Yoo, S.-E., Rhee, Y., Hwang, E. S. and Bae, M. A. (2011) 'Prominent Bone Loss Mediated by RANKL and IL-17 Produced by CD4+ T Cells in TallyHo/JngJ Mice', PLoS ONE, 6(3), pp. e18168.

Wu, C.-Z., Yuan, Y.-H., Liu, H.-H., Li, S.-S., Zhang, B.-W., Chen, W., An, Z.-J., Chen, S.-Y., Wu, Y.-Z., Han, B., Li, C.-J. and Li, L.-J. (2020) 'Epidemiologic relationship between periodontitis and type 2 diabetes mellitus', BMC Oral Health, 20(1).

Wu, L., Fritz, J. D. and Powers, A. C. (1998) 'Different Functional Domains of GLUT2 Glucose Transporter Are Required for Glucose Affinity and Substrate Specificity1', Endocrinology, 139(10), pp. 4205-4212.

Xie, J., D. Méndez, J., Méndez-Valenzuela, V. and Montserrat Aguilar-Hernández, M. (2013) 'Cellular signalling of the receptor for advanced glycation end products (RAGE)', Cellular Signalling, 25(11), pp. 2185-2197.

Xu, F., Dong, Y., Huang, X., Li, M., Qin, L., Ren, Y., Guo, F., Chen, A. and Huang, S. (2014) 'Decreased osteoclastogenesis, osteoblastogenesis and low bone mass in a mouse model of type 2 diabetes', Molecular Medicine Reports, 10(4), pp. 1935-1941.

Yagihashi, S., Mizukami, H. and Sugimoto, K. (2011) 'Mechanism of diabetic neuropathy: Where are we now and where to go?', Journal of Diabetes Investigation, 2(1), pp. 18-32.

Yamamoto, M., Yamaguchi, T., Yamauchi, M., Yano, S. and Sugimoto, T. (2008) 'Serum Pentosidine Levels Are Positively Associated with the Presence of Vertebral Fractures in Postmenopausal Women with Type 2 Diabetes', The Journal of Clinical Endocrinology & Metabolism, 93(3), pp. 1013-1019.

Yang, H., Li, Q., Lee, J.-H. and Shu, Y. (2012) 'Reduction in Tcf7l2 Expression Decreases Diabetic Susceptibility in Mice', International Journal of Biological Sciences, 8(6), pp. 791-801.

Zhou, R., Guo, Q., Xiao, Y., Guo, Q., Huang, Y., Li, C. and Luo, X. (2021) 'Endocrine role of bone in the regulation of energy metabolism', Bone Research, 9(1).

Zhou Wu, C., Hang Yuan , Y., Hang Liu , H., Sui Li , S. h., wen Zhang , B., Chen, W., jian An, Z., yu Chen , S., zhi Wu , Y., Han , B., jie Li, C. and jiang Li, L. s. a.-h. t. c. u.-i. f. f. h. r. i. w. u. x. h. g.-i.-e. (2020) 'Epidemiologic relationship between periodontitis and type 2 diabetes mellitus', BMC Oral Health, 20(204).

Zhu, Q., Yamagata, K., Miura, A., Shihara, N., Horikawa, Y., Takeda, J., Miyagawa, J. and Matsuzawa, Y. (2003) 'T130I mutation in HNF-4α gene is a loss-of-function mutation in hepatocytes and is associated with late-onset Type 2 diabetes mellitus in Japanese subjects', Diabetologia, 46(4), pp. 567-573.

Zoch, M. L., Clemens, T. L. and Riddle, R. C. (2016) 'New insights into the biology of osteocalcin', Bone, 82, pp. 42-49.

Świderska, E., Strycharz, J., Wróblewski, A., Szemraj, J., Drzewoski, J. and Śliwińska, A. (2020) 'Role of PI3K/AKT Pathway in Insulin-Mediated Glucose Uptake', Blood Glucose Levels: IntechOpen.